A Comparative Analysis of Within-host Models of Malaria Infection with Immune Response

by

Shadé Horn

Thesis presented in partial fulfilment of the requirements for the degree of Master of Science (Biochemistry) in the Faculty of Science at Stellenbosch University

Department of Biochemistry,
University of Stellenbosch,
Private Bag X1, Matieland 7602, South Africa.

Supervisor: Dr. D.D. van Niekerk
Co-supervisor: Prof. J.L. Snoep

April 2019

Stellenbosch University https://scholar.sun.ac.za

Declaration

By submitting this thesis electronically, I declare that the entirety of the work contained therein is my own, original work, that I am the sole author thereof (save to the extent explicitly otherwise stated), that reproduction and publication thereof by Stellenbosch University will not infringe any third party rights and that I have not previously in its entirety or in part submitted it for obtaining any qualification.

Date: April 2019

Copyright © 2019 Stellenbosch University
All rights reserved.

Stellenbosch University https://scholar.sun.ac.za

Abstract

With growing resistance of malaria parasites to different antimalarial treatments, there is an ever present need for new investigative approaches into disease eradication. The symptoms of the disease commonly include fever, nausea and dizziness, and can be attributed to the response of the immune system to disease. This thus emphasizes the imperativeness of the inclusion of the immune response in investigations. Within-host models are used to describe the disease dynamics within the human host during infection. Models commonly describe the change in populations of disease-associated cells within an individual, over time. Model parameters are usually incorporated as mean values from clinical data or estimated from literature. Apart from experimental error, in reality parameters can vary greatly between individuals. Consequently, it is unclear how much trust should be placed in these mathematical models to describe disease dynamics realistically.

In this project, local sensitivity, uncertainty, robustness and global sensitivity analysis was performed on within-host malaria infection models that incorporate the immune system's response. These analyses were used to determine which processes play an important role in the disease dynamics and can therefore possibly be of interest for drug targeting. The results also indicated whether the description of the disease processes can accommodate heterogeneity and uncertainty while still giving reliable and realistic model predictions. Comparison of the model analysis results in this project allowed for identifying which models would be more relevant in describing biologically realistic disease dynamics under the influence of the human immune response, and would be more suited to further studies to identify possible drug targets.

Stellenbosch University https://scholar.sun.ac.za

Opsomming

Met groeiende weerstandigheid van malaria parasiete teen verskillende anti-malariese behandeling, is daar 'n groeiende behoefte aan ondersoeke na siekte-uitwissing. Die simptome van die siekte sluit gewoonlik koors, naarheid en duiseligheid in, en kan toegeskryf word aan die respons van die immuunsisteem op die siekte. Dit beklemtoon die noodsaak vir die insluiting van die immuunsisteem in hierdie ondersoeke. Binne-gasheer modelle word gebruik om die siekte-dinamiek binne 'n mens tydens infeksie te beskryf. Modelle beskryf gewoonlik die tyd-afhanklike veranderinge in siekte-verwante selpopulasies binne 'n individu. Model parameters word gewoonlik geïnkorporeer as die gemiddelde waardes van kliniese data of geskat vanaf literatuur. Buiten eksperimentele foute, kan parameters in werklikheid dramaties varieer tussen individue. Dit is dus onduidelik hoeveel vertroue geplaas kan word in die vermoëns van hierdie wiskundige modelle om die dinamiek van die siekte realisties te kan beskryf.

In hierdie projek word sensitiwiteit-, onsekerheid-, robuustheid- en globale sensitiwiteitsanalise toegepas op binne-gasheer modelle van malaria infeksie waarin die immuunsisteem se respons ingesluit is. Hierdie analises word gebruik om te bepaal watter prosesse belangrik is vir die dinamiek van die siekte en as moontlik teikens vir farmaseutiese intervensie kan dien. Die resultate dui ook aan of beskrywings van die prosesse heterogeniteit en onsekerheid kan akkommodeer en steeds realistiese en betroubare modelvoorspellings kan lewer. Vergelyking van die model analise resultate kan gebruik word vir die identifisering van modelle wat meer relevant is vir die beskrywing van siekte-dinamiek onder die invloed van die menslike immuunsisteem en wat gebruik kan word vir verdere soeke na teikens vir farmaseutiese intervensie.

Stellenbosch University https://scholar.sun.ac.za

Contents

Stellenbosch University https://scholar.sun.ac.za

Stellenbosch University https://scholar.sun.ac.za

Stellenbosch University https://scholar.sun.ac.za

List of Figures

Stellenbosch University https://scholar.sun.ac.za

Stellenbosch University https://scholar.sun.ac.za

List of Tables

Stellenbosch University https://scholar.sun.ac.za

Stellenbosch University https://scholar.sun.ac.za

Abbreviations

ASA	Adjoint Sensitivity Analysis
DDM	Direct Differential method
eFAST	extended FAST
FAST	Fourier Amplitude Sensitivity Test
FDAP	Finite Differential Approximation
iRBC	infected red blood cell
LHS	Latin Hypercube Sampling
MC	Monte Carlo
MCA	Metabolic Control Analysis
MPSA	Multi-Parametric Sensitivity Analysis
NGM	next generation matrix
OAT	one-factor-at-a-time
ODE	ordinary differential equation
PRCC	Partial Rank Correlation Coefficient
RBC	red blood cell
RS HDMR	Random Sampling High-Dimensional Model Representation
WALS	Weighted Average of Local Sensitivities

Stellenbosch University https://scholar.sun.ac.za

Chapter 1

Introduction

Malaria is a well-known parasitic disease commonly found in the African and sub-Saharan regions. Currently, 91 countries are affected by the disease with a total of 216 million cases of infection and a mortality rate of 445 000 as reported in the malaria report of 2017 by the World Health Organization [1]. The report furthermore shows that with the increased investigations into malaria in the past few decades the overall incidence of malaria has decreased as from 2010. However, this rate of decrease has plateaued, and the reported cases are again increasing due to the development of malarial resistance to current treatments [1, 2]. This is indicative of the great need to investigate this disease with the objective of eradicating either its spread or itself.

Various different methods are currently used to investigate the malaria parasite and its life cycle, the interactions of the parasite with both the human and mosquito host, as well as the immune system's response to infection. The immune response to disease is an important area of investigation as it is associated with the clinical manifestations observed with malaria infection. One method that can integrate quantitative knowledge on all fronts, is the mathematical modelling of disease aspects. Many within-host mathematical models [3-26] of the disease dynamics of malaria infection exist. Most models focus on the time evolution of populations of different cell types, since the life cycle of the parasite in the host affects, inter alia, red blood cells and hepatocytes directly through physical infection, in addition to stimulating immune cell production indirectly (tissue-sequestered parasites and transmissible parasites that develop in the bone marrow are not yet included but could possibly have an effect on the disease dynamics). Simple models of the blood stage of infection (the most well characterized stage of infection) therefore usually describe populations of uninfected red blood cells (RBC), infected red blood cells (iRBC) and free parasites [18-21], while most models have been extended to include immune system components [3-17, 22-26]. The time evolution of these cells is mathematically described by ordinary differential equations (ODEs). In principle all processes that affect cell populations should be included in the ODEs as parametrized rates (once quantified). Not all processes are, however, equally important in the context of the disease feature of interest. The mathematical parametrization of a biological process also introduces some approximation to the dynamics that might only be realistic close to the reference

Stellenbosch University https://scholar.sun.ac.za

state. Consequently, there are some uncertainties around the outputs of mathematical models, and thus the trust that can be placed on model interpretations.

Sensitivity and uncertainty analyses are useful tools to alleviate some of the uncertainty around model outputs and determine important processes for model structure. Local sensitivity analysis is commonly used to determine the influence a small change in a process would elicit on the wild type model outputs, and can be used to investigate possible drug targets. This is possible due to a large sensitivity results indicating that the process has a large influence on the dynamics of the disease. Uncertainty analysis can be used to quantify the effect of variance in parameter values on uncertainty in model outputs that could limit trust in some interpretations made from the model. This analysis can therefore indicate which parameters should be investigated experimentally to determine actual ranges for the parameter values. Robustness analysis indicates how well model outputs for these parameter ranges correlate to the reference (wild type) model output. Lastly, global sensitivity analysis can indicate how well the local sensitivity analysis results are conserved over a larger parameter space as would be seen in a population. In combination, these analyses can assist in interpreting how well a model can account for realistic disease dynamics and where possible drug targets lie given not only the fixed mean values of parameters used for the wild type model, but taking into consideration parameter uncertainty and variance.

This project therefore focuses on reproducing published models of malaria infection, where the immune system's response is incorporated. The aim of this project is to employ uncertainty and sensitivity analysis on these within-host models, to determine which processes are important for disease dynamics (and can possibly be of interest for drug targeting) and whether the description of the disease processes can be extrapolated to account for heterogeneity and uncertainty while still giving reliable and realistic model predictions. This led to the following objectives:

- Find comparable published ODE models which include the immune response to infection.
- Reproduce the published model results to establish trust in the model descriptions, as well as the given parameter values.
- Perform local sensitivity, uncertainty, robustness and global sensitivity analyses on all models.
- Compare and interpret analysis results.

Stellenbosch University https://scholar.sun.ac.za

The following chapter will focus on background information on the malaria parasite, malaria infection, and the immune response to the disease. Chapter 3 will indicate the methodologies used in this study and elucidate on their implementation and utility. Thereafter, relevant model descriptions will be presented in Chapter 4. Chapters 5-8 will encompass the results of all the sensitivity analyses, followed by a discussion of all findings and comparison of results between models, presented in Chapter 9.

Stellenbosch University https://scholar.sun.ac.za

Chapter 2

Background information

2.1. The life cycle of the malaria parasite

Malaria is caused by five different *Plasmodium* species with *P. falciparum* being the most common as well as deadliest species [27]. The life cycle of the malaria parasite can be divided into three stages; the exo-erythrocytic, the erythrocytic and the sporogonic stage (Figure 2.1).

P. falciparum is inoculated into a human host by the female *Anopheles* mosquito during a blood feeding, where sporozoites contained within the salivary glands of the mosquito are injected into the bloodstream by their stylets [28]. Once the sporozoites enter the bloodstream, they rapidly travel to the liver where they invade the hepatocytes [29]. Here the sporozoites multiply asexually for up to 15 days to form schizonts which rupture to release merozoites in the bloodstream, marking the end of the exo-erythrocytic cycle [15].

For the erythrocytic cycle, the released merozoites roam free within the blood to infect healthy RBCs. During the replication cycle after RBC infection, a merozoite develops from an immature trophozoite to a mature trophozoite, that will form a schizont which can rupture to release the new merozoites. This process takes approximately 48 hours and leads to the release of 8 to 32 new merozoites [30].

Immature trophozoites can also undergo gametocytogenesis, developing into male and female gametocytes [29]. When an uninfected mosquito feeds, these gametocytes can be ingested with the blood, starting the sporogonic cycle. Inside the mosquito, male and female gametes combine to form zygotes, which eventually develop into oocytes. A ruptured oocyte releases sporozoites that move to the mosquito's salivary gland, completing the life cycle of the malaria parasite [15, 30].

Stellenbosch University https://scholar.sun.ac.za

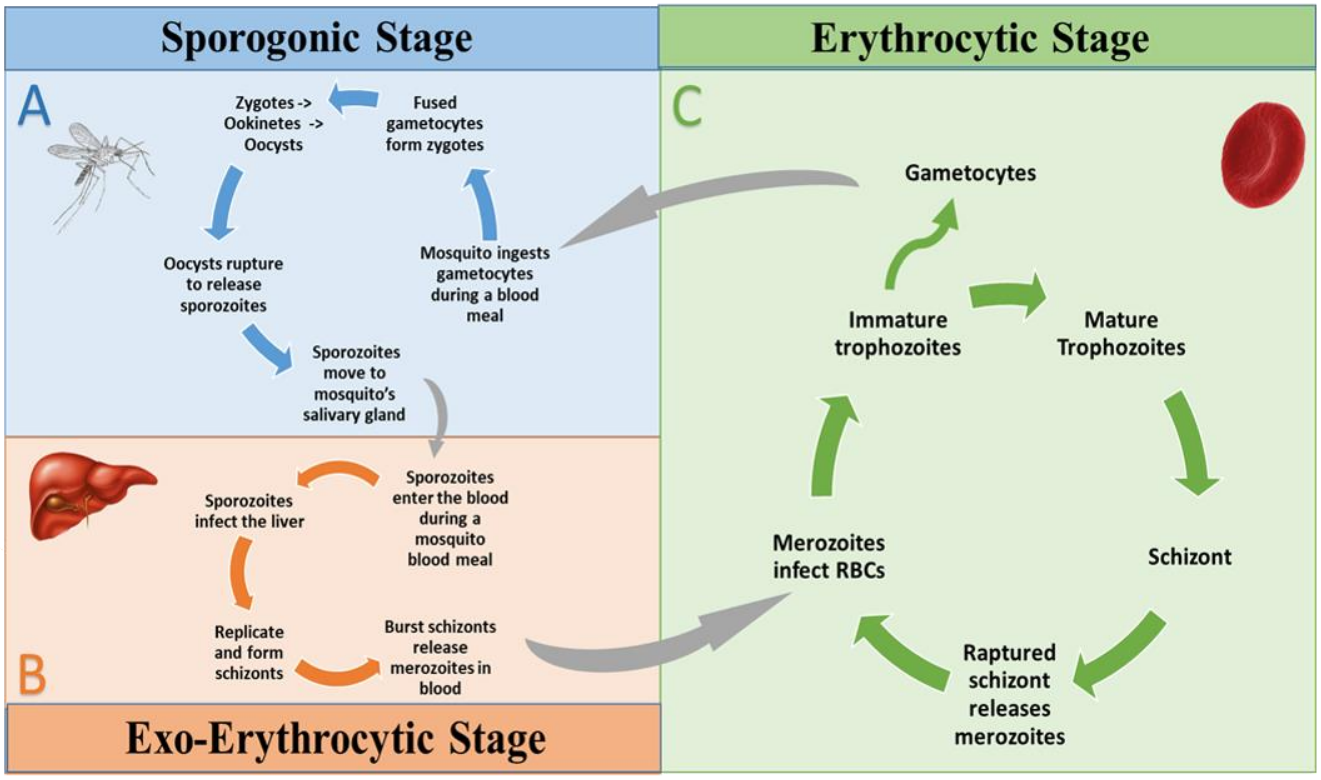

Figure 2.1. The life cycle of the malaria parasite. The life cycle is split into three stages. A – Sporogonic stage where ingested gametocytes develop into sporozoites in the Anopheles mosquito. B – Exo-erythrocytic stage cycle where sporozoites that have entered the blood stream during a blood meal develop into schizonts in the liver of the human host to release merozoites into the blood. C- Erythrocytic stage where merozoite infected RBCs can either lead to more merozoites being released within the blood or the development of male and female gametocytes for the continuation to the sporogonic stage. This scheme was constructed based on the general description of the malarial life cycle [15, 29, 30].

The erythrocytic stage of the malaria parasite is the stage that relates to the clinically observed malaria state. This is due to the released merozoites and the iRBCs that activate the immune response, leading to symptoms including fever, nausea, vomiting, malaise, abdominal discomfort as well as mild anemia [31]. Severe anemia can also exist with infection and can be attributed to the decrease in healthy RBCs due to infection as well as bursting of iRBCs [31]. Other factors that can contribute to the severe anemia are the combined death of iRBCs and possibly some uninfected RBCs due to the immune response, as well as the prohibition of the normal erythrocytic process for new healthy RBCs. [32]. In worse cases of infection symptoms can lead to a coma or even death. Since many of the clinically observed symptoms are attributed to the response of the immune system, and anti-malarial inoculation would function via the immune system, the inclusion of the immune response in studies is imperative for furthering the investigation of malaria [29].

Stellenbosch University https://scholar.sun.ac.za

2.2. Immune response to Malaria infection

The general immune response to an infection or a disease is composed of various cells and chemicals that interact both with each other and with infectious microbes to fight an infection. When protecting the body from an infection, the immune system will secrete many proteins and molecules to defend the body [33]. These secretions can then either play a role in the attack on the infectious microbes or they can protect the body by, for example, activating an inflammatory response [33]. Even though this is natural, the response can lead to clinically observed symptoms and sometimes do more harm than good. This is witnessed with auto-immune diseases where the over activation of the immune response can lead to detrimental clinical manifestations [33, 34].

Upon infection, the body has two immune responses (Figure 2.2). The first immune response is an ever-present function that rapidly attempts to protect the human at the start of an invading pathogen [35], known as the innate immune response. The innate immune response is a general response and mostly comprises of the same activity for almost all pathogens as it is not specified to any individual harmful element [35]. This response has three general purposes [36]. The first purpose is to ensure that no harmful elements enter the body through epithelial layers like the skin. The second purpose of the innate immune system is to start fighting against the microbes that passed the first defense. The body does this by secreting various proteins and cytokines as well as directly attacking the infectious agent with phagocytes or natural killer cells. This, together with the first step of defense is, however, not always sufficient to exterminate the disease and with persistent disease the adaptive immune system will be activated. The innate immune response therefore also assists the adaptive immune response and enhances its effectiveness [36].

Stellenbosch University https://scholar.sun.ac.za

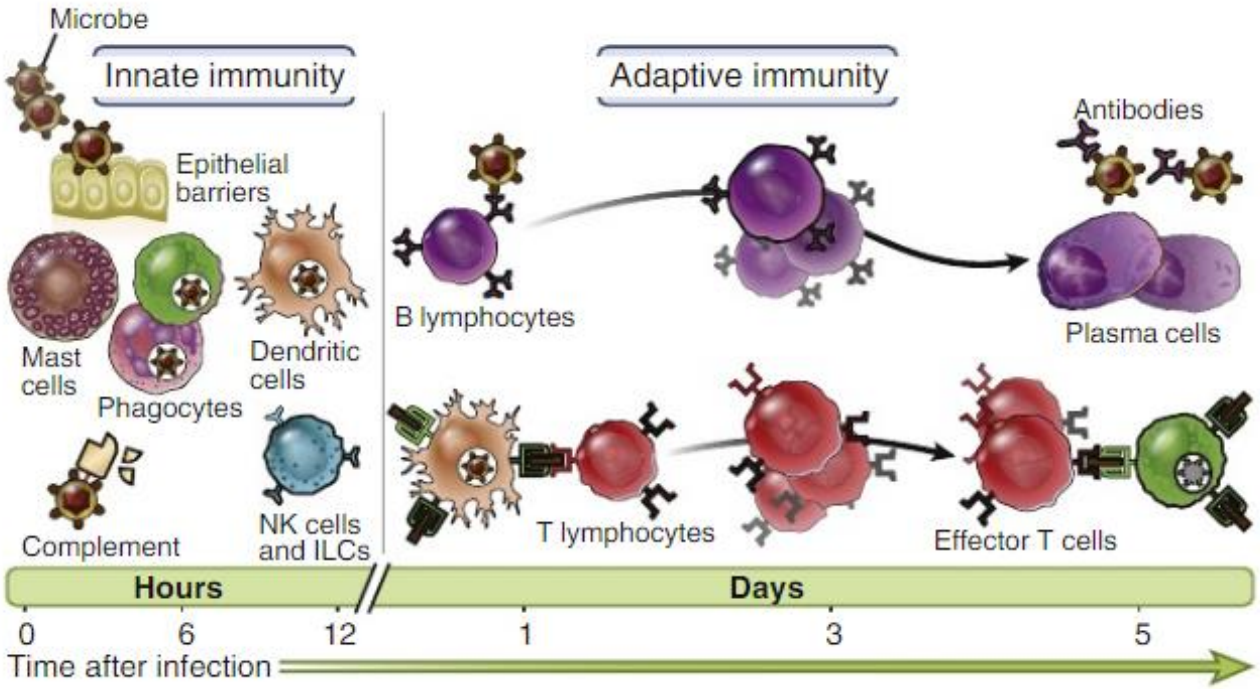

Figure 2.2. The division of the immune response into the innate and adaptive immune response. This figure shows the different cells that can be present for both the innate and adaptive immune response as well as the time after infection that each of these responses are most present. Upon entry of an infectious microbe, the innate immune system defends the body until the adaptive immune response has been specialized to the specific infection [36]. Image from [36].

The adaptive immune response takes longer to develop for a pathogen, as it is highly specific [35], and consists of T- and B-lymphocytes [37]. These two groups of cells are also indicators of the adaptive immune system's division into two types of responses, classified as the humoral and the cell-mediated immune response (Figure 2.3) [36]. The humoral immune response is specialized to act against microbes that are present outside of the host cells and consists of B-lymphocytes which produce and secrete antibodies specific to the infectious agents present within the blood and lumens of mucosal organs [36]. These antibodies from the B-lymphocytes neutralize and eliminate infectious microbes that roam free within the blood. However, as soon as the microbes infect a cell, or become phagocytized by cells such as macrophages, these defense mechanisms become redundant. The cell-mediated immune response is, therefore, composed of the T-lymphoid cells which provide defense against microbes that have entered a cell like the RBC [35]. The T-lymphocytes can differentiate into different types of T-cells, including T-helper cells and cytotoxic T-cells. Cytotoxic T-cells can directly kill infected cells by inducing apoptosis of these cells, as well as help induce B-lymphocytes to produce antibodies. T-helper cells help

Stellenbosch University https://scholar.sun.ac.za

to prime cytotoxic T cells by stimulating them to differentiate and eliminate phagocytosed microbes by producing cytokines that activate them [36].

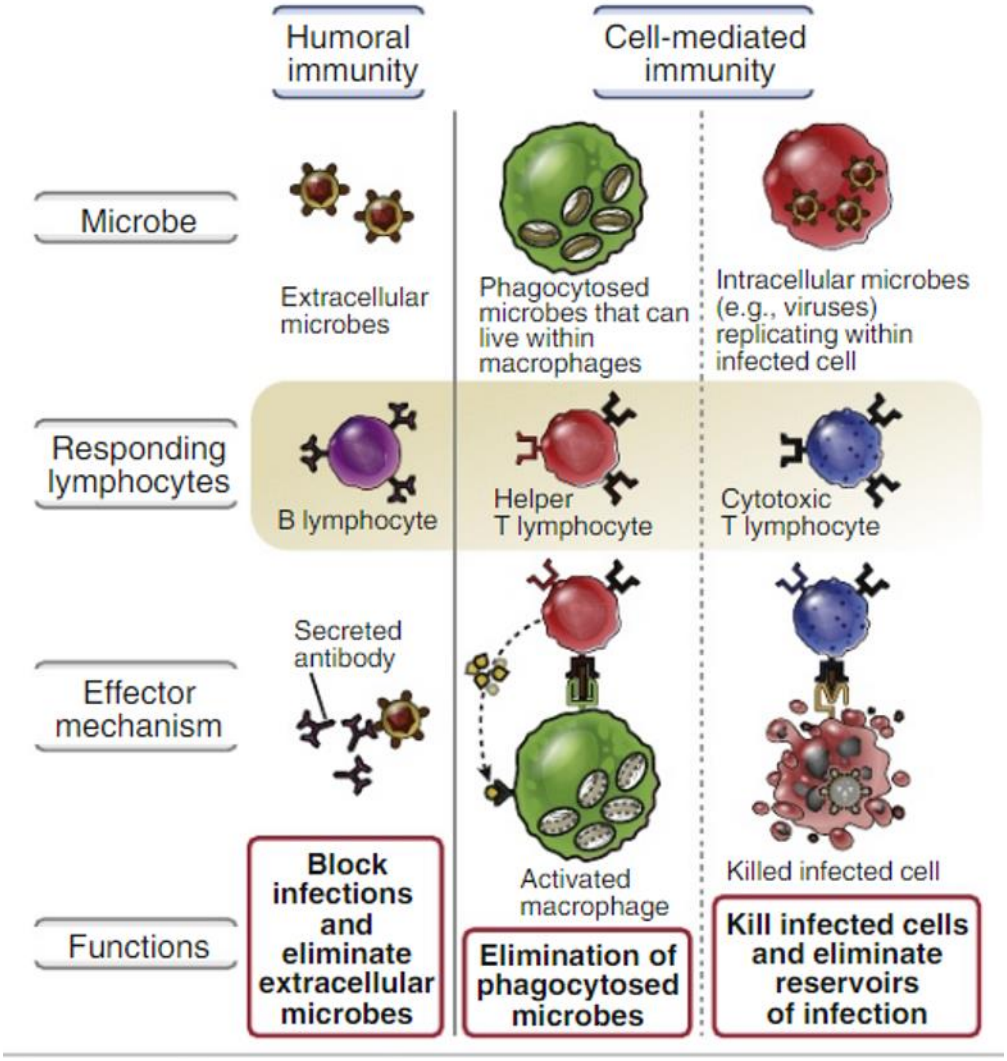

Figure 2.3. The division of the adaptive immune response. The humoral and cell-mediated immune responses differ in their lymphocytes used as well as in the mechanisms used to fight infection as explained in text [36]. Image from [36].

Considering the immune response to malaria, the collective response containing all these components can now be easily inspected. Upon first infection, the innate immune response will be present to start the fight against the infection. Dendritic cells start by capturing merozoites that roam free in the blood plasma. Dendritic cells are known as antigen presenting cells, which is a class of cells that prepare antigens to be presented to T-lymphocytes to activate the adaptive immune response [37]. Dendritic cells have a cell structure that allows them to have receptors expressed on their outer membrane known as

Stellenbosch University https://scholar.sun.ac.za

toll-like receptors (TLR) [16]. These receptors recognize infectious microbes that have entered the body, capture them and prepare them for presentation [38, 39].

Upon presentation of the antigen to the T-lymphocytes, the T-lymphocytes are activated to differentiate into T helper 1, T helper 2 and regulatory T cells (Th1, Th2 and Treg respectively) [16, 35]. Each of these T-cells plays a specific role in the immune response. Th2 cells help B-lymphocytes to produce antibodies against the microbes, Th1 cells produce compounds which can help to fight the infection and Treg cells produce compounds that ensure the immune response is stabilized [16, 40]. All these cells thus work together to fight and eradicate an infection.

An example of a compound produced by Th1 cells is interferon-gamma (IFN-gamma) which can activate cytotoxic T cells to kill pathogens directly. IFN-gamma also activate macrophages to produce inflammatory cytokines, adding to the overall inflammatory response to protect the body against infection [16, 41]. As macrophages and dendritic cells are both examples of phagocytes, these cells can phagocytose iRBCs and digest them [41]. A problem in the case of malaria is that the parasite's consumption of haem in the iRBC leads to the formation of haemozoin. Haemozoin is indigestible by the macrophages and therefore persists in activating the immune cells, leading to a continued release of pro-inflammatory cytokines that correlates to clinically observed symptoms such as the periodic fevers associated with *Plasmodium* infection [4]. Consequently, Treg cells help to regulate the immune response and can secrete anti-inflammatory compounds to counter the inflammatory response [40]. This shows the importance of a balance between fighting the disease to protect the body and regulating the response to the infectious elements to prevent severe pathology [4]. A quantitative understanding of the immune response and its components is therefore imperative for studies on infection and disease dynamics.

2.3. Mathematical modelling

Mathematical modeling is a way to simplify a complex biological system into a mathematical description, which can then be used to analyze the effect of processes in the system and to make quantitative predictions of how a system is influenced by various parameters, often through employing computational tools.

Stellenbosch University https://scholar.sun.ac.za

As stated in the introduction various mathematical models exist that represent the within-host dynamics of malaria infection, with most including the immune response and some extended to also include treatment parameters [3-26]. There are also models that only focus on certain parts of the parasite life cycle or infection, such as gametocytogenesis or antigenic variation from the parasites [11, 21-26]. Lastly, some studies investigate the within-host model components in combination with epidemiological models [42, 43].

Models of malaria can be classified according to different criteria. One such would be to classify them according to the types of processes in the system: stochastic or deterministic models [44]. Deterministic models are models where all parameters used in the model system are fixed to their experimentally determined or theoretically derived values, and a model prediction is a unique outcome of the effects of system processes and parameter values. In contrast, a stochastic model allows for variance of some parameters and as such these parameters are modeled with a probability distribution instead of a fixed value [44]. Another classification considers the organizational level at which the disease is described, e.g. epidemiological or within-host models [45]. Epidemiological models describe the disease transmission within a population focusing on different classes of people, including susceptible, infectious and recovered (SIR-models). Within-host models focus on variables within an individual and will typically include at least healthy or infected RBCs. This study focuses on deterministic within-host models on malaria infection where the immune response to infection is included.

These deterministic within-host models commonly consist of a few ODEs describing how variables (cell populations) change over time due to processes and associated parameter effects on each variable. ODEs for different variables are usually also coupled to one another through mass transfer processes which decrease one variable and concomitantly increase another at the same rate, or through stimulation or inhibition of a process proportional to the magnitude of another variable. When the ODEs are solved (typically using numerical integrators in software such as Wolfram Mathematica or MatLab) one obtains time course solutions of variable values which usually either depict continuous dynamical behavior or an equilibrium state. In the context of living systems, this equilibrium (if present), is dynamic in nature where variable and rate values remain constant and non-zero in time. This is referred to as the steady state of the system, and the rates are called fluxes [46, 47].

Stellenbosch University https://scholar.sun.ac.za

As different modelers have different preferences regarding points of interest and associated model formulations, major differences can exist in model ODEs and processes used, as well as parameter values and units. The questions thus exist: Which model describes disease dynamics and the immune response realistically and under which circumstances? How does one compare these models? Are model predictions reliable and realistic when taking heterogeneity and uncertainty of the disease processes into account? Furthermore, being able to pinpoint parameters with the largest effects on e.g. merozoites surviving in the blood, or the amount of iRBCs, can represent an important process for drug targeting [23]. To thus distinguish the important parameters from the rest and to quantify the effect of parameter variance, sensitivity analysis is performed to indicate the sensitivity of a variable population (e.g. the number of healthy RBCs) to a parameter (e.g. the number of merozoites released per bursting iRBCs).

2.4. Sensitivity analyses

Sensitivity analyses are useful tools to quantify parameter effects within a model. Thereby they can assist in elucidating biologically relevant components for disease eradication, determining the contribution of parameter uncertainty to variance in model prediction and test model robustness against parameter changes. As discussed below, these outcomes are accomplished through local sensitivity analysis, uncertainty analysis, robustness analysis and global sensitivity analysis.

2.4.1. Local Sensitivity analysis

Local sensitivity analysis entails the determination of the change in model outputs when the model inputs are allowed to change one at a time in a localized parameter space around the reference state. When parameters are changed one at a time it is designated as a one-factor-at-a-time (OAT) method [48]. An example of this would be investigating the change in variable steady states when one parameter in a model is allowed to change with a certain percentage, while all other parameters are kept constant. The same method is then applied to all parameters individually and the results, shown as sensitivity indices, can then be indicative of the importance or influence that each parameter has on the model outputs. The sensitivity indices are calculated by computing first-order derivatives of the variables regarding the parameters. Methods that exist for these computations include Finite Difference Approximation (FDAP), the Direct Differential Method (DDM), Adjoint Sensitivity Analysis (ASA) and Metabolic Control Analysis (MCA) [49]. These analyses differ in their methodologies as well as when they can be applied.

Stellenbosch University https://scholar.sun.ac.za

The FDAP method is mostly used when there is no analytical solution for a model and the model was therefore solved by numerical approximations where model outputs are approximated using different model input values. As such, for the calculations of the sensitivity coefficients, parameters are varied one by one, firstly with a small perturbation. This perturbation is then increased or decreased until there is a small or insignificant change in the sensitivity coefficients from one perturbation to another. At this perturbation the model will be indicated as robust and the sensitivity indices will be accepted [49]. The method therefore includes infinitesimal amounts of perturbations to obtain a sensitivity index and can become very time-consuming as the analysis will have to be repeated for each parameter [50, 51]. The DDM differs from the FDAP by calculating all the sensitivities of each variable to a parameter at the same time, thereby excluding the need for the infinitesimal amounts of parameter perturbations. This method does however require the construction of a Jacobian matrix (which contains the first-order partial derivatives of the sensitivity coefficient as a function of the variable) which would become computationally expensive as parameter set sizes increase [52, 53, 54]. To alleviate the time consumption of these methods, the ASA method uses a Green's function matrix where the sensitivities included within the matrix are expressed in integral instead of differential form. This method delivers the same results as obtained by DDM, while being less computationally expensive due to dependency of the method shifting to the number of variables, and not the number of parameters [55, 56]. Lastly, MCA is generally used for biological mathematical models, especially with numerous parameters, and entails calculating normalized derivatives of the sensitivity coefficients of the model variables on the parameters. Various sensitivity coefficients can be obtained by MCA, such as elasticity, concentration control, flux control, sensitivity flux control, response and time-dependent response coefficients [50], depending on the model inputs and outputs of interest, e.g. the flux control coefficient considers the rate of a reaction as the input, and the flux of the reaction in the system as a whole as an output [54]. In the systems of this project, steady states are the observables of interest and the associated sensitivity analysis therefore considers parameters as input and a steady state for each variable as an output [50] leading to so-called response coefficients. The response coefficients are indicators of the change in a steady state brought upon by a change in a parameter value [55, 56]. Response coefficients can then be used to indicate parameters important or redundant for the model predictions, as well as which parameters have a large influence on the model outputs. It thus offers information regarding potential areas for further investigation of targets in drug development.

Stellenbosch University https://scholar.sun.ac.za

2.4.2 Uncertainty analysis

Uncertainty analysis is closely related to local sensitivity analysis as it describes the contribution of uncertainty of each parameter in a model to the uncertainty in model predictions [57]. Where local sensitivity analysis gives insight on how variables are affected by small changes in parameters, it does not show how the overall uncertainty of a parameter can affect the uncertainty in the model outputs at the reference state. This method is commonly used when parameters are not set at a certain value or have been estimated from literature. Uncertainty analysis can therefore be useful to indicate which parameters should not have a large influence on the model outputs as it would contribute to the uncertainty in the model predictions. Uncertainty analysis will thus be included in this project, in conjunction with local sensitivity analysis [50, 57-59].

2.4.3. Robustness Analysis and Sampling methods

The response coefficients that will be obtained through local sensitivity analysis could be used as a model robustness indicator for small changes in parameters round their reference values. A robust model is a model that is resilient to changes in model inputs [60]. Therefore, if a parameter perturbation shows no or insignificant change to the different variables, the model will show a degree of robustness to a specific parameter. The question could however be asked how robust a model is to changes in all parameters at the same time? A typical outcome of such an analysis would thus show the different outcomes, if outcomes do differ, with variations in parameter values of a model. The different outcomes that will be obtained can then be visualized as a distribution showing the density and the lowest and highest possible variable outputs. This requires obtaining numerous parameters sets in a distribution around the reference state. Various sampling techniques exist to obtain these sets and will be discussed briefly.

Numerous factors should be kept in mind when deciding on a sampling method as the different methods rely on different mathematical and coding techniques, and inputs which can be computationally expensive for some methods. Methods reviewed included the Morris method, stratified sampling, Latin Hypercube Sampling (LHS) and Monte Carlo (MC) random sampling [50, 61-64]. The Morris method of sampling encompasses an OAT design, as each parameter is varied over a range in a step-wise manner, meaning that if a parameter range is defined as lying between 90% and 110 % of the reference parameter value, subdivided into 5 intervals, the parameters are chosen on the interval boundaries, in other words where the parameter is at 90%p, 95%p etc. [65]. Trajectories are then determined in parameter space whereby every parameter is changed in a coordinated way, thereby constructing various parameter sets,

Stellenbosch University https://scholar.sun.ac.za

and an elementary effect can be calculated for each parameter as the change in the variable outputs achieved. The mean and standard deviations of a given parameter's elementary effects from different trajectories is then used as a measure of global sensitivity [66, 67]. Stratified sampling and LHS both encompass a choice of interval amount and the range of every parameter's values is then divided into this number of equally sized intervals. A random value is chosen in each interval. If a range was divided into five intervals, there would therefore be five parameter values for each individual parameter, each falling in one of the intervals [68, 69]. The difference in these two sampling techniques lie within their constructing of parameter sets for model evaluation. Consider a scenario where there are 5 intervals for 7 parameters, (i.e. 5 values for every parameter). For LHS the construction of a parameter set uses one parameter value from any interval for each parameter. However, if a parameter from one interval has been used, it will be excluded in the construction of the next parameter set, therefore ensuring that there would only be 5 (unique) parameter sets. Stratified sampling differs in that it does not exclude a previously used parameter and ensures that all parameter combinations are used [69]. Therefore, for the same number of parameters and intervals, stratified sampling will produce 5^7, consequently 78 125, unique strata (or parameter sets). As this will increase exponentially with increase in the number of parameters incorporated in a model, or with an increase in intervals analyzed, this could become a very computationally expensive method. Lastly, MC random sampling needs a range for each parameter, in which a random value is chosen, thus creating one parameter set [70]. A value may be used more than once ensuring more parameter sets and combinations can be obtained. As the process is entirely random, the more iterations that can be run, the more likely it becomes that the parameter space is covered satisfactorily. Note that the coverage of parameters space is assumed to be more thorough for fewer sets in the case of LHS and stratified sampling by design.

As some model parameter sets included more than 30 parameters in this project, parameter space size was a necessary factor to keep in mind. MC random sampling (with a high number of parameter sets) and LHS (with a lower number of sets) was used to obtain and compare robustness results for model variables between the two methods and between models. As each method can generate unique parameter sets, with each parameter set leading to new steady states for model variables, a total range could be determined for the steady state results. This range would therefore be an indicator of model robustness to combined parameter changes.

Stellenbosch University https://scholar.sun.ac.za

2.4.4. Global Sensitivity Analysis

Local sensitivity only shows the sensitivity of a model to small perturbations or changes in one parameter at a time, and lacks the ability to show the model sensitivity in the range of model outputs arising from combined non-infinitesimal parameter changes. Global sensitivity analysis offers a different approach as it allows for large perturbations in all parameters. Intense variations in the biology of individuals and populations exist, therefore indicating that more than one steady state is achievable for each variable. Global sensitivity analysis can therefore assist in indicating unexpected sensitivities and thereby determining which of the parameters can contribute to the variation of the observed model outputs. Additionally, it can indicate if the local sensitivities is conserved over a larger parameter space as seen in individuals [50].

Global sensitivity analysis is a widely used term, with no consensus on the methods employed, that implies perturbations in all parameters simultaneously [49, 50, 71-72]. Parameter ranges used vary greatly between authors, as some would vary parameter values by 50% and others by 10%, depending on the model investigated as well as uncertainty in parameters. Nevertheless, a method that can be used for sensitivity analysis of a biological model at every point in parameter space would be MCA if every such point is treated as a reference state for a local analysis. Other general global sensitivity analysis methods used on biological models include Multi-Parametric Sensitivity Analysis (MPSA), Partial Rank Correlation Coefficient (PRCC), Morris sensitivity analysis method, Weighted Average of Local Sensitivities (WALS), Sobol method, Fourier Amplitude Sensitivity Test (FAST), extended FAST (eFAST) and Random Sampling High-Dimensional Model Representation (RS HDMR) [50]. Each of these methods have their advantages and disadvantages with various levels of computational and mathematical complexity and approximation. The MPSA method has the disadvantage of requiring a threshold value in model outputs to determine if new parameter sets are acceptable. This borders on being impossible with biological models with a large amount of parameters, as model outputs can differ vastly. The PRCC method builds on the assumption that model input and outputs share a monotonic relationship and WALS uses a combination of weighing factors and the averages of local sensitivity results for each parameter in a local parameter space in order to obtain the global sensitivity result. The Sobol method, FAST, eFAST and RS HDMR are all variance-based methods that become more computationally expensive with increase in parameter sets [50, 53, 61, 69].

Stellenbosch University https://scholar.sun.ac.za

The difference between local and global MCA analysis is that global analysis is done when all parameters are varied. As the sampling methods discussed in the previous section would create numerous parameter sets, MCA analysis is performed on each set and results are obtained in the form of response coefficients (68). For a sampling method of say a 1000 parameter sets, there would therefore be 1000 response coefficients for each parameter, thus showing a distribution of possible response coefficients for a parameter. A normal distribution with the mean and median lying on the wild type response coefficient would consequently show global robustness of the model's sensitivity for a parameter. In principle there could exist different response coefficients for these parameters within a biologically plausible parameter space.

In summary, all sensitivity analysis methods would therefore give insight into the reliability of model constructions and parameter values used. Results for global sensitivity analysis can additionally be compared between different models where if more than one model shows the same global analysis results for a parameter, this parameter might be cause for further investigation.

Stellenbosch University https://scholar.sun.ac.za

Chapter 3

Methodologies

All modeling and sensitivity analysis methods were implemented in Wolfram Mathematica v.11.3. Prior to sensitivity analysis, each model used was reproduced and simulated with standard numerical differential equation solver and root finding functions in Mathematica. This was performed to verify that the same model outputs as published could be obtained, i.e. faithful model reproduction was achieved. The reproduced results are shown in Appendix A. Functions were then coded to perform local sensitivity, uncertainty, robustness and global sensitivity analyses on all models.

3.1. Local Sensitivity Analysis

For the local sensitivity analysis of model parameters, standard methods of MCA were utilized. This method entailed the perturbation of parameters one at a time to see the effect of the perturbation on model variable outputs, indicated as the response coefficient. A response coefficient describes the percentage change of a model output – in this case the steady states of different variables V – upon a 1% change in model inputs or parameters p. The general formula of a response coefficient follows:

$$R_p^V = \frac{\partial V}{\partial p} \times \frac{p}{V}$$

Numerically, the derivative is approximated by a finite difference formula symmetrically using symmetric perturbations of size *pertSize* (e.g. 0.001 for a 0.1% perturbation) up and down from the reference parameter value:

$$R_p^V = \frac{1}{2}\left(\frac{newSSUp - wtSS}{paramUp - paramWT} + \frac{newSSDown - wtSS}{paramDown - paramWT}\right) \times \frac{paramWT}{wtSS}$$

$$= \frac{newSSUp - newSSDown}{2 \times pertSize \times wtSS}$$

Stellenbosch University https://scholar.sun.ac.za

The up and down perturbation of a parameter yields two new steady states, denoted as *newSSUp* and *newSSDown*. The difference in these two steady states is divided by the difference in parameter values (*paramUp* and *paramDown*) and then normalized to the reference state.

3.2. Uncertainty analysis

Uncertainty analysis was performed on all models to show which parameter's uncertainty would contribute the most to total uncertainty in the model outputs. The method therefore incorporates the individual variance of each parameter to attain individual uncertainties. The variance is calculated as the variance of the natural logarithm of each parameter:

$$\sigma^2(\ln p_j)$$

However, as the variance of parameters in the biological models of this thesis are not known, all parameters were modelled to have a 10% random variance in parameter value. It is therefore assumed that all parameters vary with the same percentage and the uncertainty results would thus indicate which variance has the largest effect on the model outputs. The individual contribution of each parameter variance $\sigma^2(ln\ p_j)$ on the total variance of each variable $\sigma_j^2\ (V_i)$ is then calculated using:

$$\sigma_j^2\ (V_i) = \sigma^2(\ln p_j)(\frac{\partial V_i}{\partial \ln p_j})^2$$

where $\sigma^2(\ln p_j) = \frac{1}{12}[\ln(1.1p_j) - \ln(0.9p_j)]^2$ i.e. we considered a uniform distribution with maximum and minimum determined by a 10% change in the wild type parameter value (i.e. min = 0.9p and max = 1.1p) for each parameter [73]. The total variance of each variable can be determined by summation of all of the individual contributions to uncertainty of each parameter on a variable,

$$\sigma^2(V_i) = \sum_j \sigma_j^2\ (V_i)$$

Stellenbosch University https://scholar.sun.ac.za

If the total variance of a variable has been calculated, it would therefore be possible to determine the contribution of each parameter to model output uncertainty as a percentage:

$$\%uc_{ij} = \frac{\sigma_j^2\ (V_i)}{\sigma^2(V_i)} \times 100$$

3.3. Sampling methods and Robustness analysis

Two different sampling methods were used to achieve parameter sets in preparation for robustness and global sensitivity analysis. The first sampling method utilized is a MC random sampling based method. All parameters were therefore allowed to vary at the same time within a 10% range and parameters sets were generated choosing values within the range at random. For this analysis, 10 000 parameter sets were generated per model for further analysis.

The second sampling method used was LHS, which also allowed parameters to vary with a 10% range, with the addition of the use of user defined intervals. For this analysis 1 000 evenly distributed intervals were chosen, indicating that each parameter would have 1 000 values, each value taken randomly from every interval. The parameter sets were then constructed by randomly choosing one parameter value from each parameter. Once a parameter value from a set is used, this parameter value is excluded from further parameter set constructions. As such, a 1 000 unique parameter sets could be constructed per model for this sampling method.

Once all parameter sets were generated for both sampling methods, each parameter set was used to solve for the steady state solutions of all variables. As such, 10 000 steady states were obtained for each variable in each model for the MC sampling method. This was then used to determine a distribution of steady states achieved by all parameter sets, and results are visualized with box-and-whisker plots in Chapter 7, to be used as an indicator of model robustness. The same method was applied to the parameter sets obtained by LHS.

Stellenbosch University https://scholar.sun.ac.za

3.4. Global Sensitivity Analysis

The global sensitivity analysis method employed in this thesis is the MCA analysis. The parameter sets achieved in MC and LHS provided the parameter space and at every point, MCA was used to determine the response coefficients of each variable for each parameter. The same method employed for local sensitivity analysis was therefore used on each parameter set. The obtained response coefficients for each parameter was used to construct a histogram to show the distribution of possible responses. The histograms were compared with the local sensitivity analysis response coefficients denoted as the wild type responses. The results are presented in Chapter 8.

Stellenbosch University https://scholar.sun.ac.za

Chapter 4

Model Descriptions

The comparable models that could be reproduced are described in this chapter. The reproduced model outputs obtained using Wolfram Mathematica v.11.3 are presented in Appendix A, following parameter descriptions and values used in their simulations. Many models on the within-host dynamics of malaria infection are built on the original model from Anderson *et al*. [10]. Four publications are included in this study. As some of the publications includes multiple sub-models, only the most relevant sub-models are shown and described to stipulate the differences between the individual sub-models of each publication. However, for this study our interest lies in analyzing the dynamics of models where the immune response is included, and will thus be the focus of subsequent chapters.

4.1. Anderson *et al.* [10]

The first model that is included in the investigation can be seen as the starting point of most within-host models of malaria infection, as it is one of the first of such models proposed, upon which many others were based. Anderson *et al.* [10] constructed a within-host model focusing on the erythrocytic cycle of malaria infection, including the immunological response to free roaming merozoites and iRBCs. In the absence of an immune response the model ODEs are as follows:

$$\frac{dx}{dt} = \lambda - \mu x - \beta xs \qquad 4.1.1$$

$$\frac{dy}{dt} = \beta xs - \alpha y \qquad 4.1.2$$

$$\frac{ds}{dt} = \alpha r y - ds - \beta xs \qquad 4.1.3$$

Stellenbosch University https://scholar.sun.ac.za

For this model, the variables x, y and s represent the densities of healthy RBCs, iRBCs and free roaming merozoites within the blood plasma, respectively. The ODEs above show how the different parameters and terms incorporated in each equation can influence each variable. For variable x (eq. 4.1.1), the rate of RBC recruitment from bone marrow (λ), increases the number of uninfected RBCs. The parameter μ describes the natural death rate of RBCs, and is dependent on the population of current RBCs (μx). βxs is a transfer term present for all three variables, where β denotes the probability of a merozoite infecting a healthy RBC. Thus, this term is dependent on, and influences, the population densities of merozoites (s), as well as available RBCs (x). As the term depicts the decrease of healthy RBC and free roaming merozoites as the healthy erythrocytes are infected, iRBC will be increased. This can be seen in the ODEs presented above as the term βxs is only positive in equation 4.1.2 representing the iRBC population. The death rate of iRBCs is represented by the term αy, which leads to a decrease in the density of iRBCs. However, as a bursting iRBC releases a number of merozoites r, a positive term appears for variable s as the free roaming merozoites will increase within the blood. Lastly, merozoites need to infect RBCs to survive and failure to do so will result in their death, represented by ds [10].

This model shows a simplistic form of three different cell densities important for studying malaria infection, but does not yet include the immune response to infection. It should be noted that this model was the first to be constructed on the within-host dynamics of malarial infection and was constricted at the time (1989) with a lack of information regarding the actual dynamics and involvement of the immune system [10]. The inclusion of the immune system response, as well as the parameter values used, has therefore served as a basis for further development of models. Upon inclusion of the immune system response, the authors first derived an ODE describing the immune attack on only the free roaming merozoites. Thereafter, another variable T was added, denoting the density of the antigen-specific T-lymphocytes directed at the free merozoites. This is indicative of a humoral immune response. This variable consequently also affects the variable s for merozoite density in the blood:

$$\frac{ds}{dt} = \alpha r y - ds - \beta s x - hsT \qquad 4.1.4$$

$$\frac{dT}{dt} = \gamma sT - aT \qquad 4.1.5$$

Stellenbosch University https://scholar.sun.ac.za

A new term hsT is inserted for the variable s, representing the net rate of T-lymphocytes induced death of merozoites, dependent on the antigen-specific T cell population and the merozoite density itself. The T-lymphocytes proliferate at a rate γsT proportional to the densities of both variables representing the stimulation of the immune system. To conclude the addition of the T lymphocyte equation, another term is added for the natural decay rate of T-lymphocyte, aT.

Further development of the system of ODEs to include immune response to the infection sees the alteration of the model to include cell-mediated immune response to infection. This indicates that the T-lymphocytes would then affect the number of iRBCs, y, as presented in eq. 4.1.6, showing immune attack on both disease variables, s and y. As such, another term (kyT) needs to be added to the ODE depicting T-lymphocyte density, as the differentiation of T-lymphocytes will additionally be dependent on the density of iRBCs present in the blood. As with γ, k indicates the proliferation rate of T-lymphocytes due to iRBC presence.

$$\frac{dy}{dt} = \beta xs - \alpha y - gyT \qquad 4.1.6$$

$$\frac{dT}{dt} = \gamma sT + kyT - aT \qquad 4.1.7$$

From theory, the adaptive immune response is split into two groups based on the cells used to fight the disease. The humoral component of the immune response consists of B-lymphocytes that secrete antibodies to attack free-roaming pathogens within the blood, whereas the cell-mediated component attacks infected cells within a host. The immune response incorporated in this model description therefore includes both components of the adaptive immune response, while excluding the innate immune response. As the humoral immune response is the adaptive response to free roaming merozoites within the blood, antibodies should technically be incorporated instead of T-lymphocytes to indicate the attack against merozoites. However, the model describes both types of adaptive immunity as T-lymphocytes, which could consequently rather be seen as a group of immune effectors that include both antibodies and T-lymphocytes. Although there is then only one variable to describe these T-lymphocytes, the attack is split between the ODEs themselves.

From these equations the authors constructed four different models that will be denoted as sub-models 1A-1D. Every model presented depicts different dynamics of the malaria infection and the immune

Stellenbosch University https://scholar.sun.ac.za

response thereto, by including different components or combination of components of the model. The first sub-model (1A) shows the dynamics of the different variables without an immune response and incorporates eq. 4.1.1 to 4.1.3. The second sub-model (1B) includes an antibody attack by the humoral part of the adaptive immune system, thus affecting the free roaming merozoites while excluding an attack on the iRBCs, and is represented by eq. 4.1.1, 4.1.2, 4.1.4 and 4.1.5. The third sub-model (1C) includes a cell-mediated attack on iRBC, therefore encompassing eq. 4.1.1, 4.1.2, 4.1.6 and 4.1.7; however, it excludes the attack on merozoites. As eq. 4.1.6 and 4.1.7 include parameters for antibody attack, these parameters were set to zero to incorporate this exclusion in analysis. The last sub-model (1D) includes both forms of attack and uses the same equations as the third model, but with all parameters larger than zero. The parameters used and model outcomes are indicated in Appendix A.

4.2. Li *et al.* [13]

Li *et al.* [13] showcases a same form of model as Anderson *et al.* [10] with four different ODEs for variables H (RBCs), I (iRBCs), M (Merozoites) and E (Immunity effectors). Here "immune effectors" denotes all biological immune effectors as one class and does not distinguish between innate and adaptive immunity.

$$\frac{dH}{dt} = \lambda - d_1 H - \alpha HM \qquad 4.2.1$$

$$\frac{dI}{dt} = \alpha HM - \delta I - \frac{p_1 IE}{1+\beta I} \qquad 4.2.2$$

$$\frac{dM}{dt} = \mathrm{rI} - \mu M - \frac{p_2 ME}{1+\gamma M} \qquad 4.2.3$$

$$\frac{dE}{dt} = -d_2 E + \frac{k_1 IE}{1+\beta I} + \frac{k_2 ME}{1+\gamma M} \qquad 4.2.4$$

As there is significant overlap of the processes encapsulated in this model with those in the model of Anderson *et al.* [10], only new aspects will be discussed. This model is extended from the Anderson *et al.* [10] model, as the authors included non-linear bounded Michaelis-Menten-Monod functions within their ODEs. These functions are visible as fractions in the different equations above and are included to account for saturation of the processes, as the number of infections (iRBCs and merozoites) that can be

Stellenbosch University https://scholar.sun.ac.za

eliminated by the immune effectors will plateau at some point, since this process is dependent on the efficiency of e.g. immune effectors and binding to merozoites. The first process of this kind is the removal of the iRBCs (I) by immune effectors E, represented by $p_1IE/(1+\beta I)$ in equation 4.2.2. In this term p_1 is a rate constant for the rate at which immune effectors can remove iRBCs, and $1/\beta$ is viewed as a half-saturation constant for iRBCs, as immune cells can only eliminate iRBCs if these two cell groups "bind". The same explanation can be given for the term $p_2ME/(1-\gamma M)$, where p_2 is the rate at which the immune effectors can remove the merozoites in the blood plasma, while $1/\gamma$ depicts a half-saturation constant. k_1 and k_2 are both parameters describing the proliferation rate of lymphocytes due to activation by iRBCs and merozoites, respectively, shown in the last ODE (eq. 4.2.4) of this model. Even though this publication views the immune effectors as a single variable E, the immune response is split into two components within the relevant equation 4.2.4. In equation 4.2.4, the second term (first component) shows the proliferation of the immune cells due to the activation by iRBCs and the third term (second component) shows activation by merozoites. The merozoites and iRBCs thus activate and are removed by the humoral immune effectors (rate constants p_2 and k_2) and cell-mediated immune effectors (rate constants p_1 and k_1), respectively. These processes of activation of immune effectors are saturable, meaning activation will not continue indefinitely as it is dependent on the population of the disease variables and immune effector concentration, their binding and efficiency of the process.

The authors created six different outputs from this model by changing the relevant parameter values to describe different disease responses. Four of these will be included here for analyses. The first sub-model (2A) is one with a malaria free equilibrium. The second sub-model (2B) represents malaria infection without a specific immune response, where a host lacks the defense against infection. Sub-model 2C includes a specific immune response against infection, and sub-model 2D is for an endemic state of malaria infection. These scenarios were simulated by changing parameter values as explained in Appendix A.

4.3. Niger *et al.* [15]

Niger *et al.* [15] extended on some basic existing models such as Anderson *et al.* [10] and Li *et al.* [13] to contain age compartments of the intracellular parasite stage (iRBCs), showing how the parasite matures within the infected erythrocyte. The stage of parasite maturation is indicated as compartments, where the parasites "move" from one age compartment to the next (Y_n). The term moving is used

Stellenbosch University https://scholar.sun.ac.za

artificially to model the aging of the iRBCs. Different compartments can thus designate the merozoite development as it matures from an immature trophozoites to a schizont that can release new merozoites. The compartments following the first compartment obey the same form of the differential equation; however, as noted in Appendix A differences between the growth and death rates of the parasites in each compartment are used. Niger *et al.* [15] also proposed a more biologically realistic model, as this model splits the immune effector cells into two groups, immune cells B and antibodies A. The model with healthy RBCs (X) and merozoites (M) follows:

$$\frac{dX}{dt} = \lambda_X - \beta XM - \mu_X X \qquad 4.3.1$$

$$\frac{dY_1}{dt} = \beta XM - \mu_1 Y_1 - \gamma_1 Y_1 - k_1 B Y_1 \qquad 4.3.2$$

$$\frac{dY_2}{dt} = \gamma_1 Y_1 - \mu_2 Y_2 - \gamma_2 Y_2 - k_2 B Y_2 \qquad 4.3.3$$

……

$$\frac{dY_n}{dt} = \gamma_{n-1} Y_{n-1} - \mu_n Y_n - \gamma_n Y_n - k_n B Y_n \qquad 4.3.3$$

$$\frac{dM}{dt} = r(\mu_n + \gamma_n) Y_n - \mu_M M - k_M BM - \mu\beta XM \qquad 4.3.4$$

$$\frac{dB}{dt} = \lambda_B + B(\rho_1 Y_1 + \rho_2 Y_2 + \cdots + \rho_n Y_n + \rho_{n+1} M) - \mu_B B \qquad 4.3.5$$

$$\frac{dA}{dt} = \eta BM - \mu_A A \qquad 4.3.6$$

This model corresponds with the Anderson *et al.* [10] and Li *et al.* [16] models in various ways when it comes to healthy RBCs and different birth and death rates of the variables, and as such only the immune system components, as well as the iRBCs and its age-related compartments, will be discussed. In the first stage Y_1, eq. 4.3.2 shows infection of healthy RBCs dependent on the infection rate constant β and the populations of both the merozoites (M), and healthy RBCs (X). The natural death rate μY_1 of iRBCs and the progression to the next age compartment of iRBC, are both responsible for a decrease in variable Y in each respective compartment. The immune system now additionally kills iRBCs, where k_i is the immuno-sensitivity of the stage i parasite iRBCs to immune effectors B. For the next compartment Y_2 the term βXM no longer appears (which is the rate of infection of healthy RBC). The first term is hence

Stellenbosch University https://scholar.sun.ac.za

replaced with $\gamma_1 Y_1$ to show an increase in Y_2 as cells "enter" the next stage of aging. In this publication Y_n encompass five stages with differences in parameters shown in Appendix A. The immune effectors are denoted by variable B as immune cells including the innate immune effectors, T- and B-lymphoctes, and variable A denoting antibodies specific to free merozoites. This is an important distinction in the immune effectors as innate immune cells are naturally always present, whereas antibodies are formed during the acquired immunity response. For the immune cells B we thus have a natural production of cells, λ_B, as well as a stimulation of production rate due to the presence of an infection (at rate $\rho_i Y_i$) in all infected compartments including free merozoites. For antibodies in the human body, there is no natural production but rather an increase of antibodies at a rate ηBM, dependent on populations of immune cells and merozoites.

Using these equations (eq. 4.3.1 to 4.3.6), two sub-models were published, by varying the parameter values to achieve different disease states. One sub-model (3A) shows a disease-free state, and the other (3B) shows a stable parasite-present steady state.

4.4. Okrinya [16]

The last model is a model contained within the doctoral thesis of Okrinya [16] and is added for analysis due to the incorporation of an extra variable G, denoting the population of *Plasmodium* gametocytes within the blood. This model can thus be viewed as another extension of the previous models. The model itself was published as both a dimensionalised and non-dimensionalised form. The model outputs were achieved using the non-dimensionalised form to overcome the various different time scales for the parameters used in the model system. For numerical comparison to other models, the dimensionalised form of this model is presented here. The model with healthy RBCs (X), iRBCs (Y), merozoites (M), innate immune cells (P) and antibodies (A), follows.

Stellenbosch University https://scholar.sun.ac.za

$$\frac{dX}{dt} = \lambda_X - \frac{\beta_x XM}{1+c_0 A} - \mu_X X \quad 4.4.1$$

$$\frac{dY}{dt} = \frac{\beta_x XM}{1+c_0 A} - (\mu_y + \mu_n)Y - k_y PY(1 + k_a A) \quad 4.4.2$$

$$\frac{dM}{dt} = \frac{r\mu_y(1-\theta)Y}{1+c_1 A} - \frac{\beta_x XM}{1+c_0 A} - \mu_m M - k_m PM(1 + k_b A) \quad 4.4.3$$

$$\frac{dG}{dt} = \frac{r\mu_y \theta Y}{1+c_1 A} - \mu_g G - k_g PG(1 + k_c A) \quad 4.4.4$$

$$\frac{dP}{dt} = b_m + \eta_1(Y + \phi M) - \mu_p P - P(k_d Y + k_n M) \quad 4.4.5$$

$$\frac{dA}{dt} = \eta_2\{Y(t - d_1) + g_2 M(t - d_1)\} - \mu_a(A_0 - A) - A(\eta_3 Y + \eta_4 M) \quad 4.4.6$$

To verify the model outputs from our reproduction of the model, the non-dimensionalised and dimensionalised outputs are presented in Appendix A to illustrate the differences. The sensitivity analysis will only be shown for the dimensionalised model.

This model differs from previous models not only due to its added variable G, but also due to having split the immune effectors differently. The first immune effector variable P reflects the innate immune cells and represents cells such as dendritic cells and macrophages. The second effector variable A depicts the population of adaptive immune cells and include cells like B and T cells, as well as antibodies. This shows that the immune effectors are split differently in this model compared to the Niger *et al.* [15] model, and will thus lead to different outputs in the following analyses. Comparison to the ODEs of the Niger *et al.* [15] model, also shows the difference in processes. For example, terms that include $1/(1 + c_1 A)$ indicate the efficiency of antibodies blocking the infection. The term $k_m PM(1 + k_3 A)$ depicts the successful removal of merozoites by the immune system, dependent on the innate immune cell as well as the merozoite concentration. Similar terms can be explained in the same manner when looking at parameter definitions as shown in Appendix A. An additional parameter θ in the ODEs for M and G (eq. 4.4.3 and 4.4.4) represents the fraction of merozoites that will not enter the erythrocytic cycle again, as they will develop into gametocytes. For the innate immune cell concentration, a natural birth rate as well as a stimulation rate is observed due to the presence of infection (η_1), whereas antibodies and other adaptive immune effectors are only produced due to the presence of iRBCs and merozoites. Note, however, that a time lag $(t - d_1)$ is incorporated in the equation, as there is a delay between when infection starts and when adaptive immune cells are produced.

Stellenbosch University https://scholar.sun.ac.za

Only one model output has been published for this specific model (4A) showing pathogenesis in the human host when the immune system fights the infection.

All of the publications included for analysis therefore differ in their model structure as well as their incorporations of the immune system. The Anderson *et al.* [10] and Li *et al.* [13] models use one variable to designate the immune effectors, with the Anderson *et al.* [10] model denoting this variable as T-lymphocytes while Li *et al*. [13] denotes them as an immune effector group. Both of these models do not include the innate immune response, but have split the adaptive immune response into humoral and cell-mediated immunity. The Niger *et al.* [15] and Okrinya [16] models both split the immune effectors into two variables and include the innate and adaptive immune response towards the infection. However, whereas the Niger *et al.* [15] model has split it into two variables describing all immune cells and antibodies, the Okrinya [16] model has split them into innate immune cells and all adaptive immune cells. The different divisions of the immune system would thus lead to different analysis results.

4.5. R_0 equations for models

The reproductive number (R_0) equation in a model is an indication of whether the disease will persist and is composed of a number of parameters related to the progression and death of an infection. The reproductive number can be derived using the next generation method as described by Diekman *et al.* [74]. The method involves the formation of a transmission (F) and transition (V) matrix, with the first matrix describing the production of new infections, while the second describes changes in model state. The product of the negative transmission matrix ($-F$) with the inverted transition matrix (V^{-1}) yields the next generation matrix (NGM). R_0 is equal to the dominant eigenvalue of the NGM.

The R_0 equations normally consists of parameters that would increase the infection as the numerator and parameters that would decrease the infection as the denominator. An R_0 value ≥ 1 reflects an endemic disease state, while a $R_0 < 1$ reflects a disease-free state. This would thus show that a value of 1 or above would mean disease activating parameters are greater than disease clearing parameters, whereas a lower than 1 value would show the opposite. Note that R_0 is defined relative to the disease-free system and is therefore not a direct indication of disease progression with subsequent rounds of parasite replication and the effect of immune activation. Li *et al.* [13], Niger *et al.* [15], and Okrinya [16] published their own R_0 equations (presented below), derived using the NGM. However, the R_0 equation for the Okrinya [16]

Stellenbosch University https://scholar.sun.ac.za

model was derived for the non-dimensionalised model, and we therefore converted it for the dimensionalised model as used in this project. Anderson *et al.* [10] does not incorporate a R_0 equation, but rather a ratio describing whether the disease will persist. This ratio was transformed to a R_0 equation for this project. As the ratio included disease increasing variables to decreasing variables as seen with the R_0 equation, the disease increasing variables were used as a numerator and the others as the denominator. The R_0 equations for all analyzed models are:

$$R_0 = \frac{(r-1)\beta\lambda}{d\left[\mu+\left(\frac{\beta a}{\gamma}\right)\right]} \qquad 4.5.1$$

$$R_0 = \frac{r\alpha\lambda}{d_1\mu\delta} \qquad 4.5.2$$

$$R_0 = \frac{\beta r\gamma_1\cdots\gamma_{n-1}(\gamma_n+\mu_n)\left(\frac{\lambda_x}{\mu_x}\right)}{\left[\mu_M+k_M\left(\frac{\lambda_B}{\mu_B}\right)+\mathrm{u}\beta\left(\frac{\lambda_x}{\mu_x}\right)\right]\left[\left(\mu_1+\gamma_1+k_1\left(\frac{\lambda_B}{\mu_B}\right)\right)\cdots\left(\mu_n+\gamma_n+k_n\left(\frac{\lambda_B}{\mu_B}\right)\right)\right]} \qquad 4.5.3$$

$$R_0 = \frac{\frac{\beta_x\lambda_x}{\mu_x\mu_y}r(1-\Theta)}{\left(1+\frac{\mu_n}{\mu_y}+\frac{k_y b_m}{\mu_p\mu_y}\right)\left(\frac{\beta_x\lambda_x}{\mu_x\mu_y}+\frac{\mu_m}{\mu_y}+\frac{k_m b_m}{\mu_p\mu_y}\right)} \qquad 4.5.4$$

From these equations it can be inferred which parameters have a large influence on the persistence or disease state. The R_0 value is an indicator of whether the disease will evolve or clear at the start of infection. It is noticeable that some equations include parameters of the immune system e.g. eq. 4.5.3 includes the natural birth rate of innate immune cells (λ_B), whereas other do not). This is due to the fact that parameters of the immune response can only be added if they exist at the start of infection, like the innate immune cells that have a natural birth rate and are always present, and thus not dependent on activation due to infection.

All of the models that were analyzed in this thesis and the differences between them have now been described. The Anderson *et al.* [10] model is the most primitive model whereon most within-host models have been built. The Li *et al.* [13] model is akin to that of the Anderson *et al.* [10] model with more reliably estimated parameter values. The Niger *et al.* [15] model incorporates compartmentalization of the iRBC population and has split the immune effectors into two groups as immune cells and antibodies. The Okrinya thesis model is the most extended model which further incorporates a variable for the gametocyte population in an infected individual. Models described in this chapter will be analyzed in chapters to follow.

Stellenbosch University https://scholar.sun.ac.za

Chapter 5

Local Sensitivity analyses

Local sensitivity analysis was performed on all the models described in Chapter 4 by attaining response coefficients of the variables of each model for each of its parameters, using Metabolic Control Analysis (MCA). This analysis involves the perturbation of each parameter, one-at-a-time (OAT), to quantify the possible effects it would elicit on all of the model variables. This method was used for all parameters in each sub-model described in Chapter 4. The response coefficient values thus indicate the percentage change that a 1% change in a parameter value has on the steady state of a variable and is an indication of the importance of each parameter to the stability of the whole model system at its wild type steady state. For this analysis, the absolute steady state value of each variable is not of importance, but only the effect that changes in the parameters elicit on these steady states. The results are shown in the following tables and will be followed by a comparative conclusion at the end of this chapter. Take note that response coefficient values within sub-models of a model are comparable to each other. However, care should be taken when comparing response coefficient values obtained from different sources, such as Anderson *et al.* [10] and Li *et al.* [13], as differences exist in model structure and parameter definitions. It might be more instructive to compare such models when inspecting the theory of each model, and rather focusing on comparing which parameters showed the largest response coefficients, than focusing on the absolute values of these coefficients.

Furthermore, parameters with a high response coefficient for variables such as the disease variables describing merozoite and iRBC concentration or the immune effectors, can be viewed as plausible drug targets for disease treatment or eradication. For example, a large negative response of one of the disease variables (variables indicative of disease, such as iRBCs and merozoites) on a parameter indicates that an increase in this parameter will lead to a decrease in the disease.

Local sensitivity analysis was additionally performed on the R_0 equations of all the sub-models to determine which parameters are important for the threshold of the reproductive number, as these parameters may offer targets that can lead to parasite clearance.

Stellenbosch University https://scholar.sun.ac.za

5.1. Anderson *et al.* [10]

For the Anderson *et al.* [10] sub-models, the four variables represent the populations of healthy RBC (x), iRBC (y), free roaming merozoites (s) and T-lymphocytes (T). The local sensitivity analysis of the first sub-model (1A - malaria infection and no immune response) is shown in Table 5.1A. Parameter descriptions and values of this model can be found in Appendix A. All response coefficients for this model will be discussed in detail to demonstrate the methods of interpretation, after which the other model discussions will only include significant findings.

Table 5.1A: The response coefficients for the first sub-model (1A) in the Anderson et al. [10] publication describing infection without immune response.

1A-R_p^V	$\boldsymbol{x}[\boldsymbol{t}]$	$\boldsymbol{y}[\boldsymbol{t}]$	$\boldsymbol{s}[\boldsymbol{t}]$	$\boldsymbol{T}[\boldsymbol{t}]$
$\boldsymbol{\lambda}$	0^*	1.666	1.666	-
$\boldsymbol{\mu}$	0	-0.666	-0.666	-
$\boldsymbol{\beta}$	-1	0.666	0.666	-
$\boldsymbol{\alpha}$	0	-1	0	-
$\boldsymbol{r}$	-1.067	0.711	1.777	-
$\boldsymbol{d}$	1	-0.666	-1.666	-

$\boldsymbol{x}[\boldsymbol{t}]$- healthy RBCs; $\boldsymbol{y}[\boldsymbol{t}]$– iRBCs; $\boldsymbol{s}[\boldsymbol{t}]$- free roaming merozoites; $\boldsymbol{T}[\boldsymbol{t}]$- T-lymphocytes; $\boldsymbol{\lambda}$- recruitment of healthy RBCs; $\boldsymbol{\mu}$- natural death rate of RBCs; $\boldsymbol{\beta}$- probability of infection of RBCs with free roaming merozoites; $\boldsymbol{\alpha}$- death rate of iRBCs; $\boldsymbol{r}$- merozoites released per bursting iRBC; $\boldsymbol{d}$- natural death rate of free roaming merozoites; $\mathbf{0}^*$=0 due to rounding.

Table 5.1A shows that the largest response coefficients are observed for the disease variables, y and s. Disease variables are variables indicative of disease, such as merozoite population and iRBCs. These responses are seen where there is a change in parameters λ and μ, where λ indicates an increased birthrate of healthy RBC, therefore increasing the concentration of cells that can be infected y. The increase in iRBCs can then indirectly increase the number of merozoites s produced by the infected cells. μ represents the opposite as it depicts the natural death rate of the healthy RBC and therefore decreases the cells as well as the possible infections that can exist. One would expect to see the larger response coefficient on these two parameters lying directly at the healthy RBCs population (x), as the parameters are incorporated into the ODE for healthy RBCs (eq. 4.1.1); however, analysis indicates that, in fact, a chain reaction occurs, where the steady states of y and s are affected. This indicates that with an increase

Stellenbosch University https://scholar.sun.ac.za

in a variable, such as x, that is directly influenced by a given parameter, akin to λ, the increase of the healthy RBC population would lead to an increase in a linked variable similar to y if there is a density-dependent transfer term such as βxs. As more cells are then infected and transferred from the uninfected cells x to the iRBC state y, a decrease would be seen in x. The increase in x due to its natural birthrate λ, is therefore countered by a decrease due to infection. It is therefore possible that the response coefficient could be almost zero, as the steady state of the healthy RBC concentration will change minimally.

β is present in all variable ODEs and will directly affect all variables. As this parameter is defined as the probability of a merozoite infecting a healthy erythrocyte, and its associated rate is thus dependent on the number of healthy RBCs and free roaming merozoites, an increase in this parameter will lead to a direct decrease of the healthy RBC concentration. As RBCs become infected, the iRBC population increases in turn. The merozoite population should decrease as the parameter is incorporated in the ODE of the merozoite population (eq. 4.1.4)). However, an increase is observed attributed to the increased iRBCs releasing more merozoites as the erythrocytic stage comes to an end and the iRBCs burst. α denotes the death of iRBCs and will influence this population. r represents the amount of merozoites released per bursting iRBC and will consequently influence all three variables of this model. As the amount of merozoites increases, the iRBC will increase as well, leading to a decrease in healthy RBCs. d shows the death rate of merozoites and an increase in d would therefore lead to less merozoites and consequently less iRBC, thus increasing the concentration of healthy RBCs.

For a disease model without immune response it is easy to observe and plausibly deduce some of the possible responses that changes in parameters will elicit in the steady states of the different variables. This is due to the small number of parameters incorporated in the model, as well as the simplicity of the structure and component interactions of the model. A remarkable finding is, however, the small response of x on λ as the response in the absence of infection would clearly be 1 (the steady state of the healthy RBCs would only be dependent on the birth and death rate of these cells). This analysis thus indicates that an increase in the RBC birth and death rates in the presence of an infection without an immune response, have negligible effect on the steady state of the RBC population while dramatically influencing disease variables.

For the second sub-model (1B) from the Anderson *et al.* [10] publication, an immune response directed at free roaming merozoites is included. With an increase in parameters and variable interactions, the biological mechanisms leading to the response coefficients becomes more intricate.

Stellenbosch University https://scholar.sun.ac.za

Table 5.1B: The response coefficients for the second sub-model (1B) in the Anderson et al. [10] publication describing infection with antibody-mediated immunity towards free roaming merozoites.

1B-R_p^V	$x[t]$	$y[t]$	$s[t]$	$T[t]$
λ	1	1	0^*	2.777
μ	-0.625	-0.625	0^*	-1.735
β	-0.375	-0.625	-0^*	1.735
α	0	-1	0	-0^*
r	0	-0^*	-0^*	2.962
d	0	0	0	-1.777
h	0	0^*	0	-1
γ	0.375	-0.625	-1	1.042
a	-0.375	0.625	1	-1.042

***x*[*t*]**- *healthy RBCs;* ***y*[*t*]**- *iRBCs;* ***s*[*t*]**- *free roaming merozoites;* ***T*[*t*]**- *T-lymphocytes;* λ- *recruitment of healthy RBCs;* μ- *natural death rate of RBCs;* β- *probability of infection of RBCs with free roaming merozoites;* α- *death rate of iRBCs;* r- *merozoites released per bursting iRBC;* d- *natural death rate of free roaming merozoites;* h- *rate of antibody-mediated killing of free merozoites;* γ- *proliferation rate of T-lymphocytes due to merozoites;* a- *natural death rate of T-lymphocytes;* 0^* *= 0 due to rounding.*

In Table 5.1B there is little to no response from the parameter changes on the free roaming merozoites s, with responses only from parameters γ, the proliferation rate of T-lymphocytes due to merozoites, and a, the natural death rate of T-lymphocytes. Note that the responses for these parameters with values of -0.625 and 0.625 are slightly smaller for the iRBC population y when compared to the merozoite population s. These parameters are both included in the ODE for the density of T-lymphocytes (eq. 4.1.5), with γ leading to an increase in T-lymphocytes and a leading to a decrease, corresponding respectively to a decrease and increase in merozoites. It is, however, surprising to see no response coefficient for h, the rate of antibody-mediated killing of free merozoites, affecting the merozoite population s, as it is included in a term leading to a direct decrease in the amount of free roaming merozoites hsT (eq. 4.1.5). Instead, we see a response of T with a value of -1, showing that an increase in antibody-mediated killing of the free merozoites would lower the originally obtained steady state of the T-lymphocyte population. This can be ascribed to the fact that the term incorporates both h and T. A 1% increase in the killing rate constant of merozoites (h) leads to an instantaneous decrease in the merozoites. This leads to a decrease in the merozoite-stimulated T-lymphocyte proliferation rate (γsT). The decrease in T-cells then abolishes the effect of the increased leading to no net effect on the free roaming merozoites (s) at steady state. With the added variable T, most of the sensitivity of the model

Stellenbosch University https://scholar.sun.ac.za

lies with the immune response. This is due to infection activating and directly influencing the proliferation of the immune effectors to fight the disease. Even though response coefficients of other parameter-variable pairings are observed, the largest response coefficients are seen for parameters λ and r when regarding variable T. It can thus be inferred that, for a model including immune attack against merozoites only, the largest sensitivity of the model lies with the birth rate of healthy RBC as well as the release of merozoites by a bursting iRBC. As the T-lymphocytes attack only free roaming merozoites in this model, the response coefficient of 2.962 shows that the T-lymphocytes population size will increase with 2.962% if the merozoites released r increases with 1%. For λ, the high response coefficient can be attributed to an increase in healthy RBC, leading to an increase in the amount of iRBCs that will release more merozoites, subsequently increasing the activation of T-lymphocytes. It can consequently be deduced from the analyses that this model shows the availability of healthy RBCs and the amount of free roaming merozoites to be the largest influences on T-lymphocyte activation. Furthermore, the change in steady states of the T-lymphocytes, show to have an effect on the disease variables as well, as the proliferation rate of the T-lymphocytes due to merozoite presence γ and the natural death rate of T-lymphocytes a which directly affect the T-lymphocytes in the variable ODE (eq. 4.1.5), additionally affect the iRBC and the merozoite populations, y and s. Lastly, this analysis indicates the response coefficient for the healthy RBC population x on the birth rate of these cells. has increased to a value of 1 versus a 0 seen with the infection model without an immune response. This can be attributed to the immune response inclusion, ensuring that the merozoite population does not dominate the model system.

In the third sub-model (1C) of the Anderson *et al.* [10] publication the model describes infection with an immune response to only the iRBC, and the distribution of the response coefficients have now shifted in Table 5.1C from the iRBCs y to the merozoites s.

Stellenbosch University https://scholar.sun.ac.za

Table 5.1C: The response coefficients for the third sub-model (1C) in the Anderson et al. [10] publication describing infection with cell-mediated immunity towards iRBC.

1C-R_p^V	$x[t]$	$y[t]$	$s[t]$	$T[t]$
λ	1.034	0	−0.105	2.427
μ	−0.699	0	0.071	−1.640
β	−0.301	-0^*	−0.071	1.640
α	−0.335	0	1.034	0.213
r	−0.335	0	1.034	1.825
d	0.301	0	−0.929	−1.640
a	−0.335	1	1.034	−0.787
g	-0^*	0^*	0^*	−1
k	0.335	−1	−1.034	0.787

x*[*t*]**- *healthy RBCs;* ***y*[*t*]**- *iRBCs;* ***s*[*t*]**- *free roaming merozoites;* ***T*[*t*]**- *T-lymphocytes;* ***λ- *recruitment of healthy RBCs;* ***μ***- *natural death rate of RBCs;* ***β***- *probability of infection of RBCs with free roaming merozoites;* ***α***- *death rate of iRBCs;* ***r***- *merozoites released per bursting iRBC;* ***d***- *natural death rate of free roaming merozoites;* ***h***- *rate of antibody-mediated killing of free merozoites;* ***γ***- *proliferation rate of T-lymphocytes due to merozoites;* ***a***- *natural death rate of T-lymphocytes;* ***g***- *rate of cytotoxic killing of iRBC;* ***k***- *proliferation rate of T-lymphocytes due to iRBCs;* **0*** *= 0 due to rounding.*

In this model the values for h and γ were set to zero, to ensure that the immune response is only directed at the iRBCs, and as such no responses regarding these parameters were retrieved. A shift in the response coefficients can be observed from parameters affecting the attack against merozoites, as shown in the previous model, to parameters describing an attack on iRBC (like g and k). The same trend can be seen as with sub-model B for parameters incorporated in the ODE denoting the density of T-lymphocytes (eq. 4.1.5), where the natural death rate of T-lymphocytes a leads to a decrease in T-lymphocytes and the proliferation rate γ led to an increase due to activation by merozoites. In this sub-model the parameters a and k, with k being an additional parameter responsible for the proliferation of T-lymphocytes due to the presence of iRBCs, is now respectively responsible for the decrease and increase in T-lymphocytes. λ, the natural birth rate of healthy RBCs, still elicits a large effect on T; however, the response of r, the number of merozoites release per bursting iRBC, has lowered due to the immune attack being directed towards the iRBC in this model and therefore not the merozoites. Additionally, as the iRBCs are the focus of this model, the healthy RBCs will also be affected by parameters that affect the iRBC population, as the iRBC population is highly dependent on the availability of healthy RBCs.

From the analysis of sub-model 1B and 1C, we note that the response coefficients mostly lie with the disease variable that is not the target of the immune system, e.g. when the immune system targets iRBCs,

Stellenbosch University https://scholar.sun.ac.za

the most non-zero response coefficients are observed for the merozoite population. This could thus indicate that the immune response tends to keep its target under control, leading to low response coefficient values for that target.

The last model from the Anderson *et al.* [10] publication (1D), is a model including immune response to both the free roaming merozoites as well as the iRBCs by the T-lymphocytes. In Table 5.1D, response coefficients for all parameter on all variables are observed, as the immune response is not directed at only one disease variable.

Table 5.1D: The response coefficients for the fourth sub-model (1D) in the Anderson et al. [10] publication describing infection with both antibody and cell-mediated immunity towards merozoites and iRBC, respectively.

1D-R_p^V	$\boldsymbol{x}[\boldsymbol{t}]$	$\boldsymbol{y}[\boldsymbol{t}]$	$\boldsymbol{s}[\boldsymbol{t}]$	$\boldsymbol{T}[\boldsymbol{t}]$
$\boldsymbol{\lambda}$	1.015	0.055	-0.070	1.925
$\boldsymbol{\mu}$	-0.803	-0.044	0.056	-1.524
$\boldsymbol{\beta}$	-0.197	0.044	-0.056	1.524
$\boldsymbol{\alpha}$	-0.118	-0.443	0.567	0.767
$\boldsymbol{r}$	-0.118	-0.441	0.564	1.923
$\boldsymbol{d}$	0.104	0.388	-0.496	-1.692
$\boldsymbol{h}$	0^*	0.002	-0.002	-0.008
$\boldsymbol{\gamma}$	0.093	-0.434	-0.445	0.176
$\boldsymbol{a}$	-0.212	0.988	1.015	-0.401
$\boldsymbol{g}$	-0^*	-0.002	0.002	-0.992
$\boldsymbol{k}$	0.119	-0.555	-0.569	0.225

x*[*t*]**- *healthy RBCs;* ***y*[*t*]**- *iRBCs;* ***s*[*t*]**- *free roaming merozoites;* ***T*[*t*]**- *T-lymphocytes;* ***λ- *recruitment of healthy RBCs;* ***μ***- *natural death rate of RBCs;* ***β***- *probability of infection of RBCs with free roaming merozoites;* ***α***- *death rate of iRBC;* ***r***- *merozoites released per bursting iRBC;* ***d***- *natural death rate of free roaming merozoites;* ***h***- *rate of antibody-mediated killing of free merozoites;* ***γ***-*proliferation rate of T-lymphocytes due to merozoites;* ***a***- *natural death rate of T-lymphocytes;* ***g***- *rate of cytotoxic killing of iRBC;* ***k***- *proliferation rate of T-lymphocytes due to iRBCs;* **0*** *= 0 due to rounding.*

For this model we see that the response coefficients are quite evenly distributed, complicating deductions as the results are a mixture of the results from sub-models 1B and 1C. There is still a relatively larger response for λ and r on the population of T-lymphocytes, showing that the availability of healthy RBC and free roaming merozoites is still the leading factors for increases in the number of T-lymphocytes. It is also notable that the coefficients of h, representing antibody-mediated death of merozoites due to T-

Stellenbosch University https://scholar.sun.ac.za

lymphocytes, is very small for all variables. This indicates that T-lymphocyte killing of merozoites is not ideal in this model, as an increase in the rate of merozoite killing does not greatly affect the model system. There is a larger coefficient of g on T, where an increase in g signifying an increase in the rate of iRBC killing, would decrease the amount of iRBC, therefore decreasing the need for T-lymphocytes (-0.992). These two effects of the parameters h and g, also demonstrate that the immune system targeting the iRBCs is more ideal, as a decrease in the iRBCs decreases the immune effectors more, showing a more effective immune response. As for the parameters responsible for activating T-lymphocytes due to iRBC and merozoites (γ and k), we see small coefficients, showing that the system is not so sensitive to activation due to infection. Finally, the parameter describing the natural death rate of T-lymphocytes a, is shown to increase the densities of disease variables, which showcases the importance of the presence of T-lymphocytes in controlling the disease.

In all disease sub-models from Anderson *et al.* [10] where the immune system was incorporated, the birthrate of healthy RBCs for infection, the merozoite number released, as well as the death rate of the T-lymphocytes have the largest influence on the disease persistence, and can be possible areas for investigating disease eradication.

5.2. Li *et al.* [13]

The first sub-model (2A) from Li *et al.* [13] is a model with no infection and therefore no immune effectors. In Table 5.2A the only response coefficients present are the responses of λ and d_1, showing that the response of the healthy RBC population is solely dependent on the production and death of healthy RBCs (H).

Table 5.2A:Response coefficients of the first sub-model (2A) of the Li et al. [13] publication for a disease-free model.

2A-R_p^V	$\boldsymbol{H[t]}$	$\boldsymbol{I[t]}$	$\boldsymbol{M[t]}$	$\boldsymbol{E[t]}$
$\boldsymbol{\lambda}$	1	–	–	–
$\boldsymbol{d_1}$	-1	–	–	–

$\boldsymbol{H[t]}$- healthy RBCs; $\boldsymbol{I[t]}$- iRBCs; $\boldsymbol{M[t]}$- merozoites; $\boldsymbol{E[t]}$- immune effectors; $\boldsymbol{\lambda}$- production rate of healthy RBCs: $\boldsymbol{d_1}$- decay rate of RBCs;

Stellenbosch University https://scholar.sun.ac.za

For the second sub-model (2B) malaria infection is present without the immune response and there would therefore be no response coefficients for the immune effectors variable E.

Table 5.2B: Response coefficients of the second sub-model (2B) of the Li et al. [13] publication for a disease infection model without specific immune response.

2B-R_p^V	$\boldsymbol{H[t]}$	$\boldsymbol{I[t]}$	$\boldsymbol{M[t]}$	$\boldsymbol{E[t]}$
$\boldsymbol{\lambda}$	0	9	9	–
$\boldsymbol{d_1}$	0	−8	−8	–
$\boldsymbol{\mu}$	1	−9	−8	–
$\boldsymbol{d_2}$	0	0	0	–
$\boldsymbol{\alpha}$	−1	8	8	–
$\boldsymbol{\delta}$	1	−9	−9	–
$\boldsymbol{r}$	−1	9	8	–

H*[*t*]**- *healthy RBCs;* ***I*[*t*]**- *iRBCs;* ***M*[*t*]**- *merozoites;* ***E*[*t*]**- *immune effectors;* $\boldsymbol{\lambda}$- *production rate of healthy RBCs;* $\boldsymbol{d_1}$- *decay rate of RBCs;* $\boldsymbol{\mu}$- *decay rate of malaria parasites;* $\boldsymbol{d_2}$- *decay rate of immune effectors;* $\boldsymbol{\alpha}$- *infection of RBCs by malaria parasites;* $\boldsymbol{\delta}$- *decay rate of iRBCs;* ***r- *product rate of malaria parasites;* $\mathbf{0}^*$*= 0 due to rounding.*

Sub-model 2B yielded significantly larger response coefficients than the previous results indicated in this chapter. An approach to explain these values can be to analyze these responses in terms of elasticity and control coefficients using the control matrix equation [77, 78]. However, this is beyond the scope of this thesis. The largest response coefficients (Table 5.2B) are for the iRBCs (I) and merozoites (M) in sub-model 2B, which indicates that all parameters can significantly affect the disease variables when no immune response is present. It is also observed that the natural birth rate of healthy RBCs λ shows no effect on the healthy RBC population but rather a carried over effect by increasing the iRBC population, as seen with Anderson *et al.* sub-models [10]. This shows that the availability of healthy RBCs would thus ensure that more cells are available for infection by free roaming merozoites. The response coefficient values of the iRBC and merozoite populations are the same, showing a direct correlation between these two variables. This is attributed to the absence of the transfer term αHM in the merozoite population ODE (eq. 4.2.3), where αHM describes the infection of healthy RBCs by merozoites to become iRBCs. This term is dependent on the availability of healthy RBCs and merozoites. As such, it should decrease the free merozoite concentration when merozoites are transferred into a healthy RBC; however, this decrease is not perceived. Instead the iRBCs concentration is directly dependent on the merozoite concentration, which is not dependent on the loss of merozoites when they infect a RBC.

Stellenbosch University https://scholar.sun.ac.za

The third sub-model 2C includes specific immune response to infection, and thus response coefficients for the immune effectors E is now obtained.

Table 5.2C: Response coefficients of the third sub-model (2C) of the Li et al. [13] publication for an infection model with specific immune response.

2C-R_p^V	$H[t]$	$I[t]$	$M[t]$	$E[t]$
λ	1.002	0.017	−0.020	102.9
d_1	−0.899	−0.015	0.018	−92.37
μ	0.053	0.448	−0.517	−96.93
d_2	−0.252	2.449	2.458	−24.20
α	−0.101	0.015	−0.018	92.37
δ	−0.002	−0.017	0.020	−101.9
r	−0.053	−0.448	0.517	96.97
p_1	-0^*	-0^*	0^*	−0.965
p_2	0^*	0^*	-0^*	−0.035
k_1	0.171	−1.660	−1.666	16.41
k_2	0.081	−0.789	−0.792	7.796
β	−0.116	1.125	1.129	−10.47
γ	−0.033	0.325	0.326	−3.200

$H[t]$- healthy RBCs; $I[t]$- iRBCs; $M[t]$- merozoites; $E[t]$- immune effectors; λ- production rate of healthy RBCs; d_1- decay rate of RBCs; μ- decay rate of malaria parasites; d_2- decay rate of immune effectors; α- infection of RBCs by malaria parasites; δ- decay rate of iRBCs; r- product rate of malaria parasites; p_1- removal rate of iRBCs by immune effectors; p_2- removal rate of malaria parasites by immune effectors; k_1- proliferation rate of immune effectors by iRBCs; k_2- proliferation rate of immune effectors by parasites; β- $1/\beta$ half saturation constant for iRBCs; γ- $1/\gamma$ half saturation constant for malaria parasites, 0^*= 0 due to rounding.

The largest response coefficients yielded for this model are observed for the immune effectors (Table 5.2C). The coefficients for the iRBC and merozoite populations show great similarities for parameters as with the sub-model 2B, demonstrating that there is a large dependency of the iRBCs on the merozoites. It can thus be deduced that the merozoites, and therefore processes that affect the merozoite population in this model, directly infect RBCs, reflecting the chain reaction one would expect from the biological system. The parameters with the largest response coefficients on the immune effectors are μ, α, δ, λ, d_1 and r. Excluding λ and d_1, μ, α, δ and r are all parameters associated with infection, with μ and δ depicting natural decay rates of merozoites and iRBC respectively, therefore decreasing the disease variables as well as the need for immune effectors E. The parameters d_1 and λ are the natural decay and

Stellenbosch University https://scholar.sun.ac.za

birth rates of the healthy RBCs and would respectively decrease and increase the healthy RBC population. An increase in the density of healthy RBCs (λ) would mean an increase in cells that can be infected (I) and consequently impart the necessity for immune effectors (E). An increase in r and α leads to a large response in the immune effectors, implying that the production of merozoites and infection of healthy RBCs by merozoites both increase the immune effectors. From the analysis of this sub-model we can deduce that the most important parameters for immune effector stimulation would be r and α, indicating that the release of merozoites from bursting iRBCs and infection of RBCs by merozoites would be a good investigative focus for disease elimination. Additionally, the availability of healthy RBCs increases the disease as well and can be another target for investigation.

The last sub-model (2D) for the Li *et al.* [13] publication is one showing an endemic state of disease.

Table 5.2D: Response coefficients of the fourth sub-model (2D) of the Li et al. [13] publication for an endemic disease state.

2D - $\boldsymbol{R_p^V}$	$\boldsymbol{H[t]}$	$\boldsymbol{I[t]}$	$\boldsymbol{M[t]}$	$\boldsymbol{E[t]}$
$\boldsymbol{\lambda}$	1.003	0.009	-0.028	87.02
$\boldsymbol{d_1}$	-0.902	-0.008	0.025	-78.25
$\boldsymbol{\mu}$	0.073	0.245	-0.721	-80.29
$\boldsymbol{d_2}$	-0.275	2.716	2.725	-22.02
$\boldsymbol{\alpha}$	-0.098	0.008	-0.025	78.25
$\boldsymbol{\delta}$	-0.003	-0.009	0.027	-86.05
$\boldsymbol{r}$	-0.073	-0.245	0.721	80.32
$\boldsymbol{p_1}$	-0^*	-0^*	0^*	-0.966
$\boldsymbol{p_2}$	0^*	0^*	-0^*	-0.034
$\boldsymbol{k_1}$	0.231	-2.288	-2.296	18.55
$\boldsymbol{k_2}$	0.043	-0.428	-0.429	3.469
$\boldsymbol{\beta}$	-0.156	1.542	1.547	-11.85
$\boldsymbol{\gamma}$	-0.018	0.174	0.175	-1.401

$\boldsymbol{H[t]}$*- healthy RBCs;* $\boldsymbol{I[t]}$*- iRBCs;* $\boldsymbol{M[t]}$*- merozoites;* $\boldsymbol{E[t]}$*- immune effectors;* $\boldsymbol{\lambda}$*- production rate of healthy RBCs;* $\boldsymbol{d_1}$*- decay rate of RBCs;* $\boldsymbol{\mu}$*- decay rate of malaria parasites;* $\boldsymbol{d_2}$*- decay rate of immune effectors;* $\boldsymbol{\alpha}$*- infection of RBCs by malaria parasites;* $\boldsymbol{\delta}$*- decay rate of iRBCs;* $\boldsymbol{r}$*- product rate of malaria parasites;* $\boldsymbol{p_1}$*- removal rate of iRBCs by immune effectors;* $\boldsymbol{p_2}$*- removal rate of malaria parasites by immune effectors;* $\boldsymbol{k_1}$*- proliferation rate of immune effectors by iRBCs;* $\boldsymbol{k_2}$*- proliferation rate of immune effectors by parasites;* $\boldsymbol{\beta}$*-* $1/\beta$ *half saturation constant for iRBCs;* $\boldsymbol{\gamma}$*-* $1/\gamma$ *half saturation constant for malaria parasites;* $\mathbf{0}^*$ *= 0 due to rounding.*

Stellenbosch University https://scholar.sun.ac.za

For this model the system is again shown to be most sensitive in variable E, the immune effectors. The parameters with the largest response coefficients are involved in the populations of merozoites, iRBCs and healthy RBCs, indicating that the availability of RBCs for infection and the number of merozoites and iRBCs all increase the immune effector population. This model therefore suggests, quite logically, that an effective approach to eradicate disease would be to prevent the infection of healthy RBCs and release of merozoites.

5.3. Niger *et al.* [15]

For the Niger *et al.* [15] model two different outputs were obtained, the first (3A) showing a disease-free state. In this publication the immune effectors were split into two groups: immune cells (B) and antibodies (A). Additionally, the iRBCs were split into five age-related compartments, which were unified to form a single variable (Y^*) within the response table.

Table 5.3A: Response coefficients of the first sub-model (3A) of the Niger et al. [15] publication for a disease-free state.

3A-R_p^V	$\boldsymbol{X}[\boldsymbol{t}]$	$\boldsymbol{Y}^*[\boldsymbol{t}]$	$\boldsymbol{M}[\boldsymbol{t}]$	$\boldsymbol{B}[\boldsymbol{t}]$	$\boldsymbol{A}[\boldsymbol{t}]$
$\boldsymbol{\lambda_X}$	1	0	0	0^*	0
$\boldsymbol{\lambda_B}$	0	0	0	1	0
$\boldsymbol{\mu_X}$	-1	0	0	0^*	0
$\boldsymbol{\mu_B}$	0	0	0	-1	0

$\boldsymbol{X}[\boldsymbol{t}]$- *population of healthy RBCs;* $\boldsymbol{Y}[\boldsymbol{t}]$- *population of iRBCs;* $\boldsymbol{Y}^*[\boldsymbol{t}]$- *an added value for all the compartments* $Y_{1\text{-}5}$*;* $\boldsymbol{M}[\boldsymbol{t}]$- *population of merozoites;* $\boldsymbol{B}[\boldsymbol{t}]$- *population of immune cells;* $\boldsymbol{A}[\boldsymbol{t}]$- *population of antibodies;* $\boldsymbol{\lambda_X}$- *production rate of RBCs from bone marrow;* $\boldsymbol{\lambda_B}$- *production rate of immune cells;* $\boldsymbol{\mu_X}$- *natural death rate of RBCs;* $\boldsymbol{\mu_B}$- *death rate of immune;* $\boldsymbol{0}^*$*=0 due to rounding.*

For the results of the first sub-model (Table 5.3A) there is no response for the antibodies as no antibodies will be produced without the presence of a disease. All other response coefficients are zero or negligibly small except for the response of healthy RBC population to λ_X (birth rate of RBCs) and μ_X (death rate of RBCs) as these are the only parameters influencing the model at a disease-free state. Response coefficients are also observed for λ_B and μ_B which, respectively, indicate disease-independent production and death rate of innate immune cells.

Stellenbosch University https://scholar.sun.ac.za

The second sub-model (3B) shows a disease state, and response coefficients for all parameters and variables were therefore obtained.

Table 5.3B: Response coefficients of the second sub-model (3B) of the Niger et al. [15] publication for a disease present state.

3B-R_p^V	$X[t]$	$Y^*[t]$	$M[t]$	$B[t]$	$A[t]$
λ_X	1.052	0.081	-0.854	0.262	-0.592
λ_B	0.034	-0.522	-0.552	0.008	-0.544
μ_X	-0.988	-0.076	0.802	-0.246	0.556
μ_{Yi} $(i=1)$	-0.006	-0.044	0.092	-0.144	-0.053
μ_{Yi} $(i=2)$	0.007	-0.148	-0.111	-0.141	-0.251
μ_{Yi} $(i=3)$	0.007	-0.098	-0.112	-0.141	-0.253
μ_{Yi} $(i=4)$	0.007	-0.069	-0.112	-0.141	-0.254
μ_{Yi} $(i=5)$	-0.003	0.003	0.043	0.054	0.097
μ_M	0.002	-0.011	-0.029	-0.037	-0.066
μ_B	-0.098	1.517	1.605	-0.024	1.580
μ_A	0	0^*	0^*	-0^*	-1
μ	0.023	-0.147	-0.384	0.262	-0.864
β	-0.012	0.076	-0.802	0.246	-0.556
γ_i $(i=1)$	-0.051	0.627	0.843	0.293	1.136
γ_i $(i=2-4)$	-0.015	0.059	0.243	0.302	0.545
γ_i $(i=5)$	-0.004	0.004	0.065	0.081	0.146
k_i $(i=1)$	-0.006	-0.004	0.104	-0.164	-0.060
k_i $(i=2)$	0.008	-0.169	-0.126	-0.161	-0.257
k_i $(i=3)$	0.008	-0.112	-0.127	-0.161	-0.288
k_i $(i=4)$	0.008	-0.078	-0.128	-0.161	-0.289
k_i $(i=5)$	0.007	-0.049	-0.108	-0.135	-0.242
k_M	0.010	-0.064	-0.168	-0.201	-0.377
ρ_1	0.063	-0.982	-1.039	0.016	-1.023
ρ_2	0^*	-0.006	-0.006	0^*	-0.006
ρ_3	0^*	-0.003	-0.004	0^*	-0.003
ρ_4	0^*	-0.002	-0.002	0^*	-0.002
ρ_5	0^*	-0.001	-0.001	0^*	-0.001
ρ_6	0^*	-0.001	-0.001	0^*	-0.001
η	0	0	0	0	1
r	-0.035	0.223	0.581	0.726	1.307

$X[t]$- population of healthy RBCs; $Y[t]$- population of iRBCs; $Y^*[t]$- an added value for all the compartments $Y_{1\text{-}5}$; $M[t]$- population of merozoites; $B[t]$- population of immune cells; $A[t]$- population of antibodies; λ_X- production rate of RBCs from bone marrow; λ_B- production rate of immune cells; μ_X- natural death rate of RBCs; μ_{Yi} $(i=1-5)$- natural death rate of infected cells within different compartments; μ_M- natural death rate of merozoites; μ_B- death rate of immune cells; μ_A- deterioration rate of antibodies; μ- loss of merozoites due to infection of RBCs; β- rate of infection; γ_i $(i=1-5)-$

Stellenbosch University https://scholar.sun.ac.za

progression rate of iRBCs from stage (i) to stage (i+1); $\boldsymbol{k_i}$ $(i = 1 - 5)$*- immunosensitivity of iRBCs in their various compartments;* $\boldsymbol{k_M}$*- immunosensitivity of merozoites;* $\boldsymbol{\rho_i}$ $(i = 1 - 6)$*- immunogenicity of iRBCs and merozoites;* $\boldsymbol{\eta}$*- maximum rate of increase of antibodies;* $\boldsymbol{r}$*- number of merozoites;* $\mathbf{0}^*$*=0 due to rounding.*

In Table 5.3B, μ_B, γ_1 and ρ_1 have the largest relative response coefficients on the antibody population. As the proliferation of antibodies are dependent on the disease variables concentrations, an increase in the death rate of immune cells (μ_B) will increase the concentration of disease variables merozoites (M) and iRBCs (Y), thus indirectly increasing the proliferation of antibodies A (with 1.58%). iRBC density in stage 1 decreases as the infected cells age, thus moving to stage 2 (γ_1). The increase in this disease variable in stage 2 stimulates the immune response to increase. We also note that the immunogenicity of iRBCs and merozoites, ρ_1, does not show great sensitivity to the system in compartments past the first compartment of infection, signifying that iRBCs in stage 1 activate the immune response the most. The same is shown for all parameters that are divided into compartments where the first compartment shows the largest response coefficients. For the disease parameters, the antibody population A and the innate immune cell population B have the largest response on r and γ_1, demonstrating that the release of merozoites and the iRBCs elicits the strongest effect on the immunity variables. It should however be noted that the disease variables stimulate the proliferation of antibodies (eq. 4.3.6), but the antibodies are not included in any other ODEs to fight the disease, and as such have no effect on disease dynamics. r shows the largest effect, indicating that merozoite release should be the focus of investigation into this model as drug targets, as they activate the immune cells the most.

5.4. Okrinya [16]

The Okrinya [16] publication shows only one model output and has the added variable of gametocyte population G. The model shows a disease present state with immune effectors split into two groups; adaptive (including antibodies) A and innate immune cells P.

Stellenbosch University https://scholar.sun.ac.za

Table 5.4A: Response coefficients of the model from the Okrinya [16] publication for a disease present state.

4A-R_p^V	$X[t]$	$Y[t]$	$M[t]$	$G[t]$	$P[t]$	$A[t]$
λ_x	0.358	1.248	0.970	0.976	0.170	1.220
β_x	−0.887	0.394	0.306	0.308	0.054	0.385
μ_x	−0.113	−0.394	−0.306	−0.308	−0.054	−0.385
μ_n	0.058	−0.102	−0.082	−0.080	−0.014	−0.100
μ_y	−0.424	−0.507	0.613	0.576	−0.047	−0.423
r	−0.951	0.417	1.403	1.297	0.081	0.486
μ_m	0.556	−0.244	−0.820	−0.174	−0.047	−0.284
θ	0.006	−0.003	−0.009	0.998	-0^*	−0.003
μ_g	0	0	0	−0.084	0	0
c_0	0.023	−0.010	−0.008	−0.008	−0.001	−0.010
c_1	0.044	−0.019	−0.065	−0.061	−0.004	−0.023
k_a	0.008	−0.015	−0.013	−0.012	−0.002	−0.015
k_b	0.106	−0.046	−0.153	−0.033	−0.009	−0.054
k_c	0^*	0	-0^*	−0.048	0	-0^*
k_y	0.148	−0.260	−0.222	−0.203	−0.036	−0.256
k_m	0.308	−0.135	−0.454	−0.096	−0.026	−0.157
k_g	0	0	-0^*	−0.916	0	-0^*
b_m	0.391	−0.339	−0.580	−1.043	0.805	−0.354
η_1	0.065	−0.056	−0.096	−0.172	0.133	−0.059
η_2	0.181	−0.091	−0.242	−0.161	−0.016	0.900
Φ	0.010	−0.009	−0.015	−0.027	0.021	−0.009
g_2	0.013	−0.006	−0.018	−0.012	−0.001	0.065
k_d	-0^*	0^*	0^*	0^*	-0^*	0^*
k_n	-0^*	0^*	0^*	0^*	-0^*	0^*
η_3	−0.001	0.001	0.001	0.001	0^*	−0.005
η_4	-0^*	0^*	0^*	0^*	0^*	-0^*
μ_p	−0.455	0.395	0.676	1.215	−0.937	0.413
A_0 -	0	0	0	0	0	0
μ_a	−0.180	0.090	0.241	0.160	0.016	−0.893

$X[t]$- population of healthy RBCs; $Y[t]$- population of iRBCs; $M[t]$- population of merozoites; $G[t]$- population of gametocytes; $P[t]$- population of innate immune cells; $A[t]$- population of antibodies; λ_x- rate at which RBCs are recruited; β_x- rate constant for infection rate of RBCs; μ_x- natural per capita death rate of RBCs; μ_n natural death rate of iRBCs; μ_y- conversion rate of iRBCs to merozoites; r- number of merozoites released per bursting schizont; μ_m- death rate of merozoites; θ- fraction of merozoites converting to gametocytes; μ_g- natural per capita death rate of gametocytes; c_0- efficiency of antibodies in blocking merozoite invasion; c_1- efficiency of antibodies in blocking merozoite release; k_a- antibody induced FC-dependent killing rate of iRBCs; k_b- antibody induced FC-dependent killing rate of merozoites; k_c- antibody induced FC-dependent killing rate of gametocytes; k_m- elimination rate of merozoites by innate immune cells; k_g- elimination rate of gametocytes by innate immune cells; b_m- supply rate of immune cells from stem cells; η_1- parasite induced innate immune cell production rate; η_2- parasite induced specific immune cell production rate; Φ- phagocyte growth difference between merozoites and iRBCs; g_2- antibody production difference between merozoites and iRBCs; k_d- deterioration rate of innate immune cells due to iRBC killing; k_n- deterioration rate of innate immune cells due to interaction with merozoites; η_3- deterioration rate of antibodies due to interaction with iRBCs; η_4- deterioration rate of antibodies due to interaction with merozoites; A_0- starting density of antibodies; μ_a- death rate of antibodies; 0^*=0 due to rounding.

Stellenbosch University https://scholar.sun.ac.za

This model is most sensitive to the amount of merozoites being released r, as this leads to the highest relative response coefficient (Table 5.4A) of the disease variables, increasing the merozoites M and gametocytes G. This is possible as merozoites released can either enter another erythrocytic cycle or follow gametocytogenesis. For the immune effectors, the largest coefficient is observed for the adaptive immune cells A on the birth rate of healthy RBCs λ_x. λ_x affects all variables and therefore increase the merozoite and iRBC population as well. This would subsequently lead to an increase in the concentrations of antibodies and other adaptive immune cells. From this table various chain reactions can be deduced for varying parameters on different variables; however, the number of merozoites released per bursting iRBC r and the birth rate of healthy RBCs λ_x seem to be the most important parameters for this parasite present model with λ_x dominating.

5.4. Local sensitivity analysis of R_0

We performed local sensitivity analysis on the respective R_0 equations provided in chapter 4. As the R_0 equation is an indicator of whether a disease will persist, the response coefficient of the R_0 value can demonstrate which parameters are most relevant in disease clearance. This would be observed for the parameters that have the largest negative response coefficients, as increases in these parameters largely decrease the R_0 value the most. The same would hold true for large positive response coefficients, where a decrease in these parameters can lead to a decrease in the R_0 value.

For the Anderson *et al.* [10] sub-model 1D, the largest response coefficients were for parameters r (1.07), λ (1.00) and γ (0.71), whereas the lowest response coefficients were for d (-1.00) and α (-0.71). These results demonstrate that an increase in the release of merozoites from iRBCs (r), the natural birth rate of healthy RBCs (λ) and the proliferation rate of T-lymphocytes due to merozoites (γ) all increase the reproductive number and therefore the probability that the disease will exist and persist. An increase in the natural death rate of iRBCs (α) and merozoites (d) both decrease the disease. All of these parameters are seen with the local sensitivity results of this sub-model as well, indicating the importance of investigating these parameters when using within-host models.

The Li *et al.* [13] sub-model 1D resulted in a linear correlation of all parameters included in the R_0 equation with response coefficients of parameters in the numerator as 1 and in the denominator as -1.

Stellenbosch University https://scholar.sun.ac.za

This is due to all parameters being multipliers within the equation, influencing the reproductive number equally.

Niger *et al.* [15] sub-model 3B indicated the number of merozoites released per bursting iRBC (r) and the natural death rate of immune cells (μ_B) as the parameters increasing disease, with values of 1 and 0.55 respictively. The parameters that would have the largest effect on disease clearance are the death rate of healthy RBCs μ (-0.82) and the natural birth rate of immune cells (λ_B), indicating that less RBCs and more immune cells can clear the parasites within a host.

The largest response coefficients for the Okrinya [16] model are for the release of merozoites from a bursting iRBC r (1), the natural birth rate of healthy RBCs λ_X (0.72) and the infection rate of healthy RBCs with merozoites β_X, whilst the smallest coefficients were for the death rate of healthy RBCs μ_X (-0.72) and the death rate of merozoites (μ_M).

All of the results therefore share r as a parameter that increase the infection the most, as well as the availability of healthy RBCs as an influencer of disease dynamics. These results correspond to the overall results obtained for the local sensitivity analysis on the whole model systems, as parameters that influence the availability of healthy RBCs and the release of merozoites, both influenced the model variables the most.

Stellenbosch University https://scholar.sun.ac.za

5.5. Comparative Discussion

The models differ significantly in model content and parameter values used with each having their advantages and disadvantages. The first group of sub-models by Anderson *et al.* [10] are relatively simplistic models with parameter values estimated and constructed with limited information from literature on the immunological responses of the host to malaria infection. However, for this model we could see how immune responses directed at either iRBC or merozoites can affect the sensitivity of the system to certain parameters as well as how an immune response on both disease variables would shift the response coefficients from one disease variable to another. When the immune response was directed at both disease variables in sub-model 1D, the response coefficients were mostly evenly divided between the merozoite and iRBC populations. However, it was the release of merozoites during the bursting of an iRBC r, and the recruitment of healthy RBCs λ, that elicited the largest response of the population of T-lymphocytes. The relevant parameters for the immune effectors in the Li *et al.* [13] models were shown to be λ, r and α, representing the birth rate of healthy RBCs, the number of merozoites released as well as the infection rate of healthy RBCs by free roaming merozoites, respectively. The Niger *et al.* [15] sub-model 3B is an additional example of the effect changes in r elicits on the model system where r is indicated as the parameter with the largest effect on the immune effectors. In the analysis of the Okrinya model [16], where an extra variable for gametocytes was added, the largest obtained response coefficient was for the birth rate of healthy RBCs on the adaptive immune cell population, where the iRBC and merozoite populations were increased as well. Even though the response coefficient obtained by a change in r was not large for the antibody population, it did show the largest coefficients for merozoite and gametocyte population, therefore increasing the severity of the disease. Both r and λ_x can therefore be targeted in this model. All models thus have r in common as a target, with some models additionally having λ or α. These observations can be supported when looking at the reproductive number expressions for all models, as r and λ are common in all expressions. Furthermore, local sensitivity analysis results on the R_0 equations additionally indicated the number of merozoites released per bursting iRBC as well as the availability of healthy RBCs to increase and decrease disease, respectively. From the local sensitivity analysis of these models it can thus be inferred that the release of merozoites from bursting iRBCs, the infection of RBCs and the birth of healthy RBCs that can get infected, are all possible targets for disease eradication and can be focused on to construct new models for the determination of thresholds values at which the disease can be eliminated.

Stellenbosch University https://scholar.sun.ac.za

Chapter 6

Uncertainty analysis

As biological model parameters are typically determined from experiments performed in technical and biological repeats, or from clinical data collected from a number of subjects, one could see a significant variance in biological parameter distributions. In the deterministic ODE models considered in this project, parameter values are chosen as the mean of these distributions. But variances could lead to significant changes in model outputs, such as RBC concentration and the population of the always-present innate immune cells which could have important consequences for prediction of disease dynamics within a host. Local sensitivity analysis indicated the effect of a small change in a single parameter on a variable. Uncertainty analysis differs from local sensitivity analysis as it determines how variance in a parameter can affect the variables. Results yielded by performing uncertainty analysis will indicate which parameters have the most influence on the uncertainty of the model outputs. Uncertainty analysis is performed by calculating the individual contribution of the variance of each parameter on the total variance of each variable. The uncertainty result for each parameter is then determined as a percentage, using its contribution to the total variance of a variable. As experimentally determined variances were not available for all parameters, we considered a uniform distribution with maximum and minimum determined by a 10% change in the wild type parameter value (i.e. min = 0.9p and max = 1.1p) for each parameter as inputs. The results present the two parameters that have the largest contribution to uncertainty in each variable for every sub-model.

6.1. Anderson *et al.* [10]

The Anderson *et al.* [10] publication includes four sub-models describing, 1A: disease dynamics without an immune response, 1B: disease dynamics with cell-mediated attack on iRBC, 1C: disease dynamics with an antibody attack on merozoites, and 1D: disease dynamics where both immune system responses to infection are included. The two parameters with the largest contribution to output uncertainties regarding every sub-model are presented for each variable in Table 6.1.

Stellenbosch University https://scholar.sun.ac.za

Table 6.1. Uncertainty analysis results of the Anderson et al. [10] sub-models with the two parameters with the highest contribution to uncertainty in model variables. The uncertainty is shown as a percentage contribution of each parameter to total uncertainty in model outputs.

Variables	***Sub-model 1A***		***Sub-model 1B***		***Sub-model 1C***		***Sub-model 1D***	
$\boldsymbol{x[t]}$	r	d, β	λ	μ	λ	μ	λ	μ
	38.3	31.9	55.2	21.5	48.9	22.3	56.6	35.5
$\boldsymbol{y[t]}$	λ	α	λ, α	a, β, γ, μ	a	k	a	k
	49.5	17.8	28.1	11.0	50	50	48.3	15.2
$\boldsymbol{s[t]}$	r	λ, d	a	γ	r, k, α, a	d	a	k
	32.9	28.9	50.0	50.0	20.7	16.7	42.0	13.2
$\boldsymbol{T[t]}$	-	-	r	λ	λ	r	λ	r
	-	-	30.4	26.7	30.1	17.0	22.2	22.1

x*[*t*]**- *healthy RBCs;* ***y*[*t*]**- *iRBCs;* ***s*[*t*]**- *free roaming merozoites;* ***T*[*t*]**- *T-lymphocytes;* ***λ- *recruitment of healthy RBCs;* ***μ***- *natural death rate of RBCs;* ***β***- *probability of infection of RBCs by free roaming merozoites;* ***α***- *death rate of iRBC;* ***r***- *merozoites released per bursting iRBC;* ***d***- *natural death rate of free roaming merozoites;* ***γ***-*proliferation rate of T-lymphocytes due to merozoites;* ***a***- *natural death rate of T-lymphocytes;* ***k***- *proliferation rate of T-lymphocytes due to iRBCs.*

Inspection of the results show that λ, μ, α and r are most often present as parameters contributing the highest percentage of uncertainty in model outputs. In the sub-model with no immune response, the highest uncertainty percentages are obtained for the parameter r for both healthy RBC and merozoite concentrations, indicating that the amount of merozoites released from bursting RBCs in this model is a high contributing factor to the uncertainty of these variable outputs. λ, the recruitment (birth) rate of healthy RBCs, is presented as the largest contributor to uncertainty in the density of iRBC, as uncertainty in this rate may lead to fluctuation in healthy RBC population, which affects the possible number of cells that can be infected to increase the number of iRBCs (variable y). Furthermore, λ and μ are both present in the results for sub-models 1B to 1D for variable x, with λ and r present in all results for variable T. Therefore, variance in the rates that influence the natural birth and death of healthy RBC population are the highest contributing factors to the uncertainty in the healthy RBC population. The birth rate of healthy RBC and the number of merozoites released per bursting iRBC contribute the most to the uncertainty in T-lymphocyte population, since these parameters have been shown to influence the iRBC and merozoite concentration, which in turn activate the immune system. The natural death rate of T-lymphocytes a is seen as an important contributor to uncertainty in variables y and s (iRBCs and merozoites), as uncertainty in this parameter could greatly influence the death rate of T cells and can thus lead to a significant increase (or decrease) in the survival of merozoites and iRBCs.

Stellenbosch University https://scholar.sun.ac.za

6.2. Li *et al.* [13]

The sub-models from the Li *et al*. [13] publication incorporate 2A: a parasite free model, 2B: a parasite present model without an immune response, 2C: a parasite present model with an immune response and 2D: an endemic parasite present model.

Table 6.2. Uncertainty analysis results of the Li et al. [13] sub-models with the two parameters with the highest contribution to uncertainty in model variables. The uncertainty is shown as a percentage contribution of each parameter to total uncertainty in model outputs.

Variables	***Sub-model 2A***		***Sub-model 2B***		***Sub-model 2C***		***Sub-model 2D***	
$\boldsymbol{H[t]}$	λ	d_1	μ, δ	α, r	λ	d_1	λ	d_1
	50.0	50.0	25.0	25.0	51.7	41.6	50.4	40.8
$\boldsymbol{I[t]}$	-	-	λ, δ	α, d_1, μ, r	d_2	k_1	d_2	k_1
	-	-	19.4	15.3	53.8	24.7	48.1	34.1
$\boldsymbol{M[t]}$	-	-	λ, μ, r, δ	α, d_1	d_2	k_1	d_2	k_1
	-	-	17.9	14.3	53.1	24.4	45.4	32.2
$\boldsymbol{E[t]}$	-	-	-	-	λ	δ	λ	δ
	-	-	-	-	18.3	18.0	18.4	18.0

$\boldsymbol{H[t]}$*- healthy RBCs;* $\boldsymbol{I[t]}$*- iRBCs;* $\boldsymbol{M[t]}$*- merozoites;* $\boldsymbol{E[t]}$*- immune effectors;* $\boldsymbol{\lambda}$*- production rate of healthy RBCs;* $\boldsymbol{d_1}$*- decay rate of RBCs;* $\boldsymbol{\mu}$*- decay rate of malaria parasites;* $\boldsymbol{d_2}$*- decay rate of immune effectors;* $\boldsymbol{\alpha}$*- infection of RBCs by malaria parasites;* $\boldsymbol{\delta}$*- decay rate of iRBCs;* $\boldsymbol{r}$*- product rate of malaria parasites;* $\boldsymbol{k_1}$*- proliferation rate of immune effectors by iRBCs.*

The first sub-model excludes infection and as such will not have any model outputs for disease variables iRBCs (I) and merozoites (M), as well as for immune effectors variable (E). As such only the birth rate (λ) and death rate (d_1) of RBCs would influence this model. As these are the only parameters that affect the steady state of the healthy RBC population, the uncertainty percentages are split evenly. It is therefore possible that these parameters do not actually have a high uncertainty, but due to the method of analysis that ensures all uncertainties are a fraction of the total uncertainty in the variable output, the fractions would be split 50/50. The second sub-model excluding the immune response upon infection will not have outputs for the immune effectors E. The results obtained for sub-model 2B indicate that uncertainty lies in parameters that directly influence the iRBC and merozoite densities, such as the decay rate of iRBCs δ. Uncertainty is also observed for parameters that influences the availability of healthy RBCs, like the decay rate of healthy RBCs d_1. Sub-models 2C and 2D present the same parameters as uncertainty parameters when the immune response is included. The healthy RBCs and iRBCs are sensitive to uncertainty in the parameters that influence them directly (i.e. their birth and death rates), and the merozoite concentration shows the same uncertain parameters as indicated for the iRBCs. This indicates

Stellenbosch University https://scholar.sun.ac.za

that the two parameters, d_2 and k_1, respectively representing the decay rate of the immune effectors and the proliferation rate of immune effectors due to iRBC presence, contribute the most to uncertainty in iRBCs as well as merozoites. This demonstrates that the disease variables for this model may vary greatly between individuals due to the immune effector concentration, and the uncertainty around variables that directly affect the concentrations of immune effectors. The results presented for variable E demonstrate that the uncertainty in the production rate of healthy RBCs and the decay rate of iRBC have the largest influence on the uncertainty of the output of variable E. This is due to these parameters presenting a high influence on the iRBC and merozoite concentration, as the increase in healthy RBCs will ensure that more cells can become infected, thereby increasing the amount of iRBC, and the death rate of iRBCs will directly decrease the amount of iRBCs. As sub-model 2C and 2D has been indicated to favor the immune response directed at the iRBCs, it makes sense that parameters influencing these cells will show the most uncertainty towards the output of the immune effectors.

6.3. Niger *et al.* [15]

Niger *et al.* [15] presents two sub-models; 3A: a disease-free model and 3B: a disease present model where the immune response is included.

Table 6.3. Uncertainty analysis results of the Niger et al. [15] sub-models with the two parameters with the highest contribution to uncertainty in model variables. The uncertainty is shown as a percentage contribution of each parameter to total uncertainty in model outputs.

Variables	***Sub-model 3A***		***Sub-model 3B***	
$\boldsymbol{X[t]}$	λ_X	μ_X	λ_X	μ_X
	50.0	50.0	52.6	46.4
$\boldsymbol{Y_t[t]}$	-	-	μ_B	ρ_1
	-	-	55.8	23.4
$\boldsymbol{M[t]}$	-	-	μ_B	ρ_1
	-	-	34.3	14.4
$\boldsymbol{B[t]}$	λ_B	μ_B	r	μ
	50.0	50.0	33.7	14.7
$\boldsymbol{A[t]}$	-	-	μ_B	r
	-	-	20.6	14.1

$\boldsymbol{X[t]}$- population of healthy RBCs; $\boldsymbol{Y_t[t]}$- population of iRBCs as an added value for all Y[t] compartments; $\boldsymbol{M[t]}$- population of merozoites; $\boldsymbol{B[t]}$- population of immune cells; $\boldsymbol{A[t]}$- population of antibodies; $\boldsymbol{\lambda_X}$- production rate of RBCs from bone marrow; $\boldsymbol{\lambda_B}$- production rate of immune cells; $\boldsymbol{\mu_X}$- natural death rate of RBCs; $\boldsymbol{\mu_B}$- death rate of immune cells; $\boldsymbol{\mu}$- loss of merozoites due to infection of RBCs; $\boldsymbol{\rho_i}$ $(i = 1 - 6)$- immunogenicity of iRBCs and merozoites; $\boldsymbol{r}$- number of merozoites;

Stellenbosch University https://scholar.sun.ac.za

The disease-free sub-model 3A shows large uncertainty effects only for parameters directly influencing the respective variables, and the values can again be attributed to the fact that the two parameters indicated in the table for each variable are the only parameters influencing these variables. For the parasite present sub-model 3B, the same results can be seen for healthy RBC population as with the parasite free model. The death rate of immune cells μ_B has the largest contribution to uncertainty in the total iRBC, merozoite and antibody populations. This is due to immune cells activating the proliferation of antibodies. Therefore, with a decrease in immune cells, the iRBC and merozoite populations will increase. As such, uncertainty in this parameter can elicit substantial effects on all of the variables. Uncertainty in r has the largest effect on immune cell concentration, possibly due to merozoites activating the immune system. Lastly, ρ_1 describing the immunogenicity of iRBCs and merozoites additionally contribute to uncertainty in iRBC and merozoite concentration to a lesser extent. The immunogenicity of these cell populations is an indicator of how well they activate the immune response. Uncertainty in this process can therefore affect the possible effectiveness of the immune response to disease presence.

6.4. Okrinya [16]

The Okrinya thesis [16] includes a model describing disease dynamics of malaria infection, where the immune response to infection as well as the gametocyte population as a variable is incorporated in the model.

Stellenbosch University https://scholar.sun.ac.za

Table 6.4. Uncertainty analysis results of the Okrinya [16] model with the two parameters with the highest contribution to uncertainty in model variables. The uncertainty is shown as a percentage contribution of each parameter to total uncertainty in model outputs.

Variables	***Model***	
$\boldsymbol{X[t]}$	r	β_X
	31.3	27.3
$\boldsymbol{Y[t]}$	λ_X	μ_Y
	56.7	50.0
$\boldsymbol{M[t]}$	r	λ_X
	36.7	17.6
$\boldsymbol{G[t]}$	r	μ_P
	21.7	19.1
$\boldsymbol{P[t]}$	μ_P	b_M
	55.2	40.7
$\boldsymbol{A[t]}$	λ_X	η_2
	34.7	18.8

***X*[*t*]**- *population of healthy RBCs;* ***Y*[*t*]**- *population of iRBCs;* ***M*[*t*]**- *population of merozoites;* ***G*[*t*]**- *population of gametocytes;* ***P*[*t*]**- *population of innate immune cells;* ***A*[*t*]**- *population of antibodies;* $\boldsymbol{\lambda_x}$- *rate at which RBCs are recruited;* $\boldsymbol{\beta_x}$- *rate constant for infection rate of RBCs;* $\boldsymbol{\mu_y}$- *conversion rate of iRBCs to merozoites;* $\boldsymbol{r}$- *number of merozoites released per bursting schizont;* $\boldsymbol{b_m}$- *supply rate of immune cells from stem cells;* $\boldsymbol{\eta_2}$- *parasite induced specific immune cell production rate;* $\boldsymbol{\mu_p}$ *– death rate of innate immune cells*

The number of merozoites released per bursting iRBC yields the highest contribution to the uncertainty in X, M and G (healthy RBCs, merozoites and gametocytes). λ_X (birthrate of new RBCs) affects the model uncertainty for iRBCs and antibodies populations, indicating that uncertainty in the populations of these variables can be attributed to the birthrate of healthy RBCs.

6.5. Comparative Discussion

While differences are observed for the respective parameters contributing the most to uncertainty in sub-models of the same general model, specific parameters can be observed to be present as high contributing factors throughout the analyses of all models. This includes parameters that directly influence the amount (and therefore availability) of healthy RBCs, like the birthrate of healthy RBCs, as well as parameters incorporated into the ODEs of the different disease variables (e.g. merozoites, iRBCs and gametocytes), such as the number of merozoites released per bursting iRBC. With the more detailed models, e.g. Niger *et al.* [15] and Okrinya [16], some parameters of the immune system show uncertainty as well.

Stellenbosch University https://scholar.sun.ac.za

Parameters were varied with 10% to obtain uncertainty analysis results. However, most parameters vary more in practice and can therefore have an even larger effect on the model system. The amount of merozoites released was used at a value of $r = 16$ in most models to obtain model outputs. Assuming a 10% variance of this value will hold true, the range of r used for uncertainty estimation would be 14.4 to 17.6. However, the actual range of r can be 8 to 32 [30], showing a significantly larger variance than used in this chapter, indicating that the uncertainty in model outputs due to uncertainty in the parameter r can be even larger.

Furthermore, as stated, most parameters can be hard to determine experimentally and additionally can vary due to various factors. The natural birth rate of healthy RBCs λ has been present over all model results, showing that the uncertainty in this parameter contributes to uncertainty in outputs. The value of λ used differs between models, and can differ significantly experimentally as well as between humans, depending on age, diet, etc. [75]. This also indicates the high variability that the birthrate of healthy RBCs has, leading to more uncertainty in model outputs.

For both parameters, the model outputs can therefore differ largely between individuals and within an individual, as different values for the parameters are possible. Additionally, both parameters play roles in all R_0 equations for the persistence of the disease, substantiating the importance of these variables. Individuals can therefore, theoretically, have all other parameters exactly the same (which is highly unlikely) but differ in their amount of merozoites released per infected RBCs, and one would become disease free (according to the model reproductive number) while the other would have a persistent infection due to their variances in the value of r. It is therefore important to know the uncertainty contributions of different parameters on the variable outputs as these parameters should always be kept in mind when interpreting model outputs and sensitivity analysis results.

Stellenbosch University https://scholar.sun.ac.za

Chapter 7

Robustness analysis

Robustness analysis is a useful tool to investigate the outputs that can be achieved when all inputs of a model are varied simultaneously. With biological models, there is an expected range in which populations of cells can fall as the number of e.g. healthy RBCs differ between individuals as well as within an individual. It is, therefore, possible that all individuals will have varying parameter sets, and thus various steady states of cell populations within their bodies. Robustness analysis can indicate the possible outcomes achieved by a model for individuals or populations. This analysis differs from the previous analysis, as it does not indicate the effect or uncertainty of a single parameter on a variable, but rather demonstrates the achievable ranges of the model outputs if all parameters were allowed to change, thereby yielding various parameter sets.

Two sampling methods were employed for the generation of parameter sets within a 10% up and down perturbation of the reference parameter set, and were used for robustness and global sensitivity analysis (Chapter 8). Monte Carlo (MC) random sampling was used to obtain 10 000 parameter sets and Latin Hypercube Sampling (LHS) was used to obtain 1 000 parameter sets. MC random sampling generates parameter sets by randomly using a parameter value from each parameter where they have been perturbed by 10%. LHS also allows for a perturbation of all parameters, where the parameter values fall in evenly distributed intervals in the 10% range. In every interval a random value of the parameter is chosen once, and parameter sets are generated by randomly combining the values of different parameters. LHS furthermore differs from MC random sampling as a previously used parameter value is excluded in following generation of parameter sets, therefore yielding unique and non-overlapping parameter sets.

All respective models were solved using each parameter set generated in order to determine steady states for every variable. Upon initial analysis some models included negative variable ranges. The results therefore exclude parameter sets that achieve steady states of any variables that are below zero as a negative cell population does not exist and as such only valid steady states are included. The results are presented to show the range of steady states in box-and-whisker plots.

Stellenbosch University https://scholar.sun.ac.za

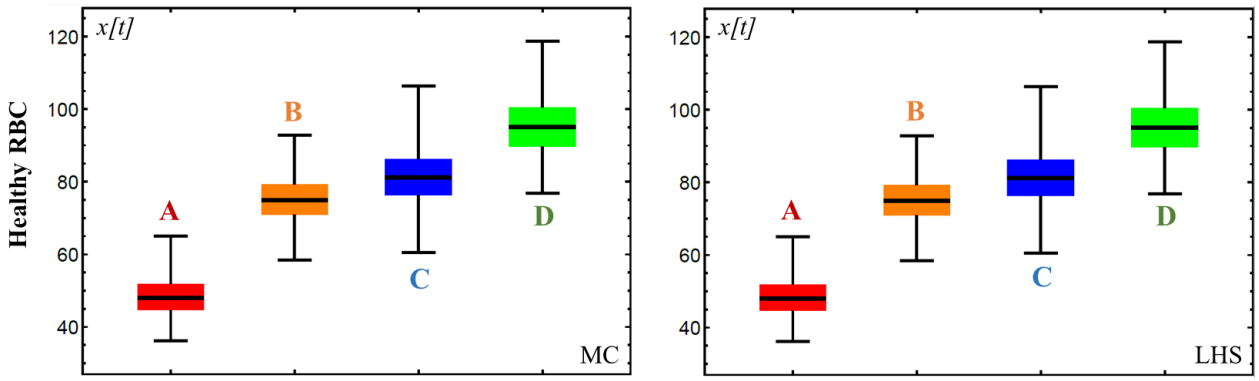

Figure 7.A: Box-and-whisker plots indicating the results obtained through robustness analysis. The results of MC random sampling are presented on the left and LHS results on the right. Four boxes can be seen in each graph, representing each of the sub-models (1A-1D) presented in the Anderson et al. publication [10]. The results present the range in possible steady states obtained for the healthy RBC population (variable x) between sub-models.The y-axis is in arbitrary units as units were not specified for this model. The whiskers of the box-and-whisker plots include outliers in data.

Figure 7A presents the robustness analysis results for a single variable (healthy RBC population) using MC sampling (left) and LHS (right) techniques for sub-models of Anderson *et al.* [10]. Here the high degree of similarity between LHS and MC methods is evident and as such only the robustness analysis of the MC sampling will be discussed further.

In terms of robustness of the model outputs, the different components of the box-and-whisker plot should be investigated. The "box" of the plot presents 50% of the yielded steady states that lie around the median and each "whisker" shows 25% of the steady states achieved above and below the 50% "box". The whiskers include outliers and can therefore be much larger than the box parts as the outliers might stretch the whiskers. Furthermore, it is possible that the data is more distributed at the whiskers and therefore denser within the box of the box-and-whisker plot. This can be observed in Figure 7A, as each whisker is larger than the whole box of the box-and-whisker plots, indicating that 25 % (the whisker) of the data has a larger range and is therefore more distributed, than 50 % (the box) of the data. The robustness of the model outputs will be discussed in terms of the box parts only. The whiskers of the plots can be used as a reference of the extremes of the model outputs. A good robustness result shows that the 50% of steady states achieved (boxes) lie closer to the median and each other within a sub-model. The robustness of each box can thus be described by the relation between the size of the box compared to the median value, where if the box is larger than one order of magnitude of the median, it would indicate poorer robustness results. In all cases we verified that the median correlates closely to the reference steady state.

Stellenbosch University https://scholar.sun.ac.za

7.1. Anderson *et al.* [10]

Robustness analysis results for the Anderson *et al.* [10] sub-models show how the distribution of the steady states obtained change between sub-models describing different malaria disease states and immunological response (Figure 7.1).

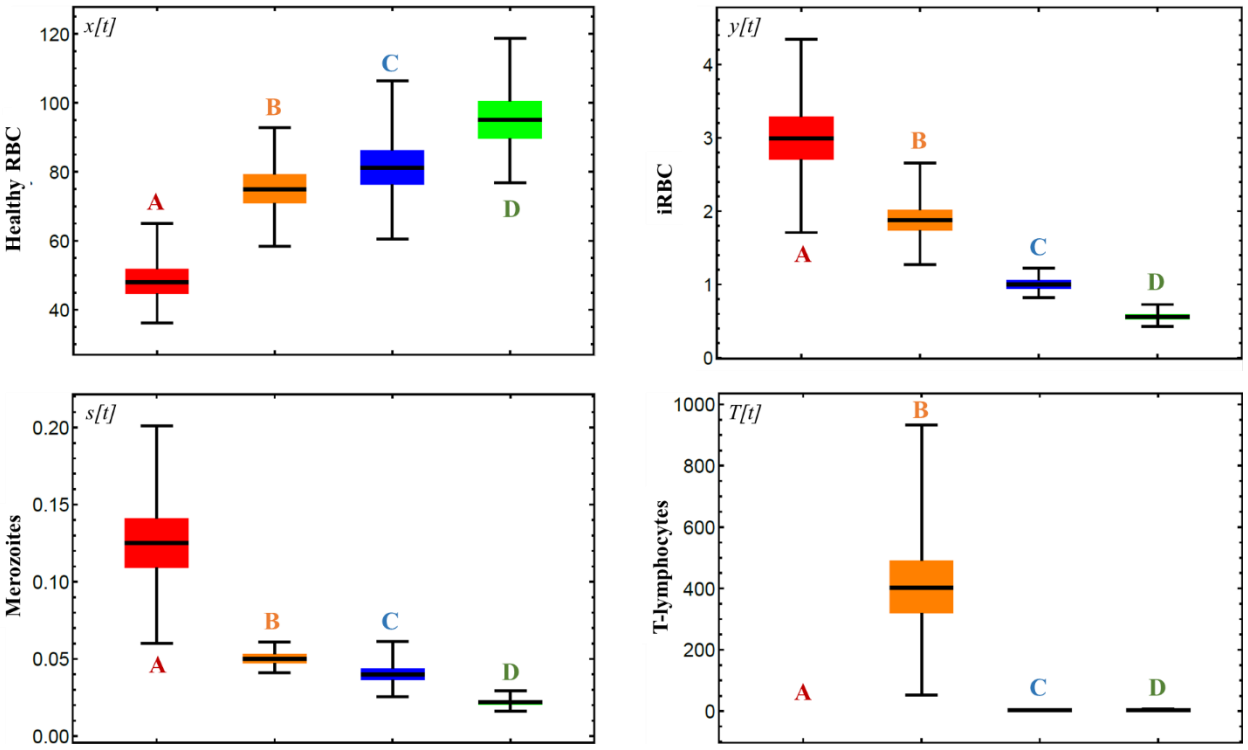

Figure 7.1. The robustness analysis results for the Anderson et al. sub-models A-D [10]. The sub-models are denoted as A: parasite present with no immune response, B: parasite present with antibody mediated attack of T-lymphocytes on merozoites, C: parasite present with cell-mediated immune attack of T-lymphocytes on iRBCs and D: parasite present with both immune attacks incorporated. Four boxes can be seen in each graph, representing each of the sub-models (1A-1D) presented in the Anderson et al. publication [10]. The results present the range in possible steady states obtained. The y-axis is in arbitrary units as units were not specified for this model. The whiskers of the box-and-whisker plots include outliers in data.

All of the individual boxes presented in Figure 7.1 show good robustness in terms of the box size versus the median. The steady state distributions of variable x denoting the healthy RBC population (Figure 7.1 top left), indicates how the steady state distribution moves upwards with each sub-model. For the disease variables y (Figure 7.1 top right) and s (Figure 7.1 bottom left) a downward movement is seen with steady states reaching minimum values in sub-model D. The T-lymphocytes (Figure 7.1 bottom right) demonstrate a large distribution for sub-model B, with low steady states reached for sub-models C and D. The progression from A to D shows how each variable output changes from a model with no immune

Stellenbosch University https://scholar.sun.ac.za

response to one incorporating an immune response on the merozoites and the iRBCs. For no immune response, the healthy RBC population (Figure 7.1 top left) is the lowest. The presence of RBCs is observed to increase with every sub model following the first, as immune responses are added to the model. The steady states yielded for this variable are also lower for an immune attack on iRBCs than for an attack on merozoites. This indicates that, for model D, cell-mediated immune response on the iRBCs is a better response to infection than an antibody-mediated response on merozoites. However, the T-lymphocytes analysis presents higher distributions for antibody-mediated response, dropping to a range of ± 3 for sub-model 1C (Figure 7.1 bottom right). This makes sense if reasoned in terms of the effectiveness if the T-lymphocytes. From previous analysis it has been deduced that the immune response to iRBC proves more effective for disease eradication than when the immune response is directed at the merozoites in this model. It is therefore possible, with an immune response on the merozoites (sub-model B), that this less effective response to disease would lead to the continuous activation of the immune system, as merozoites are not efficiently removed. In contrast, when the immune system is directed at the iRBCs, it effectively fights the disease, therefore omitting the need for more T-lymphocytes. This reasoning is substantiated by the dependence of increase in the population of T-lymphocytes on the variables y (iRBC) and s (merozoites), incorporated in the ODE for T-lymphocyte population (eq. 4.1.7). The full model output thus indicates the combined response to be most effective.

In terms of robustness outputs of these sub-models, the healthy RBC population's boxes (Figure 7.1 top left) increase in size with each sub-model, as more RBCs are present with each addition of the immune system to fight the disease. For the iRBC populations (Figure 7.1 top right), the robustness results are the best where the immune response is directed at iRBCs in sub-model C, whereas for the merozoite population results (Figure 7.1 bottom left) are best at sub-model B where the immune response is directed at the free roaming merozoites. This indicates that the robustness results are dependent on the immune effectors and their targets. As for the T-lymphocyte population (Figure 7.1 bottom right), sub-models C and D show good robustness, whereas sub-model B presents a very larger box, indicating poor robustness.

Stellenbosch University https://scholar.sun.ac.za

7.2. Li *et al.* [13]

The robustness analysis of the Li *et al.* [13] sub-models differs from the Anderson *et al.*[10] sub-models as it additionally presents a sub-model (2A) where there is no disease present, thus showcasing the possible cell concentrations in an uninfected individual. With initial analysis sub-models 2B to 2D obtained invalid steady states as the merozoite, iRBC and immune effector populations included negative results. The parameter sets that yielded theses results were therefore excluded in further analysis. The results for the four sub-models are visualised in Figure 7.2.

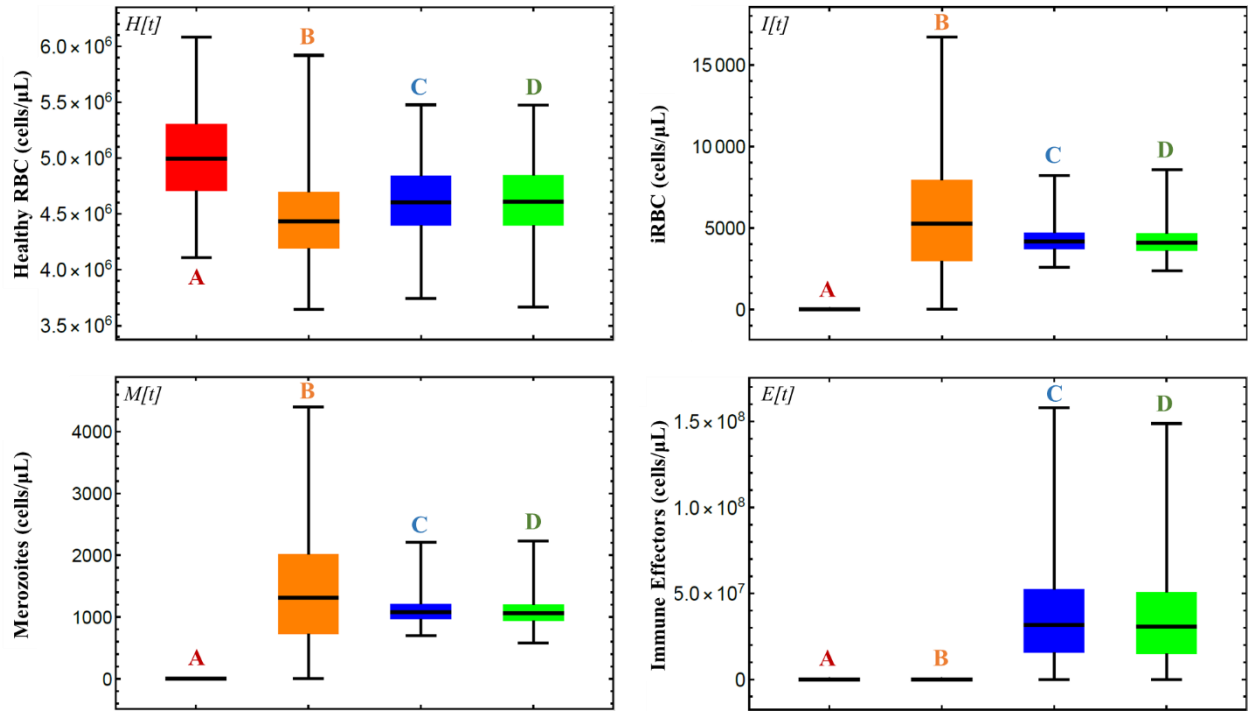

Figure 7. 2. The robustness analysis results for the Li et al. sub-models [13]. The sub-models are denoted as A: parasite free, B: parasite present without an immune response, C: parasite present with an immune response and D: endemic parasite present state. The y-axis indicates the concentration of the different variables in cell/µl. The whiskers of the box-and-whisker plots include outliers in data.

The robustness of each box shown in Figure 7.2 presents good results as none of the box sizes are larger than one order of magnitude of the median. The highest distribution for the healthy RBCs (Figure 7.2 top left) was obtained where there is no infection (sub-model A). For malaria infection without an immune response in sub-model B, the highest distribution was obtained for the iRBCs *I* (Figure 7.2 top right) and merozoites *M* (Figure 7.2 bottom left) as there is no response to infection, therefore additionally yielding the lowest results for healthy RBC population (Figure 7.2 top left). In sub-model C an immune response

Stellenbosch University https://scholar.sun.ac.za

is present, showing a decrease in the merozoite and iRBC concentrations, and an increase in immune effectors. Furthermore, the addition of an immune response increases the amount of healthy RBCs (Figure 7.2 top left), although not to the normal amount observed for the disease free sub-model. The same results are seen for sub-model 2D describing an endemic state of infection. Robustness again increases for disease vaiables (Figure 7.2 top right and bottom left) when the immune system is incorporated into the model, as presented in sub-models C and D.

As previously mentioned, robustness analysis determines the steady states of the different parameter sets, and results exclude parameter sets that can lead to a negative steady state for any of the variables. Prior to this exclusion, the Li *et al.* [13] sub-models C and D, indicated the disease variable (iRBCs and merozoites) reaching steady states of zero, indicating that it would be possible to achieve a disease-free state. However, upon exclusion of immune effector and disease variable steady states below zero, this was not observed. This is a drawback in the model itself as it thus indicates that a negative concentration of immune cells could lead to disease eradication.

7.3. Niger *et al.* [15]

The Niger *et al.* [15] model is composed of two sub-models presenting a disease-free state and a parasite present state incorporating an immune response to infection. As such it is only the healthy RBC concentration and the immune cells concentration that are comparable between the sub-models.

Stellenbosch University https://scholar.sun.ac.za

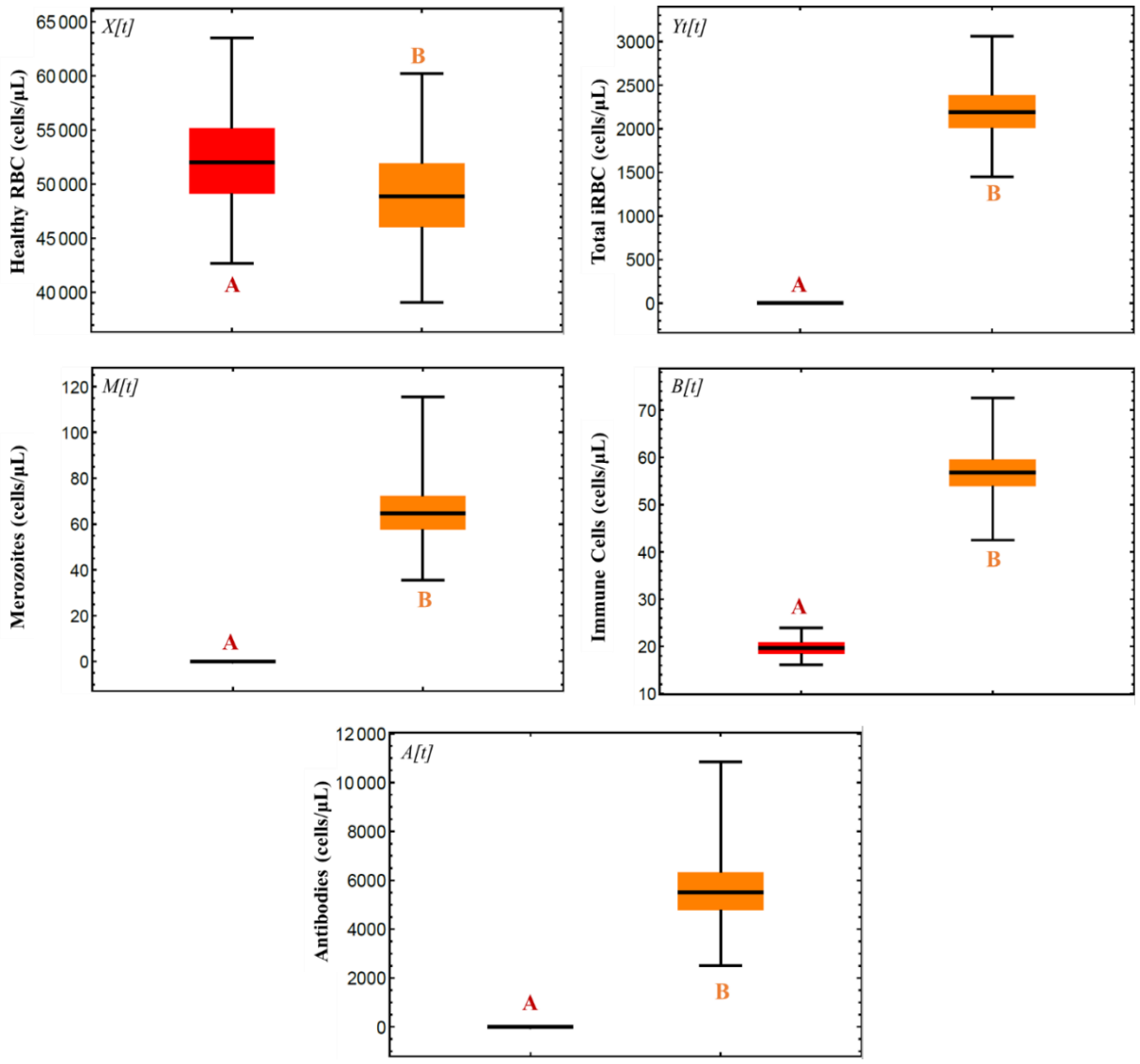

Figure 7.3. The robustness analysis results for the Niger et al. sub-models [15]. The sub-models are denoted as A: parasite free, B: parasite present with an immune response. The y-axis indicates the concentration of the different variables in cell/µl. The whiskers of the box-and-whisker plots include outliers in data.

Shown in Figure 7.3 (at the top left) as with the previous models, the healthy RBC distribution decreases with infection (sub-model 3A to 3B). What separates this model from the previous models is the differentiation of the immune effectors into immune cells B and antibodies A. The model contains an always-present immune effector concetration with a natural birth and decay rate, λ_B and μ_B respectively. Therefore, we observe a small distribution at low values for immune cells in sub-model A (Figure 7.3 middle right), due to no stimulation from infection, and no results for antibodies (Figure 7.3 bottom), where both species distributions increase with infection (eq. 4.3.4 and 4.3.5). Furthermore, even though the merozoites and immune cells stimulate the production of antibodies (eq. 4.3.5), the antibodies do not

Stellenbosch University https://scholar.sun.ac.za

affect the results yielded for the disease variables, and the fight against infection is solely due to the immune cells *B*. This is due to the absence of antibodies in the ODEs of the disease variables.

7.4. Okrinya [16]

The Okrinya model describes dynamics of an active malaria infection [16]. Whilst splitting the immune effectors into innate immune cells and antibodies, another species is also added to track the dynamics of gametocytes in the human host during infection.

Stellenbosch University https://scholar.sun.ac.za

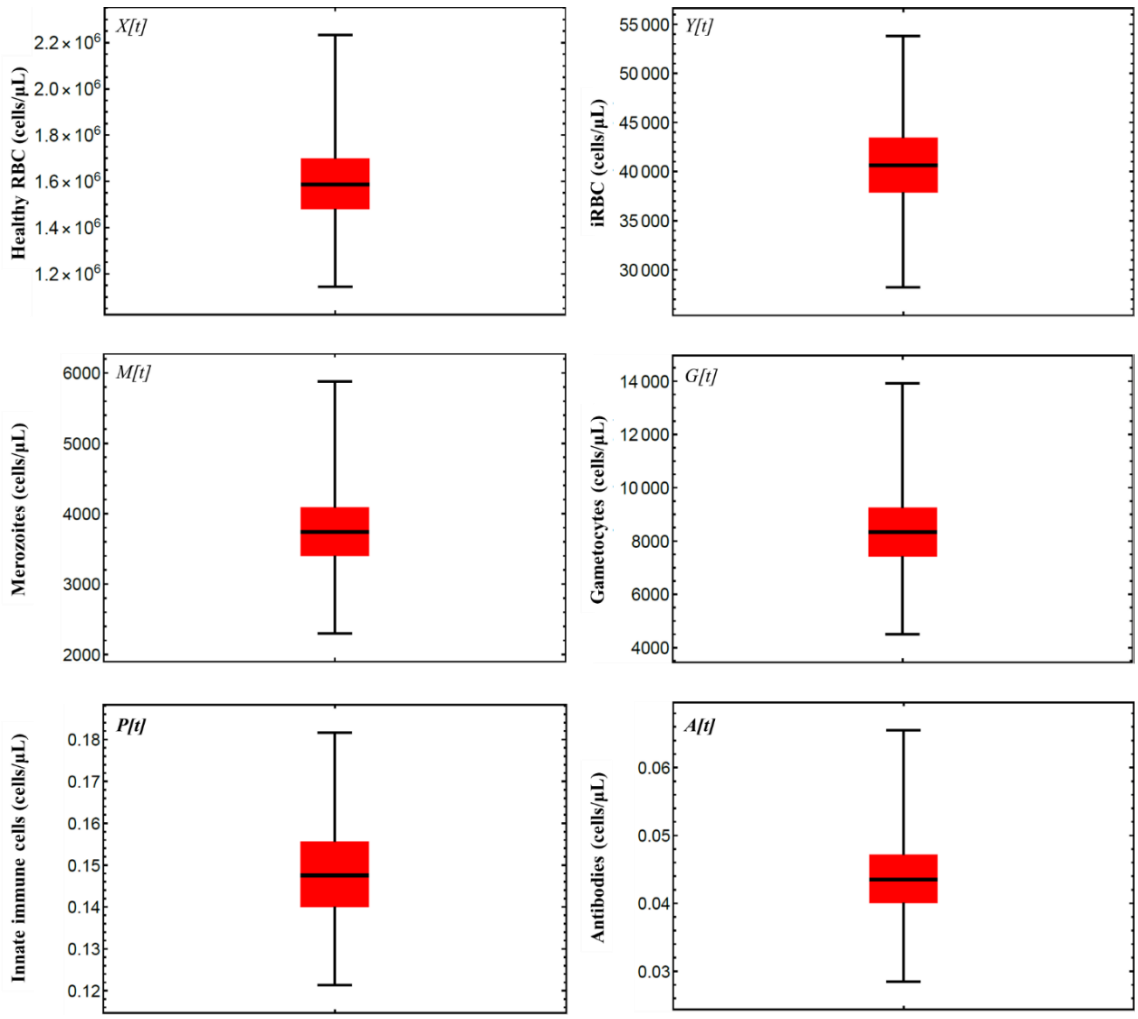

Figure 7.4. The robustness analysis results for the Okrinya model [16]. The y-axis indicates the concentration of the different variables in cell/µl. The whiskers of the box-and-whisker plots include outliers in data.

The boxes in the results for the Okrinya [16] model (Figure 7.4) are all smaller than one magnitude of the size of the median, therefore indicating good individual robustness.

7.5. Comparative Discussion

The overall robustness of models analyzed is tricky to quantify as a 10% perturbation in all parameter values leads to some variables showing large ranges where others show smaller ranges. However, robustness can be reasoned when considering the inter-quartile-range (box). The box part of the box-and-whisker diagram will include 50% of the steady states that were obtained on the parameter sets, whereas each whisker contains 25% of the data, whilst additionally including the outliers of the data. It was

Stellenbosch University https://scholar.sun.ac.za

therefore noticeable between sub-models of the publications that the robustness increased when the immune system was incorporated which can be reasoned to be due to better inter-variable regulation. With the implementation of the immune response, the range sizes of the disease variables lower for the Anderson *et al.* sub-models B to D [10] and the Li *et al.* sub-models C and D [13], showing that the immune response's incorporation increases the robustness of the disease variables, plausibly due to stabilization of the system by decreasing the merozoite and iRBC concentrations.

The results can also be compared to known cell population variances. The healthy RBC populations in individuals without infection can range between $4.41 - 6.68 \times 10^6\ cells/\mu l$ [75], which corresponds with the range observed in the infection free models of Li *et al*. [13] sub-model 2A, indicating good results for the robustness output. The RBC population when an individual is infected with malaria has in interquartile range (IQR that corresponds to the box of a box-and-whisker plot) from $3.78 - 4.80 \times 10^6\ cells/\mu l$ [76]. This corresponds with the Li *et al.* [13] sub-models. The infection models from Anderson *et al.* [10] and Okrinya [16] do not correspond with literature. The Niger *et al.* [15] models do not correspond with literature as some parameters are a few orders of magnitude off from the values used in the Li *et al.* [13] model. Lastly, a general range is given for white blood cell (WBC) count in infected individuals. WBCs include cells from the innate and adaptive immune system. As such this count should incorporate all immunity variables within a model and is therefore the added steady state ranges of the innate and adaptive immune effectors in each model. The IQR from literature is $4.52 - 7.99 \times 10^3\ cells/\mu l$ [76] which- corresponds with sub-model B of Niger *et al.* [15].

Model predictions therefore differ vastly between publications and is highly dependent on what the focus of each study was (i.e. the Anderson *et al.* [10] model was developed to investigate different immune responses to infection). From the robustness analysis, the models of Li *et al.* [13] and Niger *et al.* [15] show to be more realistic representations of the possible steady state outcomes of different cells during infection where the immune system is incorporated.

Stellenbosch University https://scholar.sun.ac.za

Chapter 8

Global Sensitivity analysis

Global sensitivity analysis is a helpful tool to determine how sensitive model outputs are to simultaneous changes in parameter values. The necessity of such an analysis when investigating biological models, is evident if one considers that variations of processes influencing the concentrations of biological components exist within and between hosts. Global sensitivity analysis can therefore assist in determining which parameters have large contributions to variations in model outputs, as well as determining if the local sensitivity analysis results are conserved over a parametric range.

This chapter will focus on global sensitivity analysis of models including infection and immune response from the publications under review, to ensure that the most descriptive models are used for comparison. Consequently, Anderson *et al*. sub-model A [10], Li *et al*. sub-models A and B [13], as well as Niger *et al*. sub-model A [15] will be excluded from this chapter as they do not incorporate the required elements.

Analysis was performed on the parameter sets obtained via MC random sampling and LHS as explained in the previous chapter. Metabolic control analysis (MCA) was conducted on the solution at every point in parameter space, yielding a response coefficient for the effect of every parameter perturbation on every variable. The response coefficient indicates the % change that a 1% change in a certain parameter would elicit on the steady state of a given variable. Note that the same parameter sets that achieved valid steady states for the robustness analysis were used in the global sensitivity analysis. The number of response coefficients explaining one parameter-variable interaction therefore matches the number of parameter sets generated by sampling methods, i.e. 10 000 response coefficients per parameter for MC random sampling and 1 000 for LHS. A probability distribution histogram was constructed for each parameter elicited response on each variable, showing the possible response coefficients on the x-axis and the probability that they will occur on the y-axis. Therefore, global sensitivity analysis of the model proposed by Okrinya [15], containing 29 parameters and 7 variables, would generate $29 \times 7 = 203$ histograms. To our knowledge, there is no definitive quantitative measure for global sensitivity analysis results, and as such histograms were included for discussion based on the self-defined criteria set out in Figure 8A.

Stellenbosch University https://scholar.sun.ac.za

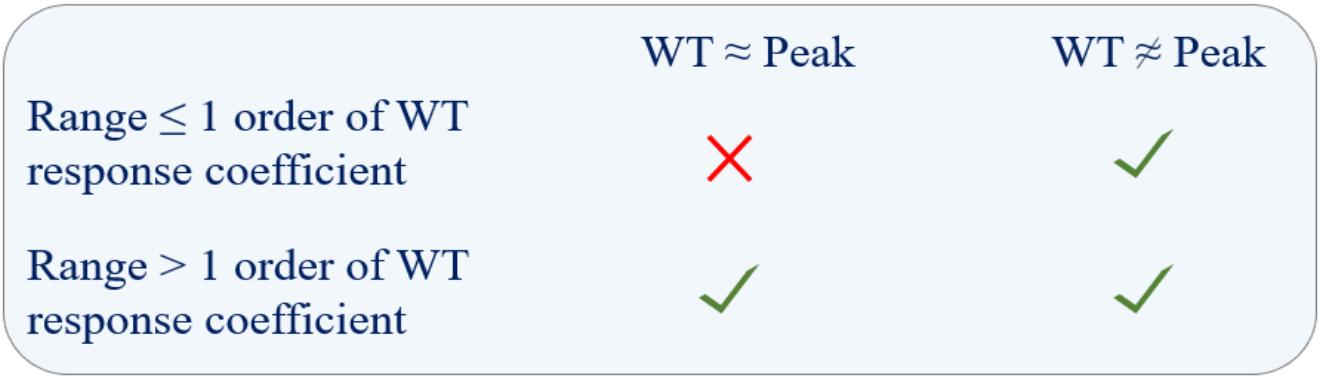

Figure 8A. The inclusion criteria for global sensitivity analysis results in the discussion. Results omitted indicate good global sensitivity results (i.e. conservation of local sensitivity across parameter space). WT represents the wild type response coefficient obtained with local sensitivity analysis and peak represents the peak of histograms obtained that represents the most probable response coefficient in the histograms. The range is determined by a 1 order decrease and increase in the wild type response coefficient. The cross indicates when results will be omitted and the ticks indicate when results will be included.

The scheme represents the criteria by which results were sifted to present the most relevant results, depicting parameter-variable sets that did not yield good global sensitivity results. As the MCA is conducted on all parameter sets generated by sampling, response coefficients will vary for different parameter sets as new steady states with new sensitivities will be obtained. If the response coefficient values fall within a range smaller than 1 order, the expected response coefficients lie in close proximity to the reference response coefficient, therefore showing a level of conservation of the local sensitivity results over a range of parameter sets. This would thus be indicative of good global sensitivity results. However, if the range increases it would indicate that in a population, with variations in parameter sets in each individual, very different responses would be elicited and the global sensitivity results would be poor. A large difference between the local response coefficient (wild type response shown as black dashed line on histograms) and the most probable response coefficient (peaks of histograms), would also indicate poor results. As some of these responses could be detrimental to health, for example if the death rate of healthy RBCs as a parameter induces a change in the variable lowering the healthy RBC population to a state of anemia, these responses should be considered in model analysis.

As MC random sampling constructed more parameter sets than LHS, the histograms displaying the MCA results show a smoother profile for the analysis on the MC random sampling parameter sets (Figure 8B). Both results, however, show the same general distribution of response coefficients, with differences

Stellenbosch University https://scholar.sun.ac.za

observed attributed to parameter set sizes (Figure 8B histograms A and B). Therefore, only MCA results obtained using the MC random sampling constructed parameter sets will be shown further on.

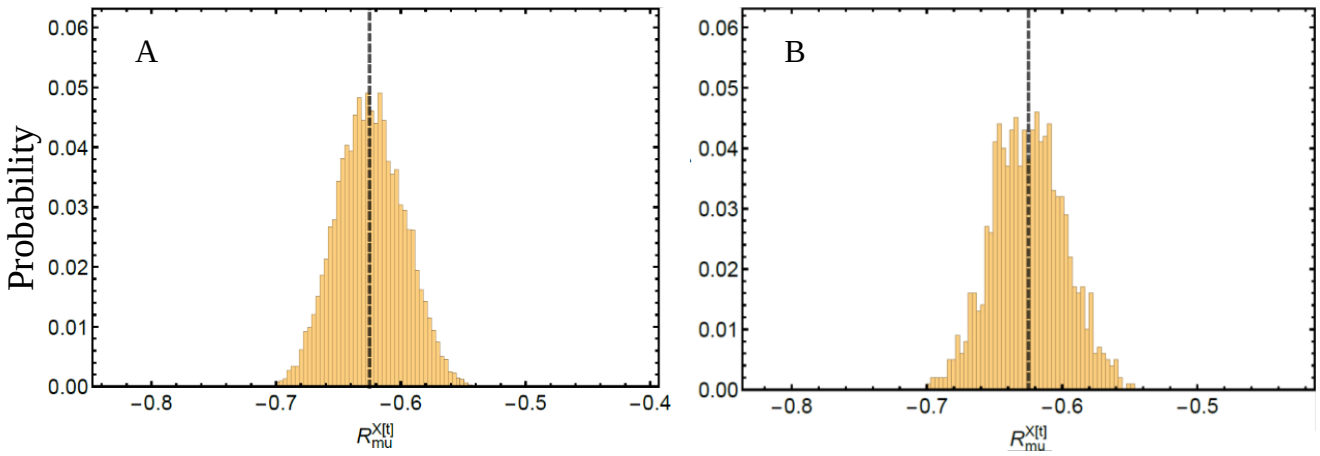

Figure 8B. The results for the global sensitivity analysis of the Anderson et al. sub-model B [10]. A) MCA analysis for the 10 000 parameter set generated by MC random sampling and B) MCA analysis for the 1 000 parameter sets obtained with LHS are shown as a response coefficient distribution histogram to present the probability of different response coefficients for variable X (RBC population) elicited by a perturbation in parameter μ (death rate of RBCs). The wild type response coefficient obtained with local sensitivity analysis is shown as a dashed black line. These results are included to present the similarities between the two sampling methods.

8.1. Anderson *et al.* [10]

For sub-models of Anderson *et al.* [10], the largest response coefficient distributions yielded by global sensitivity analysis are seen for parameters affecting variable T, denoting the T-lymphocyte population of the host. This corresponds well with results obtained from local sensitivity analysis, as the largest response coefficients were obtained for this variable. Sub-model B, representing infection with immune response directed at the free roaming merozoites, presented no significant results as good global sensitivity results were obtained with all wild types corresponding to the peaks of the respective histograms. Sub-model C presents infection with the immune response directed at the iRBCs only and results are presented in Figure 8.1A.

Stellenbosch University https://scholar.sun.ac.za

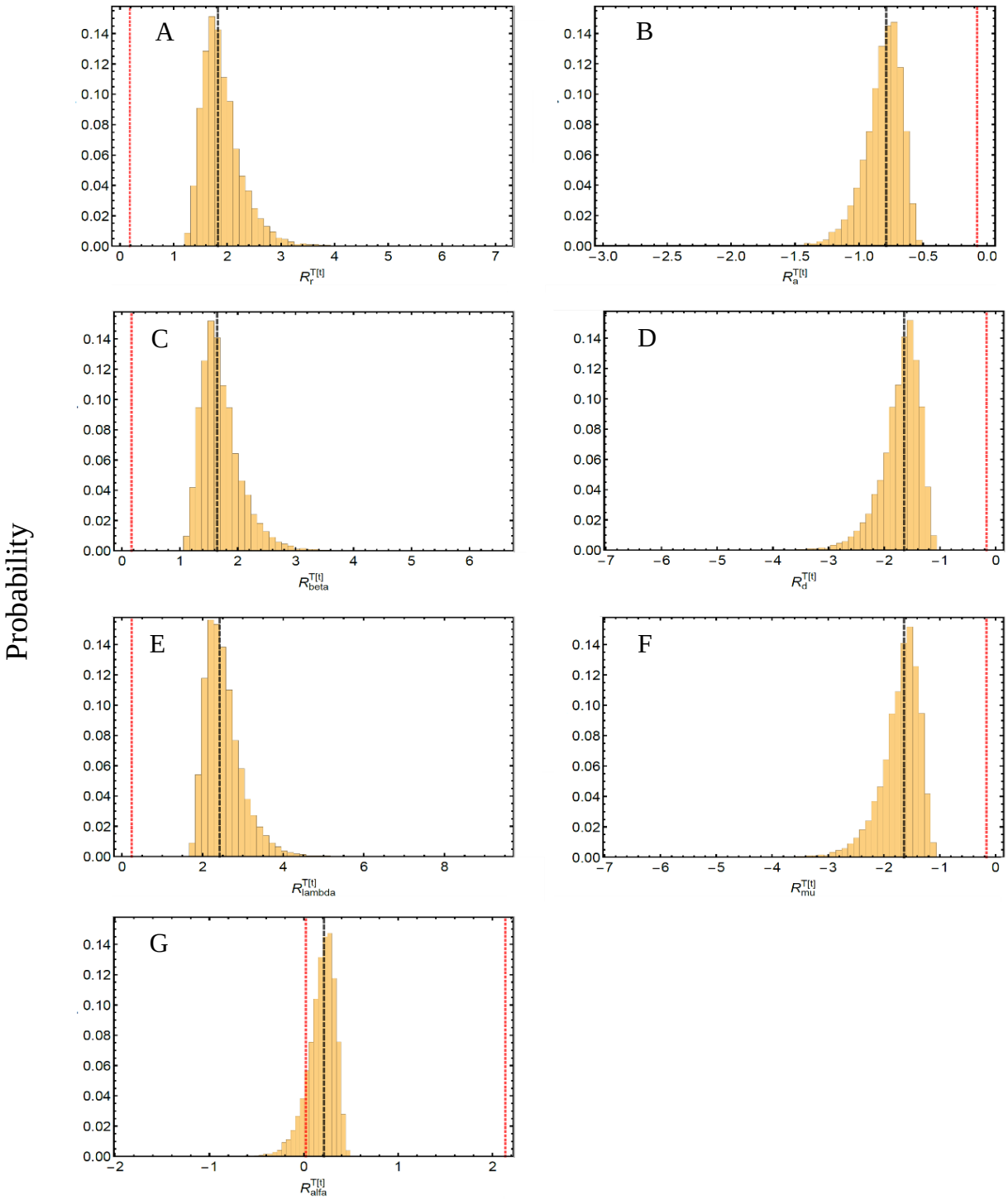

Figure 8.1A: Global sensitivity analysis results for Anderson et al. [10] sub-model C. The response coefficient distributions of the T-lymphocyte population on the parameters are presented for parameters A: "r" the number of merozoites released per bursting iRBC, B: "a" the natural death rate of T-lymphocytes, C: "β" probability of infection of RBC with free roaming merozoites, D: "d" natural death rate of free roaming merozoites, E: "λ" birth rate of healthy RBCs, F: "μ" natural death rate of healthy RBCs, and G: "α" the death rate of iRBCs. The wild type response coefficients obtained with local sensitivity analysis are visualized as black dashed lines and the red dashed lines represent the upper and lower bounds expected for the results based on a 1 order increase and decrease in the wild type response coefficient. Bounds not shown lie outside of the range of the respective histogram.

Stellenbosch University https://scholar.sun.ac.za

All results from sub-model C showed the global sensitivity results of the T-lymphocyte population that could not be excluded based on criteria set out in Figure 8A. Six of the seven plots presented (Figure 8.1A, histograms A to F) are included for discussion due to the wild type response coefficients not corresponding to the most probable response coefficients. These histograms in Figure 8.1A are for the following parameters, A: the number of merozoites released per bursting iRBC r, B: the natural death rate of T-lymphocytes a, C: the probability of infection of healthy RBCs by merozoites β, D: the natural death rate of free roaming merozoites d, E: the birth rate of healthy RBCs λ and F: the natural death rate of healthy RBCs μ. For all of these parameters the local sensitivity results are shown to be fairly well conserved in the parameter space as the probable responses lie close the reference response coefficients, whilst results also indicate that there is a more probable response coefficient than the wild type. This demonstrates that in a population with varying parameter sets, the most probable response coefficient would be slightly larger (peak on the right side of the wild type) or smaller (peak on the left side of the wild type) than the response coefficient yielded for the parameter set used in this sub-model. It should however be noted that the differences in most probable and wild type response coefficients are fractional, therefore still showing relatively good global sensitivity results.

As for histogram G in Figure 8.1A the left tail of the histogram passes the lower bound of the acceptable range in which the response coefficients may fall and furthermore indicates that negative response coefficients can exist for the response of the T-lymphocyte population on the death rate of iRBCs (α). The death rate of iRBCs lowers the amount of iRBCs and should accordingly lower the amount and need for T-lymphocytes within this model. However, most response coefficients including the wild type indicate an increase in T-lymphocytes. In the local sensitivity analysis chapter, results indicated that an increase in the death rate of iRBCs would increase the amount of merozoites and consequently the amount of T-lymphocytes. This deviates from what is expected, as the T-lymphocytes are directed at the iRBCs in sub-model 2C, though it should be noted that the response coefficients are very small. With varying parameter sets we see that a small number of response coefficients is indicated to be negative for this variable-parameter pair, indicating a possibility that for some individuals, an increase in the death rate of iRBCs will lead to a decrease in the number of T-lymphocytes at steady state. This is more reasonable as T-lymphocytes are stimulated by the presence of iRBCs.

Stellenbosch University https://scholar.sun.ac.za

In Figure 8.1B the results are presented for the global sensitivity analysis of sub-model D, which includes infection with immune response directed at both the free roaming merozoites and the iRBCs.

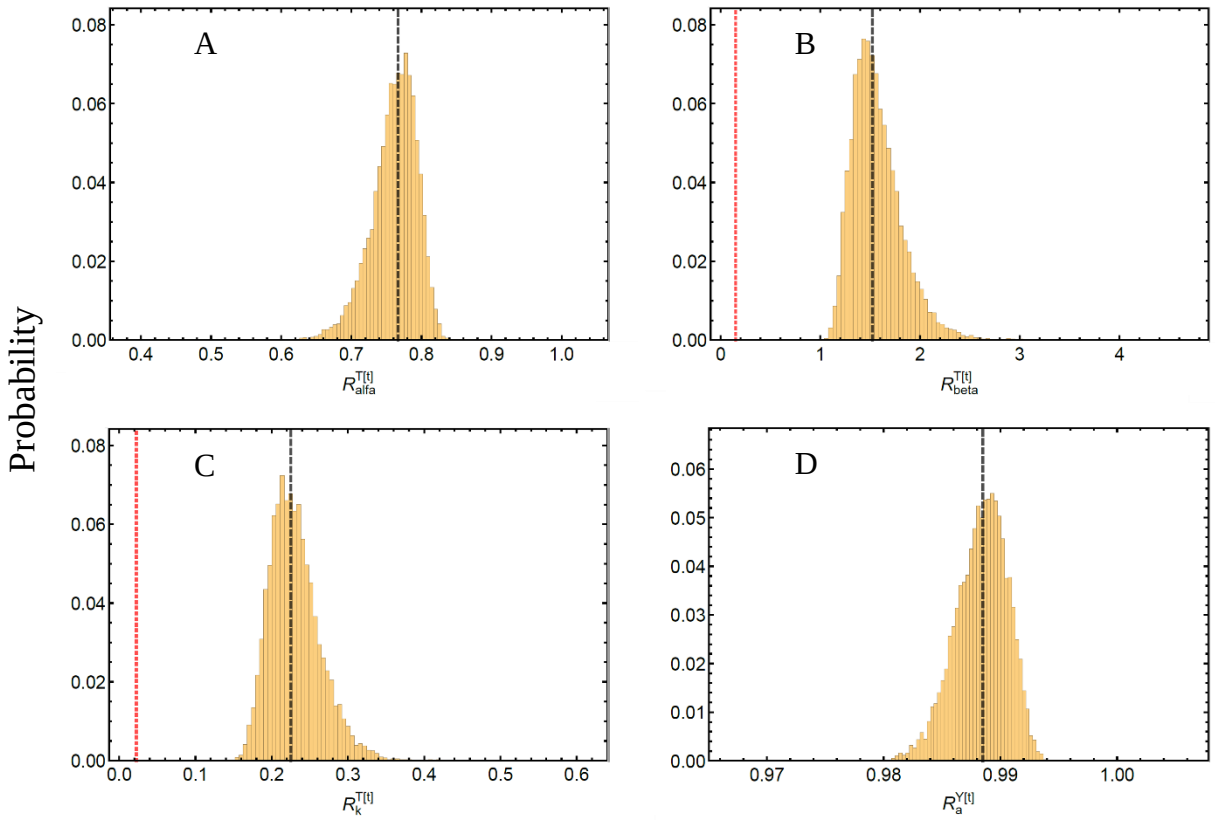

Figure 8.1B: Global sensitivity analysis results for Anderson et al. [10] sub-model D. The response coefficient distributions of the variable populations on the parameters are presented for A: "T" the T-lymphocyte population on "α" the death rate of iRBCs, B: "T" the T-lymphocyte population on "β" the probability of infection of RBC with free roaming merozoites, C: "T" the T-lymphocyte population on "k" the proliferation rate of the T-lymphocytes due to iRBCs, and D:"Y" the iRBC population on "a" the natural death rate of T-lymphocytes. The wild type response coefficients obtained with local sensitivity analysis are visualized as black dashed lines and the red dashed lines represent the upper and lower bounds expected for the results based on a 1 order increase and decrease in the wild type response coefficient. Bounds not shown lie outside of the range of the respective histogram.

All histograms are now shown to be in bounds, with almost negligible discrepancies only observed between the wild type response coefficient and the most probable coefficient. Parameters presented in Figure 8.1B histograms A to F are shown to follow the same trend as observed for sub-model C (Figure 8.1A). Histogram A in sub-model D (Figure 8.1B) represents better global sensitivity results for the same parameter-variable pair as histogram G in sub-model C (Figure 8.1A). This is likely due to the immune response being directed at both disease variables where merozoites and iRBCs activate the immune

Stellenbosch University https://scholar.sun.ac.za

response. Histogram B represents the same results as histogram C in Figure 8.1A. A new parameter-variable pairing is presented (histogram C) for the results of sub-model D, as the influence of the proliferation rate of T-lymphocytes due to iRBCs k on the T-lymphocyte concentration, is presented, with differences between the wild type and most probable response coefficient again being fractional. The last histogram presented, D, shows a larger response coefficient than the wild type for the iRBC population on the death rate of T-lymphocytes a, indicating that in a population, the death in iRBCs increase the T-lymphocytes slightly more than expected for the parameter set published.

Overall, the global sensitivity analysis showed good results for the Anderson *et al.* [10] sub-models as results were mostly presented due to differences in peaks and wild type response coefficients, and differences furthermore being marginally small.

8.2. Li *et al.* [13]

Two sub-models (C and D) were included from the Li *et al.* [13] publication for global sensitivity analysis. The first sub-model (C) indicates the disease dynamics of an infected individual with an immune response. The results are presented in two parts, Figure 8.2A(1) and 8.2A(2).

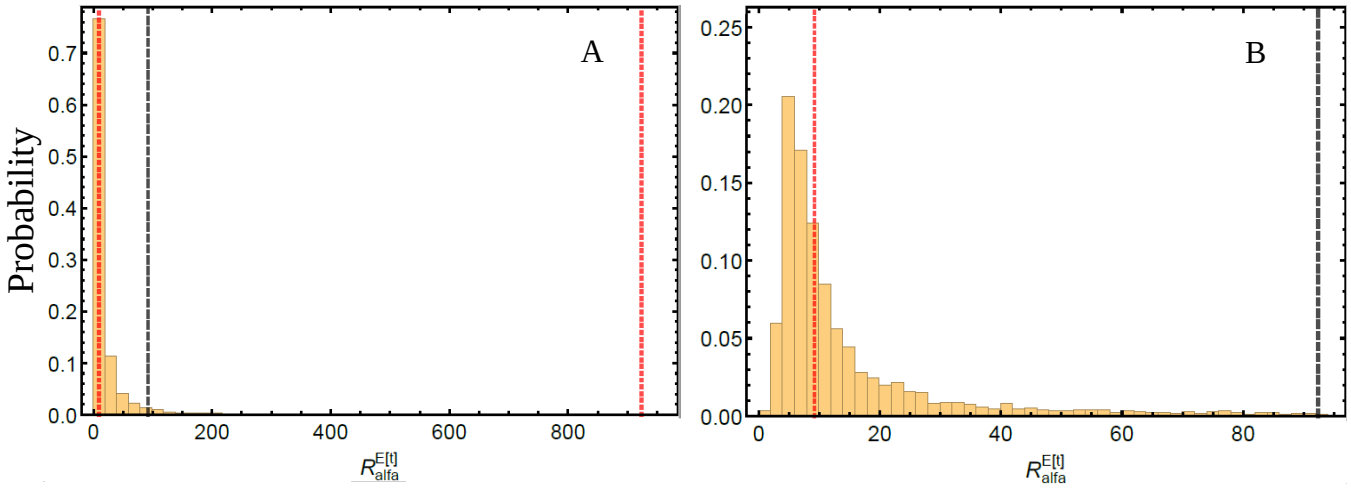

Figure 8.2A(1): Global sensitivity analysis results for Li et al. [13] sub-model C (Part 1). The response coefficient distributions of the immune effectors' population "E" on "α" the infection of RBCs with malaria parasites is presented. Histogram A presents the results as determined by analysis and Histogram B is an enlargement of histogram A where the response coefficients are concentrated. The wild type response coefficients obtained with local sensitivity analysis are visualized as black dashed lines and the red dashed lines represent the upper and lower bounds expected for the results based on a 1 order increase and decrease in the wild type response coefficient. Bounds not shown lie outside of the range of the respective histogram.

Stellenbosch University https://scholar.sun.ac.za

The results presented in Figure 8.2A(1) show the large difference between the wild type and most probable response coefficient. The wild type response coefficients determined with local sensitivity analysis were all determined to be quite large for the immune effectors E on perturbations in most parameters. Histogram A in Figure 8.2A(1), however, indicates that the most probable response coefficient is much lower and seems to be tending towards zero. With enlargement of the part of the histogram where the response coefficients are concentrated, it is possible to observe the most probable response coefficient (Figure 8.2A(1), histogram B). The most probable response coefficient lies closer to a value of 5 than to zero. The same observations were made for all of the parameters that had a large response coefficient for the immune effectors in the local sensitivity analysis chapter, and parameters include: the birth rate of healthy RBCs λ, the product rate of merozoites r, the decay rate of merozoites μ, the decay rate of healthy RBCs d_1, and the decay rate of iRBCs δ. These results demonstrate that in a population, the immune response could, more possibly, not react as drastically to changes in biological processes (parameters), as indicated by the local sensitivity analysis at wild type. This large difference between the wild type response coefficient and the most probable response coefficient can be attributed to the R_0 value used in the publication as 1.25. Due to this value lying close to the threshold, it would be possible that some parameter sets alter the value of the reproductive number to lower than 1, changing the model to a disease free state. However, this reasoning does not correlate with the robustness results (Figure 7.2), as there are no steady states for the disease variables close to zero, where the disease is eradicated and R_0 is smaller than one.

The more plausable explanation would follow on further revision of the Li *et al*. [13] publication. The authors investigated the stability of the models and determined bifurcation parameters that produced oscillatory effects on the model variables when certain values were used. An example of one of the parameters used is k_1, where a value of $4.5001 \times 10^{-5}\ \mu l/cell/day$ showed stable steady state analyses [13]. However, as this value increases to a value larger than $4.5045 \times 10^{-5}\ \mu l/cell/day$, a periodic solution occurs instead of steady states, indicating an unstable model solution [13]. These values indicate the extremely small variation in some parameters, can lead to a large alteration in the model outputs. Furthermore, the stability of their model outcomes were defined as ratios e.g. $\frac{k_2}{\gamma} < d_2 < \frac{k_1}{\beta}$ with specific parameter values for other parameters, indicating that more than one parameter can influence the stability of the model outputs. It is therefore possible that different parameter sets would lead to greatly varying response coefficients.

Stellenbosch University https://scholar.sun.ac.za

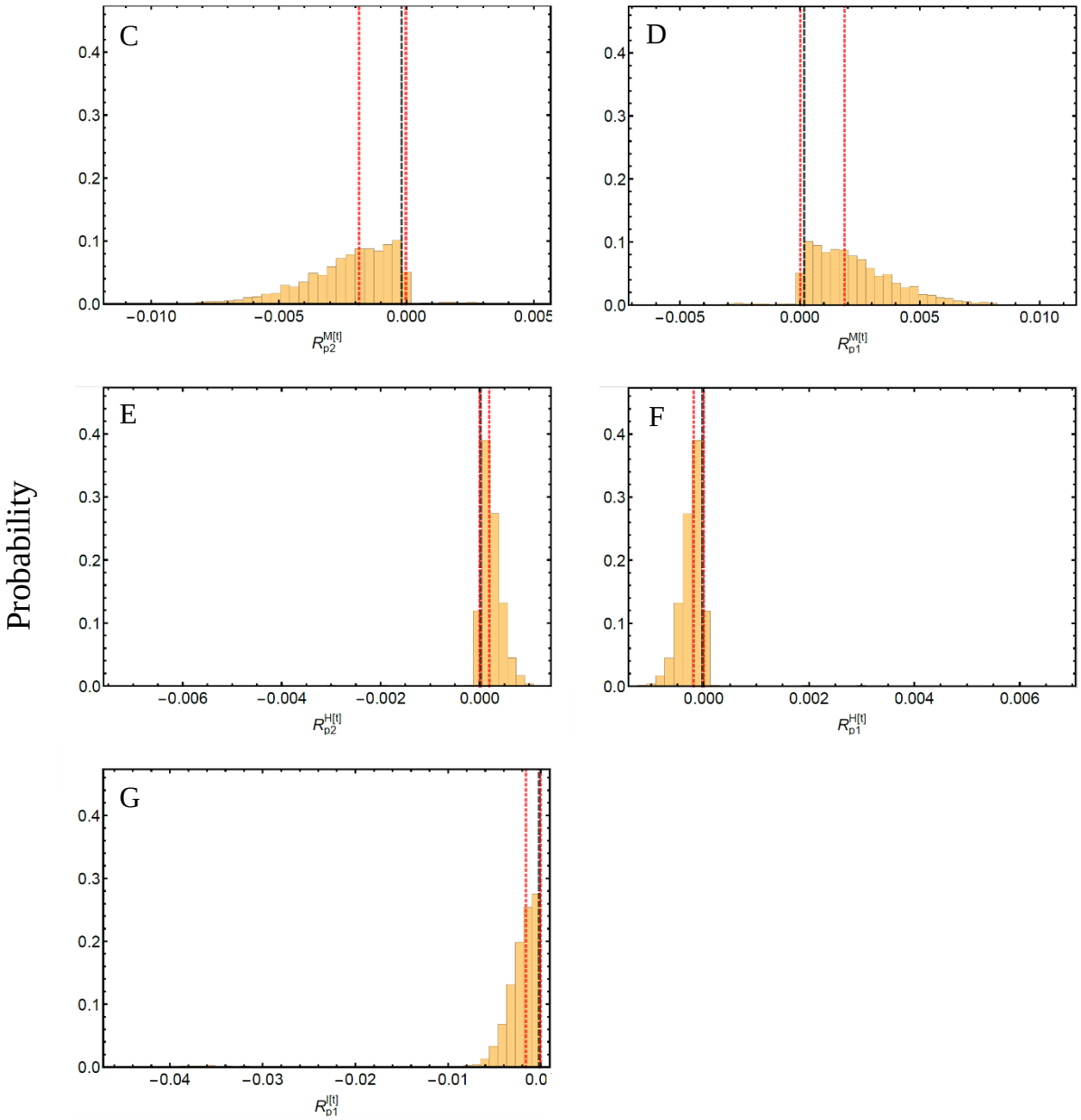

Figure 8.2A(2): Global sensitivity analysis results for Li et al. [13] sub-model C (Part 2). The response coefficient distributions of the variable populations on the parameters are presented for C: "M" merozoites on "p_2" the removal rate of merozoites by the immune effectors, D: "M" merozoites on "p_1" the removal rate of iRBCs by the immune system, E: "H" healthy RBCs on "p_2" the removal rate of merozoites by the immune effectors, F: "H" healthy RBCs on "p_1" the removal rate of iRBCs by the immune system, and G: "I" iRBCs on "p_1" the removal rate of iRBCs by the immune system. The wild type response coefficients obtained with local sensitivity analysis are visualized as black dashed lines and the red dashed lines represent the upper and lower bounds expected for the results based on a 1 order increase and decrease in the wild type response coefficient. Bounds not shown lie outside of the range of the respective histogram.

Figure 8.2.A(2) presents the second set of results for sub-model C and indicates the removal of merozoites and iRBCs by the immune effector, p_1 and p_2 respectively, resulting in poor global sensitivity

Stellenbosch University https://scholar.sun.ac.za

results. Here the tails of the histograms pass the allowed bounds of the possible response coefficients according to the inclusion criteria set out at the start of this chapter. The removal of merozoites by the immune effectors p_1, is indicated in histograms D, F and G, where it shows the response coefficients for the merozoite population M, the healthy RBCs H and the iRBCs I, respectively. The removal of iRBCs by the immune effectors p_2 is indicated in histograms C and E, where the variables shown are M and H respectively. The wild type response coefficients for these parameter-variable pairings are extremely small. Additionally, as the bounds are determined as an order difference increase and decrease in the wild type response coefficient, the range of acceptable response coefficients would therefore also be quite small. As an example, in histogram C the wild type response coefficient is rounded to zero and the lower bound is ten times that value at ± 0.002. These ranges are extremely small and the response coefficients that lie outside of these ranges are minimal and can still be seen as insignificant. These results thus only indicate that the removal rate of the disease variables will in some individuals have a very small influence on their cell populations under investigation.

The global sensitivity results of the Li *et al.* [13] sub-model D showed similar results to that of sub-model C, with three extra parameters included that had the same observations as within Figure 8.2A(1). These results were for the immune effector E resoponse on β - the $1/\beta$ half saturation constant for iRBCs, d_2 - the decay rate of immune effectors, and k_1 - the proliferation rate of immune effectors by iRBCs. The same type of results is observed as for sub-model C where the most probable response coefficient is much lower in absolute value than the wild type response coefficient.

Taking into account all of the results for the global sensitivity analysis of the Li *et al.* [13] sub-models, the results indicate that there are more probable response coefficients closer to zero than the wild type response coefficient. This is more realistic as an increase of e.g. 5% in the immune effector concentration due to a 1% increase in a parameter is much more plausible than a 92% increase.

Stellenbosch University https://scholar.sun.ac.za

8.3. Niger *et al.* [15]

The Niger *et al.* [15] publication included only one sub-model (B) that describes infection with immune response. The global sensitivity results are presented in Figure 8.3A(1) and 8.3A(2). All results are shown to be on the disease variable Yt (i.e. Y total), which represents the total amount of iRBCs, as this model has split the iRBCs into compartments based on the stages in which the iRBC is.

Stellenbosch University https://scholar.sun.ac.za

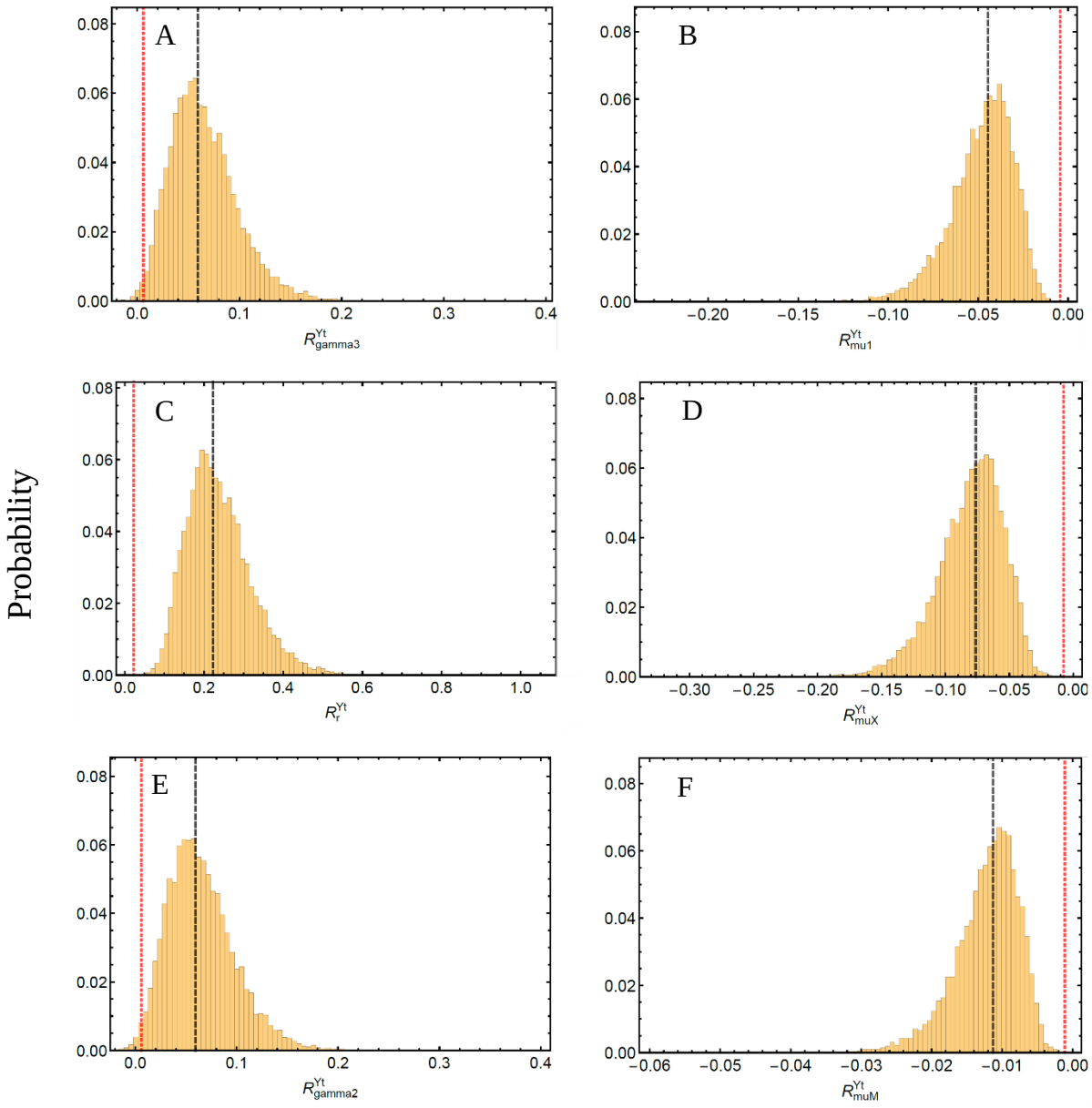

Figure 8.3A(1): Global sensitivity analysis results for Niger et al. [15] sub-model B (Part 1). The response coefficient distributions of the total iRBC population "Yt" on the parameters are presented for parameters A: "γ_3" progression rate of iRBCs from stage 3 to 4, B: "μ_1" natural death rate of iRBCs in stage 1, C: "r" number of merozoites released per bursting iRBC, D: "μ_X" natural death rate of healthy RBCs, E: "γ_2" progression rate of iRBCs from stage 2 to 3, and F: "μ_M" natural death rate of merozoites. The wild type response coefficients obtained with local sensitivity analysis are visualized as black dashed lines and the red dashed lines represent the upper and lower bounds expected for the results based on a 1 order increase and decrease in the wild type response coefficient. Bounds not shown lie outside of the range of the respective histogram.

Stellenbosch University https://scholar.sun.ac.za

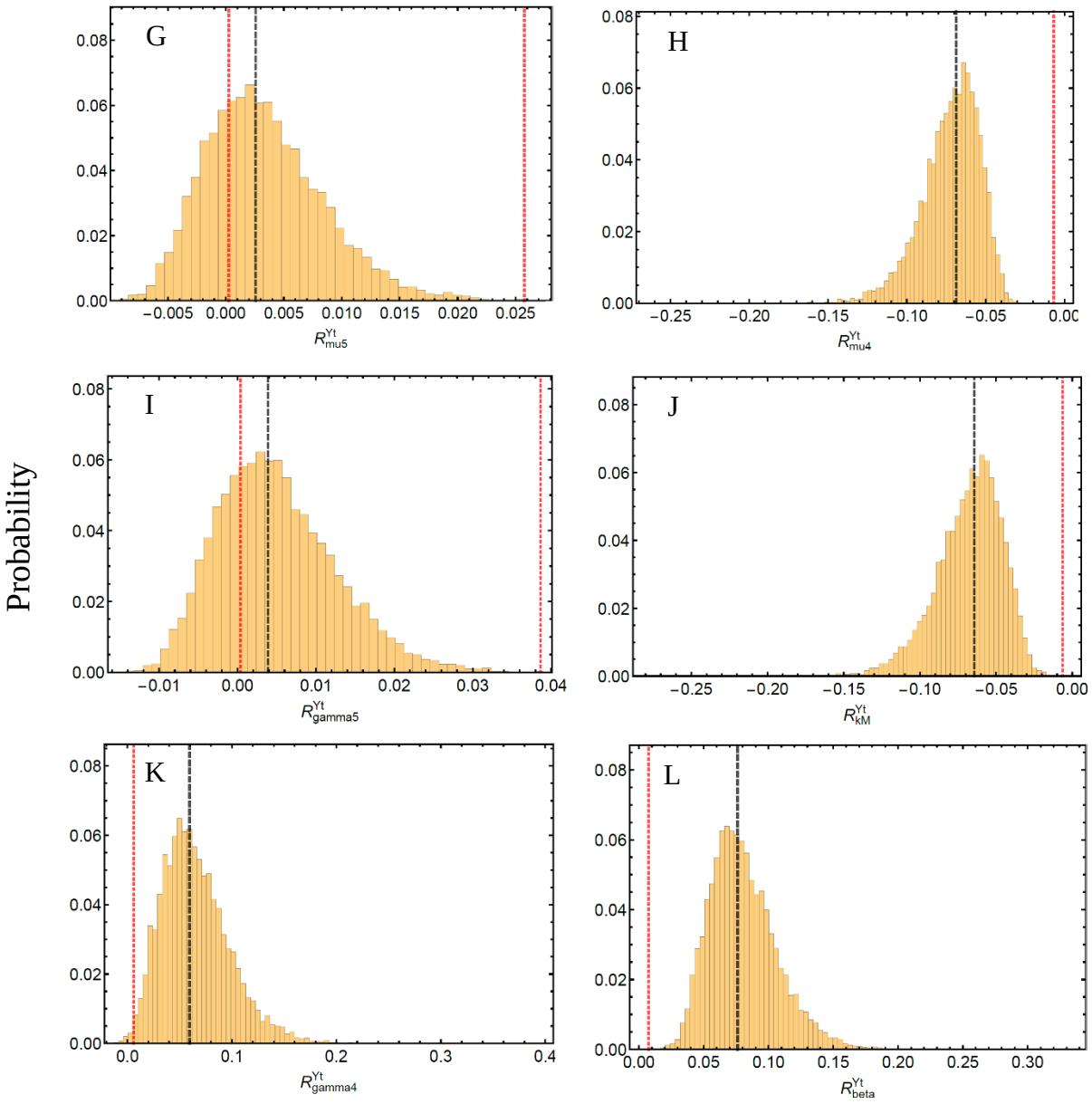

Figure 8.3A(2): Global sensitivity analysis results for Niger et al. [15] sub-model B (Part 2). The response coefficient distributions of the total iRBC population "Yt" on the parameters are presented for parameters G: "μ_5" natural death rate of iRBCs in stage 5, H: "μ_4" natural death rate of iRBCs in stage 4, I: "γ_5" progression rate of iRBCs from stage 5 to 6, J: "k_M" immunosensitivity of merozoites, K: "γ_4" progression rate of iRBCs from stage 4 to 5, and L: "β" rate of infection. The wild type response coefficients obtained with local sensitivity analysis are visualized as black dashed lines and the red dashed lines represent the upper and lower bounds expected for the results based on a 1 order increase and decrease in the wild type response coefficient. Bounds not shown lie outside of the range of the respective histogram.

Stellenbosch University https://scholar.sun.ac.za

For the results presented in the first part of Figure 8.3A(1), most of the histograms present only a difference between the wild type response coefficient and the most probable response coefficient. The differences between these two are, however, minimal. Two histograms, A and E, present distribution tails that are over the lower bounds of the acceptable range in which the response coefficients may fall. These graphs represent the response coefficients of the iRBCs on γ_3, the progression rate of iRBCs from stage 3 to 4, and γ_2, the progression rate of iRBCs from stage 2 to 3. The total amount of iRBCs is determined by adding the iRBCs of all the stages. It can therefore be reasoned, as γ_2 will increase the amount of iRBCs in stage 3, a positive response coefficient will be achieved here, however, it would decrease stage 2, therefore expecting a negative response coefficient here. This can thus explain the small distribution tail of possible response coefficients observed at these two parameters.

The same reasoning is applied to γ_4 and γ_5 in Figure 8.3A(2), histogram K and I. It should be noted that γ_1 is not included in the results, as this would increase all stages from stage 2 to 5. Even though it would decrease stage 1, this stage has various other influential factors incorporated into its ODE (eq. 4.3.3). The other histograms in Figure 8.3A(2) indicate differences between the peaks and the wild types and as such only indicate that the wild type response coefficient is not the most likely response coefficient in a population.

For this model the changes in observed response coefficients are very small, consequently the model yielded good global sensitivity analysis results.

8.4. Okrinya [16]

The Okrinya publication includes only one model and the results of the global sensitivity analysis is presented in Figure 8.4A.

Stellenbosch University https://scholar.sun.ac.za

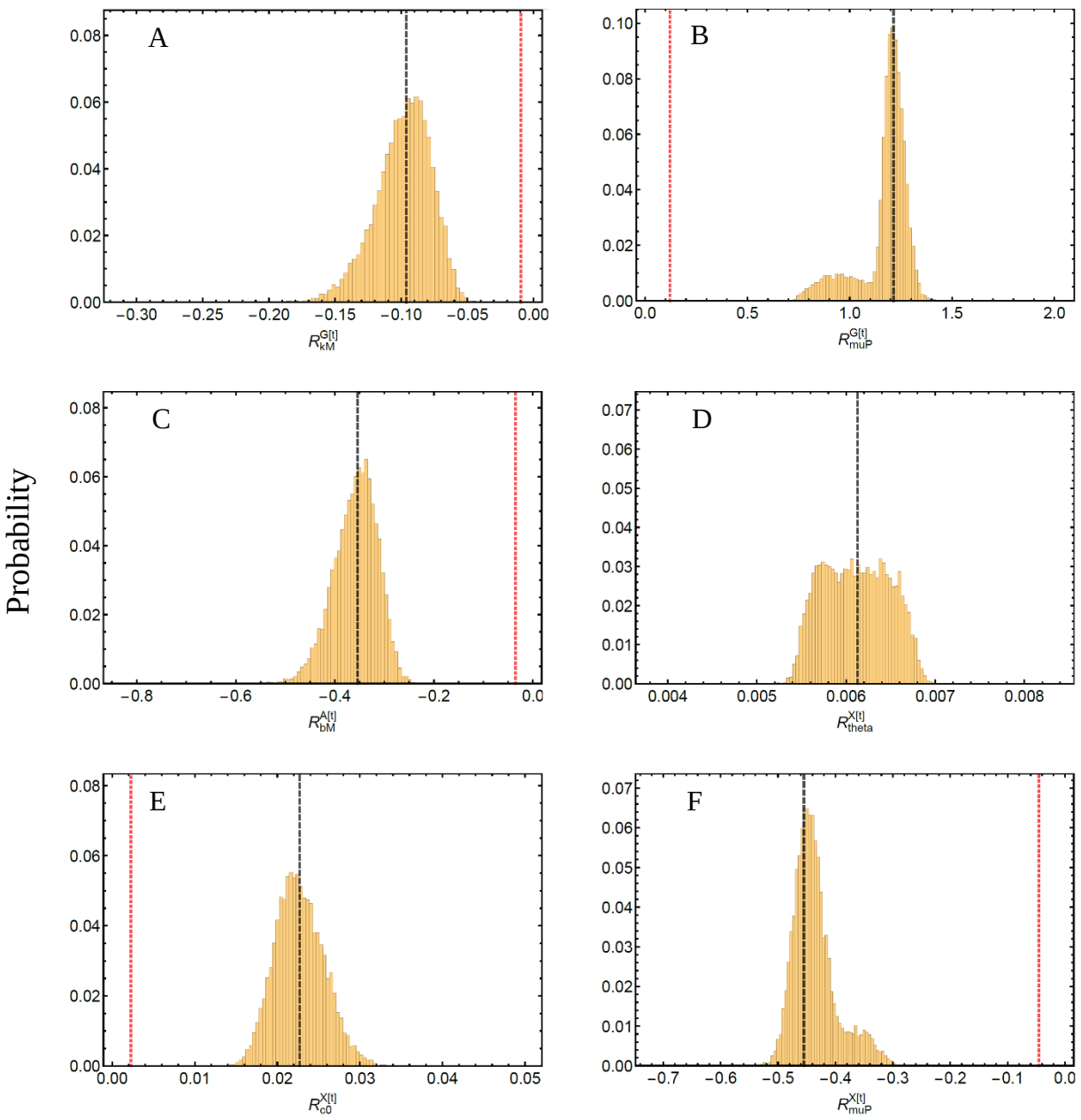

Figure 8.4A: Global sensitivity analysis results for Okrinya [16] model. The response coefficient distributions of the variable populations on the parameters are presented for A: "G" gametocytes on "k_M" the elimination rate of merozoites by innate immune cells, B: "G" gametocytes on "μ_P" natural death rate of innate immune cells, C: "A" adaptive immune cells on "b_M" the supply rate of immune cells from stem cells, D: "X" healthy RBCs on "θ" the fraction of merozoites converting to gametocytes, E: "X" healthy RBCs on "c_0" the efficiency of antibodies blocking merozoite invasion, and F: "X" healthy RBCs on "μ_P" natural death rate of innate immune cells. The wild type response coefficients obtained with local sensitivity analysis are visualized as black dashed lines and the red dashed lines represent the upper and lower bounds expected for the results based on a 1 order increase and decrease in the wild type response coefficient. Bounds not shown lie outside of the range of the respective histogram.

Histograms A, C and E were included as the wild type response coefficient and the most probable coefficient did not correlate. Histograms B and F were included due the observance of an additional small

Stellenbosch University https://scholar.sun.ac.za

peak on each of these graphs. μ_P, representing the natural death rate of innate immune cells, shows the possibility of having a slightly larger response coefficient for the healthy RBCs and a slightly lower response coefficient for the gametocyte population. The healthy RBC population presents a negative wild type response coefficient for the increase in the death of the innate immune cells, indicating that less innate immune cells will lead to more infected cells and consequently less healthy RBCs. The results indicate that it is possible that the influence of this rate on the RBCs might be smaller in some individuals in a population. The same reasoning is used for the gametocyte population. With an increase in the rate of the innate immune cell deaths, gametocytes can survive with better survival observed in some hosts (the second smaller peak). It should however be noted that the differences are yet again fractional between the two peaks.

For histogram D, θ, the conversion rate of merozoites to gametocytes shows no definite peak, indicating that the local sensitivity response coefficient is not the most possible response coefficient. There is, however, no response coefficient that is more probable than the other, but rather a very small range in which these responses can lie (0.005 to 0.007). This range is marginally small and would therefore not influence the overall global sensitivity analysis results of the whole model.

Overall, the model shows good results, with only six histograms presented based on inclusion criteria set out at the start of this chapter. Additionally, the differences between wild type and most probable response coefficients are negligible, indicating that this model system shows stable model outputs and response coefficients are preserved over a widened parameter space.

8.5. Comparative Discussion

The results of the global sensitivity analysis on the models incorporated into this study has demonstrated how well response coefficients are conserved over a parameter space and also where models can possibly lack in accuracy of physiological description. The models are ranked according to their global sensitivity results when considering overall results of the model as well as the ratio of poor to good global sensitivity results within a sub-model. The Okrinya [16] model investigated showed the best global sensitivity analysis results with Anderson *et al.* [10] sub-model B to D and Niger *et al.* [15] sub-model B following closely. In the Anderson *et al.* [10] sub-models results are presented for the variable denoting T-lymphocytes, representing the immune response. This model was built with limited information on the

Stellenbosch University https://scholar.sun.ac.za

immune system components and as such poor global sensitivity results could be observed for this variable. The Niger *et al.* [15] sub-model B showed results for the total number of iRBCs which was split into compartments, with most outlier results including parameters that influence these compartments directly. All of the models from these three publications consequently showed good global sensitivity results overall. The Li *et al.* [13] sub-models showed the poorest results as the immune effectors E was susceptible to changes in all parameters. Additionally, for this variable, almost all of the wild type response coefficients did not correspond to the much lower, most probable response coefficient. Care should therefore be taken with conclusions drawn from this model as a population shows various possible response coefficients.

Stellenbosch University https://scholar.sun.ac.za

Chapter 9

Conclusion

Within-host models describing the immune response to malaria infection were analyzed to investigate the differences in model structure, outputs obtained, and parameters used. Sensitivity and uncertainty analyses were conducted on specific sub-models from the publications as tools for model comparisons to each other as well as to human host biology. As models differ significantly from each other regarding the focus of a modeler's investigation as well as the parameters used, each model yielded different outputs. The tools used in this project can elucidate which models are more relevant in describing the disease dynamics within an individual as well as in a population, whilst additionally giving insight into parameter necessity for a model, as well as possible drug targets.

The aim of this project was to use sensitivity and uncertainty analysis on within-host mathematical models of malaria infection where the immune response is included. These analyses were used to identify important parameters for the disease dynamics that could be possible drug targets. The results were additionally used to determine whether the description of the disease processes can accommodate heterogeneity and uncertainty, while still presenting realistic model predictions. These analyses include local sensitivity, uncertainty, robustness and global sensitivity analysis. As set out in the objectives of this project, models were reproduced using published model description and parameter values to establish trust in the publications, where after the models were subjected to analyses.

Local sensitivity analysis was used to determine important parameters for the disease dynamics of each sub-model and gave insight into which parameters have a large influence on the disease variables or the immune effectors of a model – and can therefore serve as possible focus points for treatment development. Uncertainty analysis differs from local sensitivity analysis as it does not show an important parameter-variable interaction, but rather how variance in parameters can influence the uncertainty of model predictions. Robustness analysis does not form part of sensitivity and uncertainty analysis as it does not show individual parameter effects, but rather how the model outputs are affected with simultaneous changes in all parameters. This analysis can therefore determine the range of different variables with numerous parameter sets. Here, good robustness results were interpreted as model outputs that do not deviate largely from the reference model outputs, while also correlating with experimentally

Stellenbosch University https://scholar.sun.ac.za

determined variable values. Lastly, global sensitivity analysis was used to determine if local sensitivity analysis results are conserved over a larger parameter space (as one would encounter in a population). Although the different analysis results are not comparable with each other, the models used in this project can be compared when inspecting all results in combination.

Local sensitivity analysis completed on all sub-models under investigation indicated the highest response coefficients for parameters and processes that influence the availability of healthy RBCs and the release of merozoites from a bursting iRBC. These response coefficients were for the T-lymphocyte population in the Anderson *et al.* [10] sub-models. The same parameters were indicated in results for the Niger *et al.* [15] sub-model B, the Okrinya [16] model and the Li *et al.* [13] sub-models. The parameters obtained from local sensitivity analysis are additionally indicated within the local sensitivity analysis of the reproductive number (R_0) equations of all the models, and therefore have a direct influence on disease persistence. Furthermore, the local sensitivity response coefficients were the largest for the immune effector variables throughout all of the models. This indicates the strong need for an immune response to infection. The large sensitivity of the immune system to parameters integrated within the R_0 equations, show how the immune response can possibly decrease the R_0 threshold to eradicate disease.

When interpreting results for possible drug targets, care should be taken to note the model description and disease state, as difference states can indicate different drug targets. For example, in the Anderson *et al.* [10] and Li *et al.* [13] sub-models for an infected state with no immune response, the birth rate of new RBCs showed no effect on the steady state of the healthy RBC population, but increased the disease variables. This indicates that in an immune-deficient individual, an increased stimulation of healthy RBC production (to counter loss due to parasite lysis) would show no effect on the RBC population, but would increase the disease. In the sub-models where the immune response was incorporated this was not the case.

Uncertainty analysis can be helpful to determine which parameters have a large influence on the uncertainty in model outputs and therefore the trust we can have in models to represent the actual biology and dynamics behind a disease given inevitable uncertainties in inputs. Parameter values were all varied with 10 % for analysis, however, the actual variance of parameters can be much larger as parameter values can be hard to determine experimentally and can vary within a human due to different diets, ages etc., whilst also varying in a population. Uncertainty analysis distinguished the same parameters (λ and r) as observed for local sensitivity analysis present in all models as the highest contributing factors to uncertainty in model outputs. These parameters directly influence the availability of healthy RBCs and

Stellenbosch University https://scholar.sun.ac.za

the release of merozoites from bursting iRBCs. Additionally, these parameters play a role in the determination of R_0, and uncertainty in the parameters can be the difference between an infected individual and a disease-free individual with the exact same parameter values for all other parameters. The uncertainty analysis highlights the necessity for the precise determination of parameter values and their ranges as this would greatly improve model reliability as well as inter-model comparisons.

Robustness analysis of the sub-models indicated that individual model robustness improved with model complexity and the inclusion of the immune response, probably due to better control of the model system when more processes influence the disease dynamics. This indicates that a better control of the model system by e.g. the inclusion of the immune response, would ensure that model outputs do not vary greatly when all parameters are altered, but stays close to the reference model steady states. Robustness can also be interpreted when comparing results to literature ranges of the different variables. For the disease-free state, the results of Li *et al.* [13] correlated well with experimental ranges. The RBC population range when an individual is infected with malaria corresponded with the Li *et al.* [13] sub-models where infection and the immune response was included. Lastly, it was only the Niger *et al.* [15] models that corresponded with literature on the range for immune effectors. The robustness results therefore indicate that the Li *et al.* [13] models are more likely to realistically describe physiologically relevant disease dynamics, with the Niger *et al.* [15] model realistically describing the dynamics of the immune cells.

Global sensitivity analysis demonstrated how well response coefficients are conserved over a parameter space. The results showed good global sensitivity over all sub-models as the response coefficients were mostly preserved over a parameter space. It was only the results of the Li *et al.* sub-models that indicated poor global sensitivity results, where the large response coefficients observed in local sensitivity analysis did not correspond with the most probable response coefficient, which was significantly lower. The results for the Li *et al*. [13] models do, however, indicate the necessity of global sensitivity analysis, as it is a perfect example in where local sensitivity analysis may lack.

From the collective analysis on all models the different models can be ranked from the most realistic model to the least. The Niger *et al*. [15] model showed the best results as the best sensitivity analysis results were obtained, however, the robustness results were a few orders of magnitude off from literature. The Li *et al*. [13] model comes second as the robustness analysis results correspond so closely to ranges observed experimentally and in literature. The parameter values should however be closely inspected for this model as alterations in the values can lead to unexpected results evident in the local sensitivity analysis, therefore showing model instability. The Okrinya [16] model would be third best as it showed

Stellenbosch University https://scholar.sun.ac.za

great conservation of the local sensitivity results during the global sensitivity analysis, however it did not meet the robustness analysis standards. The Anderson *et al.* [10] model has a good model construction as it showed good global sensitivity analysis results; however, as this model was the first of its kind to be constructed, and taking into account that parameter values used were mostly estimated with limited knowledge of the dynamics of the human immune systems, the robustness analysis showed poor results.

The analysis of all of the models therefore emphasize the advantages of the immune response on the disease dynamics of malaria infection and indicate parameters that should be investigated for disease eradication. Future work would be to investigate the uncertainty of parameter values and the effects it can elicit on disease persistence, as this would establish more trust in within-host models. Furthermore, the amount of merozoites released as well as the availability of healthy RBCs can be investigated to determine threshold values for these parameters when integrated with other parameters presented in the equations of the reproductive numbers, to establish values at which the disease can be eradicated. The Niger *et al.* [15] model can be used as a basis for further model development, starting at the integration of the antibodies into the rest of the model system to inspect the influence on the disease variables. Additionally, parameters values can be changed for the Niger *et al.* [15] models to improve robustness results, and more components can be added to the model of Niger *et al.* [15], such as immune effector components important for inflammation, to investigate new approaches or parameters that may greatly influence the disease dynamics of malaria infection for possible drug targets. Lastly, the Okrinya [16] model showed great promise with local and global sensitivity results. As this model includes more descriptive immune system components, it should also be investigated to see if the desired robustness results can be achieved.

Stellenbosch University https://scholar.sun.ac.za

References

1. WHO (2017) *World Malaria Report 2017, World Health Organization*.
2. Hanboonkunupakarn, B. and White, N. J. (2016) 'The threat of antimalarial drug resistance', *Tropical Diseases, Travel Medicine and Vaccines*, 2(1).
3. Yan, Y., Adam, B., Galinski, M., Kissinger, J.C. and Moreno, A. (2015) 'Mathematical model of susceptibility, resistance, and resilience in the within-host dynamics between a *Plasmodium* parasite and the immune system', *Mathematical Biosciences*, 270, pp. 213–223.
4. Chiyaka, C., Garira, W and Dube, S. (2008) 'Modelling immune response and drug therapy in human malaria infection', *Computational and Mathematical Methods in Medicine,* 9(2), pp.143-163.
5. Tumwiine, J., Mugisha, J. Y. T. and Luboobi, L. S. (2008) 'On global stability of the intra-host dynamics of malaria and the immune system', *Journal of Mathematical Analysis and Applications*, 341(2), pp. 855–869.
6. Hellreigel, B. (2018) 'Modelling the Immune Response to Malaria with Ecological Concepts: Short-Term Behaviour against Long-Term Equilibrium', *Proceedings: Biological Sciences,* 250(1329), pp. 249–256.
7. Molineaux, L., Diebner, H. H., Eichner, M., Collins, W. E., Jeffery, G. M. and Dietz, K. (2001) '*Plasmodium falciparum* parasitaemia described by a new mathematical model', *Parasitology*, 122(Pt 4), pp. 379–391.
8. McKenzie, F. E. and Bossert, W. H. (1997) 'The dynamics of *Plasmodium falciparum* blood-stage infection', *Journal of Theoretical Biology*, 188(1), pp. 127–140.
9. Eckhoff, P. A. (2012) 'Malaria parasite diversity and transmission intensity affect development of parasitological immunity in a mathematical model', *Malaria Journal*, 11(419).
10. Anderson, R. M., May, R. M. and Gupta, S. (1989) 'Non-linear phenomena in host—parasite interactions', *Parasitology*, 99(S1), p. S59 – S79.
11. Anderson, R. M. (1998) 'Complex dynamic behaviours in the interaction between parasite populations and the host's immune system', *International Journal for Parasitology*, 28(4), pp. 551–566.
12. Kwiatkowski, D. and Nowakt, M. (1991) 'Periodic and chaotic host-parasite interactions in human malaria', *Population Biology*, 88, pp. 5111–5113.
13. Li, Y., Ruan, S. and Xiao, D. (2011) 'The Within-Host dynamics of malaria infection with immune response', *Mathematical Biosciences and Engineering*, 8(4), pp. 999–1018.

Stellenbosch University https://scholar.sun.ac.za

14. Tabo, Z., Luboobi, L. S. and Ssebuliba, J. (2017) 'Mathematical modelling of the in-host dynamics of malaria and the effects of treatment', *Journal of Mathematics and Computer Science*, 17(1), pp. 1–21.
15. Niger, A. M. and Gumel, A. B. (2011) 'Immune response and imperfect vaccine in malaria dynamics', *Mathematical Population Studies*, 18(2), pp. 55–86.
16. Okrinya, A. (2014). 'Mathematical modelling of malaria transmission and pathogenesis', doctoral thesis, Loughborough University, Leicestershire, https://dspace.lboro.ac.uk /2134/17160.
17. Gurarie, D. and McKenzie, F. E. (2006) 'Dynamics of immune response and drug resistance in malaria infection', *Malaria Journal*, 5(86).
18. Orwa, T.O., Mbogo, R.W. and Luboobi, L.S. (2018) 'Mathematical Model for Hepatocytic-Erythrocytic Dynamics of Malaria', *International Journal of Mathematics and Mathematical Sciences*, 2018(1), pp. 1-18.
19. Nannyonga, B., Mwanga, G.G., Haario, H., Mbalawata, I.S. and Heilio, M. (2014) 'Determining parameter distribution in within-host severe *P. falciparum* malaria', *BioSystems*,126(2014), pp. 76-84.
20. Dietz, K., Raddatz, G. and Molineaux, L. (2006) 'Mathematical model of the first wave of *Plasmodium falciparum* asexual parasitemia in non-immune and vaccinated individuals', *American Journal of Tropical Medicine and Hygiene*, 75(SUPPL. 2), pp. 46–55.
21. Diebner, H. H., Eichner, M., Molineaux, L., Collins, W. E., Jeffery, M. and Dietz, K. (2000) 'Modelling the transition of asexual blood stages of *Plasmodium falciparum* to gametocytes', *Journal of Theoretical Biology*, 202(2), pp. 113–127.
22. Eichner, M., Diebner, H. H., Molineaux, L., Collins, W. E., Jeffery, G. M. and Dietz, K. (2001) 'Genesis, sequestration and survival of *Plasmodium falciparum* gametocytes: parameter estimates from fitting a model to malaria therapy data', *Transactions of the Royal Society of Tropical Medicine and Hygiene*, 95, pp. 497–501.
23. Klein, E. Y. Graham, A. L., Llinás, M. and Levin, S. (2014) 'Cross-reactive immune responses as primary drivers of malaria chronicity', *Infection and Immunity*, 82(1), pp. 140–151.
24. De Leenheer, P. and Pilyugin, S. S. (2008) 'Immune response to a malaria infection: Properties of a mathematical model', *Journal of Biological Dynamics*, 2(2), pp. 102–120.
25. Gurarie, D., Karl, S., Zimmerman, P. A., King, C. H., St. Pierre, T. G. and Davis, T. M. E. (2012) 'Mathematical modeling of malaria infection with innate and adaptive immunity in individuals and agent-based communities', *PLoS ONE*, 7(3), pp. 1–13.

Stellenbosch University https://scholar.sun.ac.za

26. Antia, R., Nowak, M. A. and Anderson, R. M. (1996) 'Antigenic variation and the within-host dynamics of parasites', *Proceedings of the National Academy of Sciences*, 93(3), pp. 985–989.
27. Autino, B., Noris, A., Russo, R. and Castelli, F. (2012) 'Epidemiology of malaria in endemic areas', *Mediterranean Journal of Hematology and Infectious Diseases*, 4(1).
28. Lee, R.M.K. and Craig, D.A. (1983) 'Maxillary, Mandibulary, and Hypopharyngeal Stylets of Female Mosquitoes (Diptera:Culcidae); A scanning electron microscope study' *The Canadian Entomologist,* 115, pp. 1503-1512.
29. Siciliano, G. and Alano, P. (2015) 'Enlightening the malaria parasite life cycle: bioluminescent *Plasmodium* in fundamental and applied research', *Frontier in Microbiology*, 6(391).
30. Cowman, A. F., Healer, J., Marapana, D. and Marsh, K. (2016) 'Malaria: Biology and Disease', *Cell*. Elsevier Inc., 167(3), pp. 610–624.
31. White, N. J. (2004) 'Review series: Antimalarial drug resistance', *The Journal of Clinical Investigation*, 113(8), pp. 1084–1092.
32. Yan, Y., Adam, B., Galinski, M., Kissinger, J.C. and Moreno, A. (2015) 'Mathematical model of susceptibility, resistance, and resilience in the within-host dynamics between a *Plasmodium* parasite and the immune system', *Mathematical Biosciences*, 270, pp. 213–223.
33. Raje, N. and Dinakae, C. (2015) 'Overview of Immonodefeciency Disorders', *Immunology and Allergy Clinics in North America*, 35(4), pp. 599–623.
34. McCusker, C. and Warrington, R. (2011) 'Primary immunodeficiency', *Allergy, Asthma & Clinical Immunology*, 7(Suppl 1): S11.
35. Hato, T. and Dagher, P. C. (2015) 'How the innate immune system senses trouble and causes trouble', *Clinical Journal of the American Society of Nephrology*, 10(8), pp. 1459–1469.
36. Abbas, A., Litchman, A. and Pillai, S. (2015) *Basic Immunology: Functions and Disorders of the Immune System*, 5th ed. Elsevier Inc. pp.1-146.
37. Bonilla, F. A. and Oettgen, H. C. (2010) 'Adaptive immunity', *Journal of Allergy and Clinical Immunology*, 125(2), pp. S33–S40.
38. Stevenson, M and Urban, B. (2006) 'Antigen presenting and dendritic cell biology in malaria' *Parasite Immunology*, 28. pp. 5-14
39. Modlin, R. L. and Doherty, P. (2013)' Host-pathogen interactions: Host defense against microbial pathogens- the immune systems weapons of mass destruction', *Current Opinion in Immunology,* 15 (4), pp. 393-395.

Stellenbosch University https://scholar.sun.ac.za

40. Riley, E., Wahl, S., Perkins, D and Schofield, L. (2006) 'Regulating immunity to malaria', *Parasite Immunology*, (28): 35-49.
41. Plebanski, M and Hill, A. (2000) 'The immunology of malaria infection.' *Current Opinion in Immunology*. (12) 437-441.
42. Legros, M. and Bonhoeffer, S. (2016) 'A combined within-host and between-hosts modelling framework for the evolution of resistance to antimalarial drugs', *Journal of the Royal Society Interface*, 13.
43. Cai, L., Tuncer, N. and Martcheva, M. (2017) 'How does within-host dynamics affect population-level dynamics? Insights from an immuno-epidemiological model of malaria', *Mathematical Methods in the Applied Sciences*.
44. Choisy, M., Guégan, J. F. and Rohani, P. (2007) 'Mathematical Modeling of Infectious Diseases Dynamics', *Encyclopedia of Infectious Diseases: Modern Methodologies*, pp. 379–404.
45. Garira, W. (2017) 'A complete categorization of multiscale models of infectious disease systems disease systems', *Journal of Biological Dynamics*, 11(1), pp. 378-435.
46. Furrer, G., Westall, J. and Sollins, P. (1989) 'The study of soil chemistry through quasi-steady-state models: I. Mathematical definition of model' *Geochimica et Cosmochimica Acta*, 53(3), pp.595-601.
47. Cakir, T. and Khatibipour, M.J. (2014) 'Metabolic network discovery by top-down and bottom-up approaches and paths for reconciliation', *Frontiers in Bioengineering and Biotechnology*, 2(62), pp. 1-11.
48. Charzyńska, A., Nałęcz, A., Rybiński, M. and Gambin. A (2012) 'Sensitivity analysis of mathematical models of signaling pathways', *Journal of Biotechnology, Computational Biology and Bionanotechmology*, 93(3), pp. 291-308.
49. Zi, Z. (2011) 'Sensitivity analysis approaches applied to systems biology models', *IET Systems Biology*, 5(6), pp. 336–346.
50. De Pauw, D. J. W. and Vanrolleghem, P. A. (2006) 'Practical aspects of sensitivity function approximation for dynamic models', *Mathematical and Computer Modelling of Dynamical Systems*, 12(5), pp. 395–414.
51. Borgonovo, E. and Plischke, E. (2016) 'Sensitivity analysis: A review of recent advances', *European Journal of Operational Research*, 248, pp. 869–887.
52. Cacuci, D. G., Ionescu-Bujor, M. and Navon, M. N.(2005) *Sensitivity and Uncertainty Analysis: Applications to Large-Scale Systems. Volume II*, USA, CRC Press, pp. 26-29.

Stellenbosch University https://scholar.sun.ac.za

53. Haaker, M. P. R. and Verheijen, P. J. T. (2004) 'Local and global sensitivity analysis for a reactor design with parameter uncertainty', *Chemical Engineering Research and Design*, 82(A5), pp. 591–598.
54. Nägele, T. and Weckwerth, W. (2013) ' Eigenvalues of Jacobian Matrices Report on Steps of Metabolic Reprogramming in a Complex Plant-Environment Interaction', *Applied Mathematics*, 4 pp. 44-49.
55. Jurina, T., Tušek, A. J. and Čurlin, M. (2015) 'Local Sensitivity Analysis and Metabolic Control Analysis of the Biological Part of the BTEX Bioremediation Model', *Biotechnology and Bioprocess Engineering*, 20, pp. 1071–1087.
56. Wildermuth, M. C. (2000) 'Metabolic control analysis: biological applications and insights', *Genome Biology*, 1(6) pp. 1–5.
57. Schuster, S. and Heinrich, R. (1992) 'The definitions of metabolic control analysis revisited', *BioSystems*, 27, pp. 1–15.
58. Zádor, J., Zsély, I. G. and Turánui, T. (2006) 'Local and global uncertainty analysis of complex chemical kinetic systems', *Reiability Engineering and Systems Safety*, 91, pp. 1232–1240.
59. Saltelli, A. Ratto, M., Andres, T., Camolongo, F., Cariboni, J., Gatelli, D., Saisana, M. and Tarantola, S. (2008) *Global Sensitivity Analysis. The Primer*. England, John Wiley & Sons Ltd., pp. 109-133.
60. Zhu, Y., Wang, Q. A. and Cai, X. (2018) 'Analytic uncertainty and sensitivity analysis of models with input correlations', *Physica A*, 494, pp. 140–162.
61. Kitano, H. (2004) 'Biological Robustness', *Nature Reviews*, 5, pp. 826-837.
62. Marino, S., Hogue, I. B., Ray, C. J. and Kirschner, D. E. (2008) 'A methodology for performing global uncertainty and sensitivity analysis in systems biology', *Journal of Theoretical Biology*, 254, pp. 178–196.
63. Saltelli, A., Tarantola, S. and Campolongo, F. (2015) 'Sensitivity Analysis as an Ingredient of Modeling', *Statistical Science*, 15(4), pp. 377–395.
64. Shields, M. D. and Zhang, J. (2015) 'The generalization of Latin hypercube sampling', *Reliability Engineering and System Safety*, 148, pp. 96–108.
65. Beckman, R. J. and Conover, W. J. (2010) 'A Comparison of Three Methods for Selecting Values of Input Variables in the Analysis of Output from a Computer Code', *Technometrics*, 42(1), pp. 55–61.
66. Morris, M. D. (1991) 'Factorial Sampling Plans for Preliminary Computational Experiments', *Technometrics*, 33(2), pp. 161–174.

Stellenbosch University https://scholar.sun.ac.za

67. Link, K. G., Stobb, M. T., Di Paola, J., Neeves, K. B., Fogelson, L., Sindi, S. S. and Leiderman, K. (2018) 'A local and global sensitivity analysis of a mathematical model of coagulation and platelet deposition under flow', *PLoS ONE,* 13(7).
68. Herman, J. D., Kollat, J. B., Reed, P. M. and Wagener, T. (2013) 'Technical Note: Method of Morris effectively reduces the computational demands of global sensitivity analysis for distributed watershed models', *Hydrology and Earth System Sciences,* 17, pp. 2893–2903.
69. Helton, J. C. and Davis, F. J. (2003) 'Latin hypercube sampling and the propagation of uncertainty in analyses of complex systems', *Reliability Engineering and System Safety,* 81, pp. 23–69.
70. Tong, C. (2006) 'Refinement strategies for stratified sampling methods', *Reliability Engineering and System Safety,* 91, pp. 1257–1265.
71. Saltelli, A. Ratto, M., Andres, T., Camolongo, F., Cariboni, J., Gatelli, D., Saisana, M. and Tarantola, S. (2008) *Global Sensitivity Analysis. The Primer*. England, John Wiley & Sons Ltd., pp. 183-211.
72. Kent, E., Neumann, S., Kummer, U. and Mendes, P. (2013) 'What Can We Learn from Global Sensitivity Analysis of Biochemical Systems?', *PLoS ONE,* 8(11).
73. Ross, S. (2002) 'The Uniform Random Variable*', A First Course in Probability, Sixth Edition,* Prentice Hall, Upper Saddle River, pp. 195-199.
74. Diekmann, O., Heesterbeek, J. A. P. and Roberts, M. G. (2010) 'The construction of next-generation matrices for compartmental epidemic models', *Journal of the Royal Society. Interface,* 7, pp. 873-885.
75. Omuse, G., Maina, D., Mwangi, J., Wambua, C., Radia, K., Kanyua, A., Kagotho, E., Hoffman, M., Ojwang, P., Premji, Z., Ichihara, K. and Erasmus, R. (2018) 'Complete blood count reference intervals from a healthy adult urban population in Kenya', *PloS ONE,* 13(6), pp. 1-19.
76. Kotepui, M., Phunphuench, B., Chupeerach, C. and Duangmano, S. (2014) 'Effect of malarial infection on haematological parameters in population near Thailand-Myanmar border', *Malaria Journal,* 13(218), pp. 1-7.
77. Heinrich, R. and Schuster, S. (1996) 'The regulation of cellular systems', Chapman & Hall, New York.
78. Hofmeyer, J.H. and Cornish-Bowden, A. (1996) 'Co-response analysis; a new strategy for experimental metabolic control analysis', *Journal of Theoretical Biology*, 182, pp.371-380.

Stellenbosch University https://scholar.sun.ac.za

Appendix A

A.1. Anderson *et al.* [10]

Table A1. Parameter values and initial concentrations for Anderson et al. [10].

Parameter	Parameter description	Value	Unit
$\boldsymbol{\lambda}$	Recruitment rate of healthy RBCs	1	$/day$
$\boldsymbol{\mu}$	Natural death rate of RBCs	0.00833	$/day$
$\boldsymbol{\beta}$	Probability of infection of RBC with free roaming merozoites	0.1	$/day$
$\boldsymbol{\alpha}$	Death rate of iRBCs	0.2	$/day$
$\boldsymbol{r}$	Merozoites released per bursting iRBC	16	$/day$
$\boldsymbol{d}$	Natural death rate of merozoites roaming free	72	$/day$
$\boldsymbol{h}$	Rate of antibody-mediated killing of free merozoites	0.1	$/day$
$\boldsymbol{\gamma}$	Proliferation rate of T-lymphocytes due to merozoites	1.0	$/day$
$\boldsymbol{a}$	Natural death rate of T-lymphocytes	0.05	$/day$
$\boldsymbol{g}$	Rate of cytotoxic killing of iRBCs	0.05	$/day$
$\boldsymbol{k}$	Proliferation rate of T-lymphocytes due to iRBCs	0.05	$/day$
$\boldsymbol{x(0)}$	Initial density of healthy RBCs	120	–
$\boldsymbol{y(0)}$	Initial density of iRBCs	0	–
$\boldsymbol{s(0)}$	Initial density of merozoites after infection	1	–
$\boldsymbol{T(0)}$	Initial density of T-lymphocytes	0.01	–

The parameters as shown in Table A1 were used to construct 4 different sub-models (1A to 1D), with some parameter shifts to display differences in models indicating unique biological events. Additionally, the published value for γ is 0.1 $/day$; however, the model outputs could not be correlated to published outputs using this value. With a shift to a new value of 1.0 $/$ day, the first sub-model output was obtained. To obtain the other sub-models the parameter shifts were used as published and shown below. Additionally, no initial values were provided by the published article, as such parameter values were input based on visual inspection of the published model outputs. The initial density of RBCs was taken from the published graphs, and $s(0) = 1$ was used as at least 1 merozoite is needed to start infection.

Stellenbosch University https://scholar.sun.ac.za

The initial density of the T lymphocytes proved difficult to determine, and was tested using a vast range of initial estimated. A value of 0.01 was the only input that yielded desired outputs. This shows that the model is sensitive to initial conditions of the T-lymphocyte population, and that it could possibly influence the obtained results. The published and reproduced model outputs are presented in Figure A1.

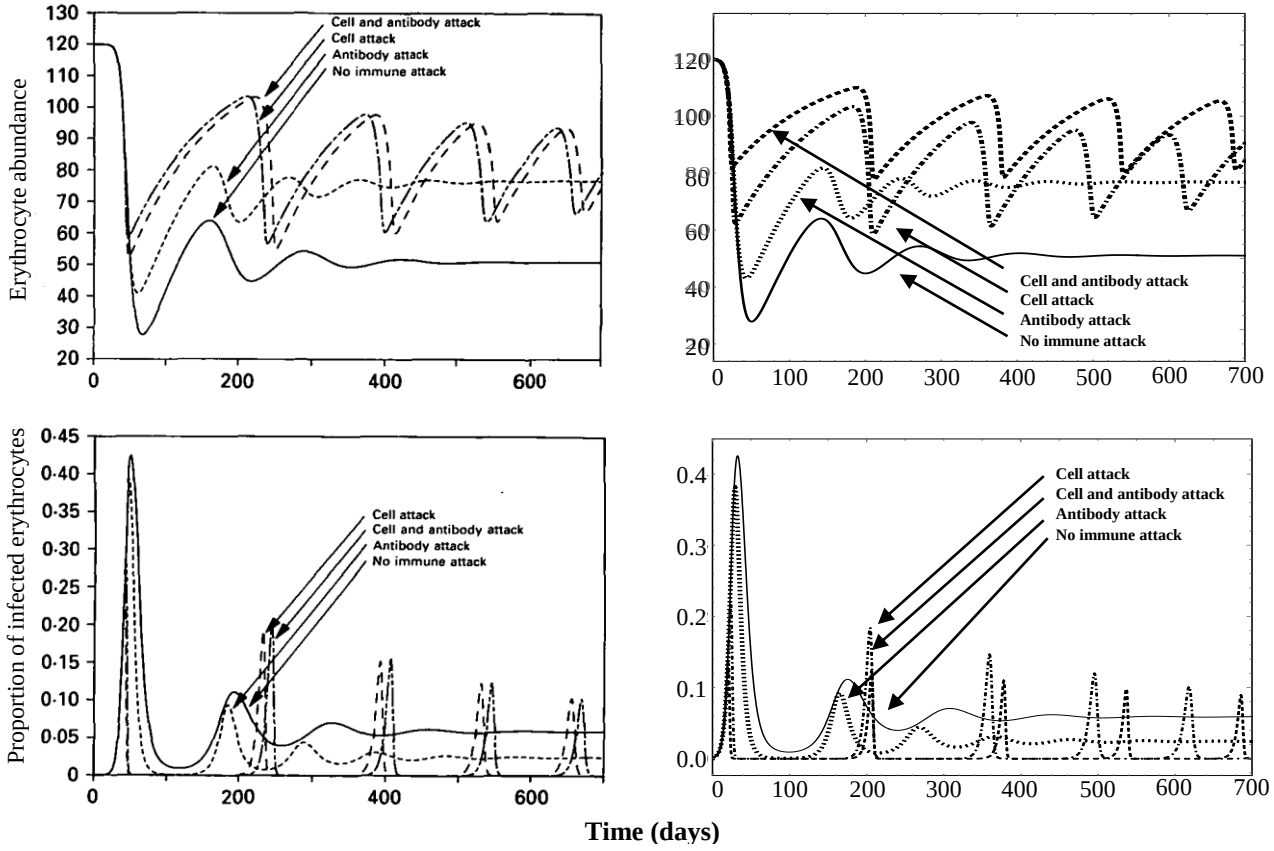

Figure A1. The Anderson et al. [10] models as published are shown on the left hand side and the reproduced models are shown on the right. Discrepancies can be attributed to modelling challenges, such as estimation of initial parameter values, as well as altered values required for precise model outputs. The solid line represents sub-models without an immune system and eq. 1.1 – 1.3 was used with parameters as shown in table A1. The long-dashed line indicates a model where the immune response includes only antibody attack against merozoites and thus encompasses eq. 1.1, 1.2, 1.4 and 1.5. Parameters used here are shown in table A1. The dashed-dotted line showcases the immune response with only cell-mediated attack against iRBCs and uses eq. 1.1, 1.4, 1.6 and 1.7, with $h = \gamma = 0$. In the model depicted as dashed lines both immune responses are included where the same equations were used as in the previously mentioned model. Here all parameters are as in Table A1.

Stellenbosch University https://scholar.sun.ac.za

A.2. Li *et al.* [13]

Table A2. Parameter and initial values for Li et al. [13].

Parameter	Parameter Description	Value	Unit
$\boldsymbol{\lambda}$	Production rate of RBCs	$4.15\ x\ 10^{6}$	$cells/\mu l/day$
$\boldsymbol{d_1}$	Decay rate of RBCs	$8.3\ x\ 10^{3}$	$/day$
$\boldsymbol{\mu}$	Decay rate of malaria parasites	48	$/day$
$\boldsymbol{d_2}$	Decay rate of immune effectors	0.05	$/day$
$\boldsymbol{\alpha}$	Infection of RBCs by malaria parasites	$2\ x\ 10^{-9}$	$\mu l/cell/day$
$\boldsymbol{\delta}$	Decay rate of iRBCs	1.0	$/day$
$\boldsymbol{r}$	Product rate of malaria parasites	12	$/day$
$\boldsymbol{p_1}$	Removal rate of iRBCs by immune system	10^{-8}	$\mu l/cell/day$
$\boldsymbol{p_2}$	Removal rate of malaria parasites by immune system	10^{-8}	$\mu l/cell/day$
$\boldsymbol{k_1}$	Proliferation rate of immune effectors (E) by iRBCs (I)	$2.5\ x\ 10^{-5}$	$\mu l\ /cell/day$
$\boldsymbol{k_2}$	Proliferation rate of immune effectors (E) by merozoites (M)	$4.69\ x\ 10^{-5}$	$\mu l/cell/day$
$\boldsymbol{\beta}$	1/ β half saturation constant for iRBCs (I)	$5\ x\ 10^{-4}$	$\mu l/cell$
$\boldsymbol{\gamma}$	1/γ half saturation constant for malaria parasites (M)	$6.67\ x\ 10^{-4}$	$\mu l/cell$
$\boldsymbol{H(0)}$	Initial population of RBCs	$5\ x\ 10^{6}$	$cells/\ \mu l$
$\boldsymbol{I(0)}$	Initial population of iRBCs	0	$cells/\ \mu l$
$\boldsymbol{M(0)}$	Initial population of malaria parasites	10^{4}	$cells/\ \mu l$
$\boldsymbol{E(0)}$	Initial population of immune effectors	10^{-4}	$cells/\ \mu l$

The table shows parameter values used for the model of eq. 4.2.1 to 4.2.4. Four different sub-models (2A to 2D) were achieved by changing some parameter values to show different dynamical results explaining various possibilities to be discussed. The parameter values were used as is to obtain the first sub-model with a disease free equilibrium. To obtain the second sub-model where the disease persists with no specific immune response, α was changed to a value of $9 \times 10^{-7}\ \mu l/cell/day$ and d_2 was changed to a value of $0.13\ /day$, therefore implicating a higher infection rate of malaria parasites to healthy RBCs and a faster decay rate of immune effectors, respectively. For sub-model 2C, the same value was used

Stellenbosch University https://scholar.sun.ac.za

for α as in the second model. However, here the value for d_2 was changed to $0.09\ /day$, showing a slightly lower decay rate as stated for model 2B. Additionally, the value for k_1 was altered to $4.5001 \times 10^{-5}\ \mu l/cell/day$ showing an increase in the proliferation rate due to infection. Lastly, in the fourth sub-model (2D) an endemic equilibrium is obtained and d_2 is now chosen as $0.04\ /day$ and here k_1, and not k_2, was changed to $1.03 \times 10^{-5}\ \mu l/cell/day$. The different model outputs are shown below in Figures A2.1- A2.4.

Stellenbosch University https://scholar.sun.ac.za

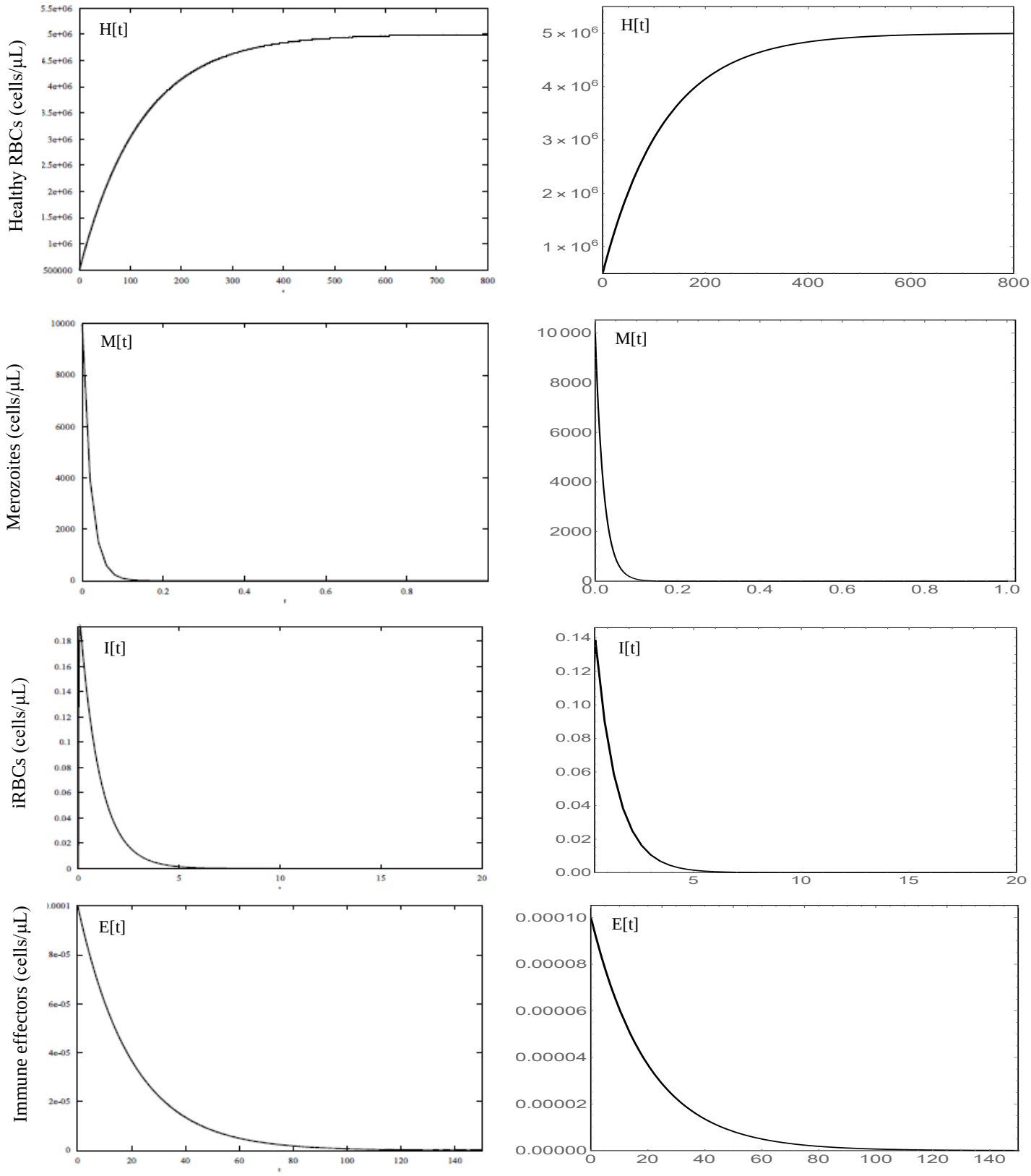

Figure A2.1: The results of the Li et al. [13] sub-model A showing a disease-free state. Parameter values were used as in Table A2. On the left hand side are all the published graphs and on the right hand side the graphs that were reproduced. $H[t]$ represents the population of healthy RBCs; $M[t]$ merozoites; $I[t]$ iRBCs and $E[t]$ immune effectors.

Stellenbosch University https://scholar.sun.ac.za

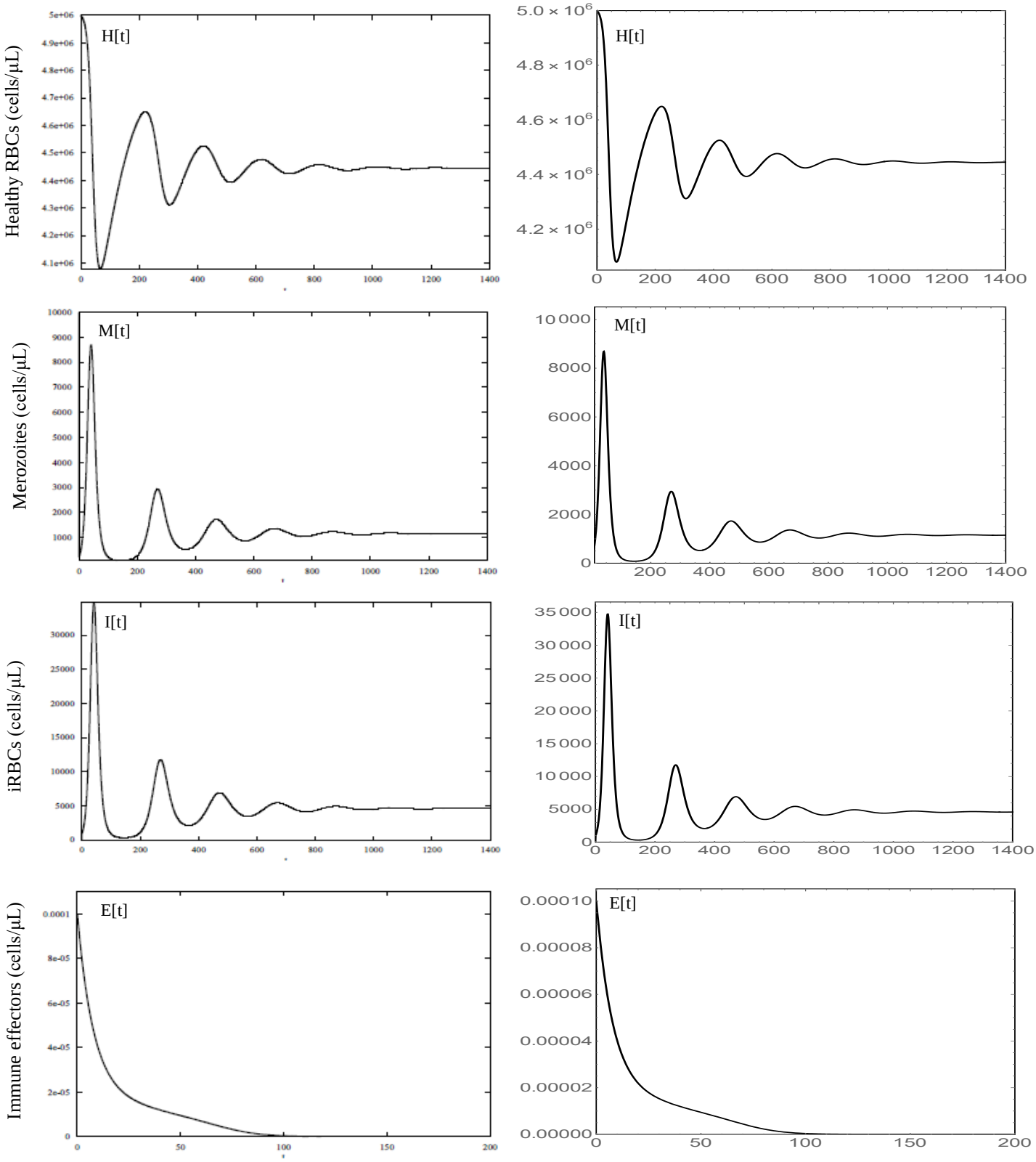

Figure A2.2: The results of the Li et al. [13] sub-model B showing an infection model without specific immune response. Parameter values were used as in Table A2 except for $\alpha = 9 \times 10^{-7}$ *and* $d_2 = 0.13$*. On the left hand side are all the published graphs and on the right hand side the graphs that were reproduced.* $H[t]$ *represents the population of healthy RBCs;* $M[t]$ *merozoites;* $I[t]$ *iRBCs and* $E[t]$ *immune effectors.*

Stellenbosch University https://scholar.sun.ac.za

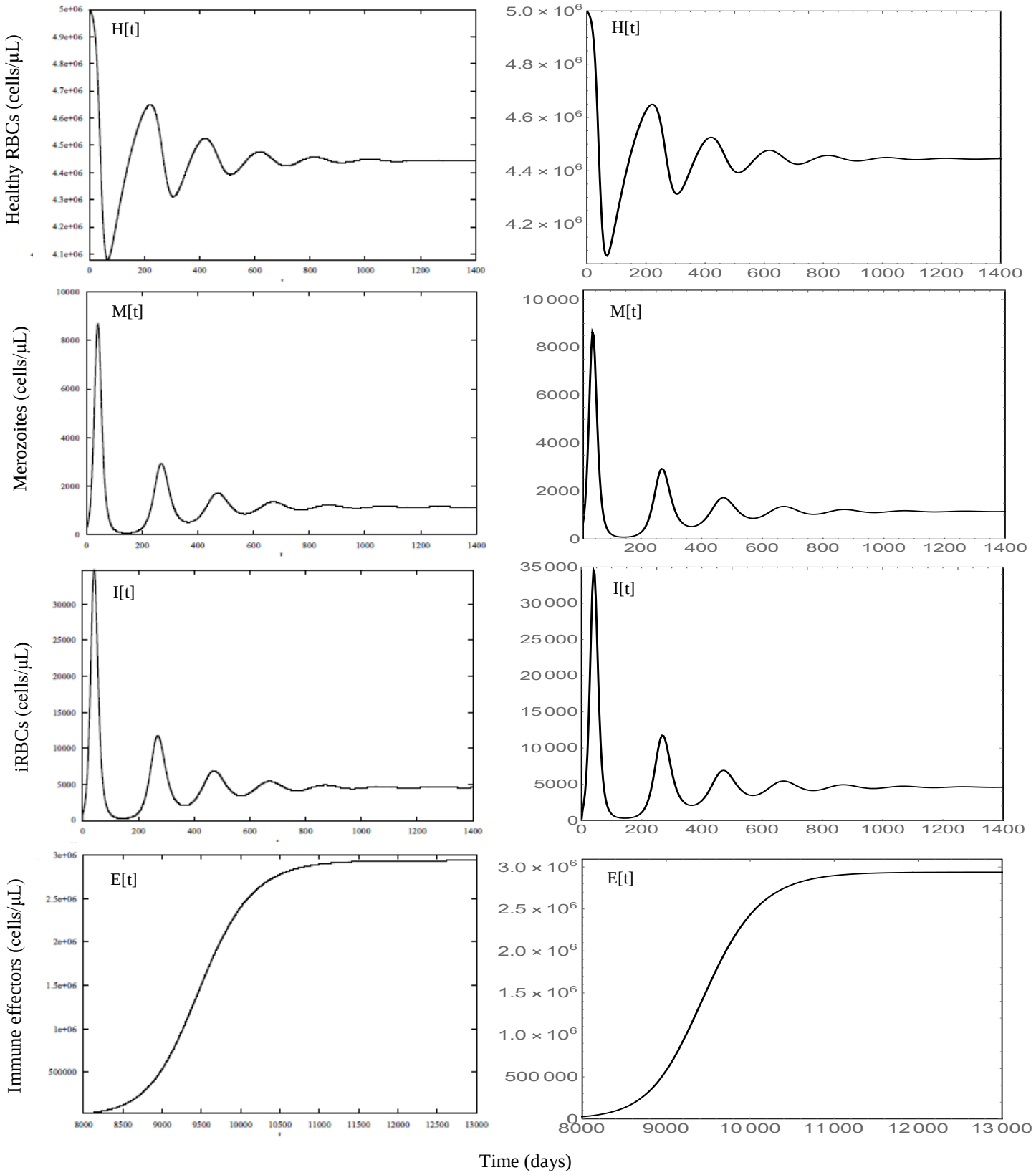

Figure A2.3: The results of the Li et al. [13] sub-model C showing an infection model with specific immune response. Parameter values were used as in Table A2 except for $\alpha = 9 \times 10^{-7}$, $d_2 = 0.09$ *and* $k_1 = 4.5001 \times 10^{-5}$. *On the left hand side are all the published graphs and on the right hand side the graphs that were reproduced.* $H[t]$ *represents the population of healthy RBCs;* $M[t]$ *merozoites;* $I[t]$ *iRBCs and* $E[t]$ *immune effectors.*

Stellenbosch University https://scholar.sun.ac.za

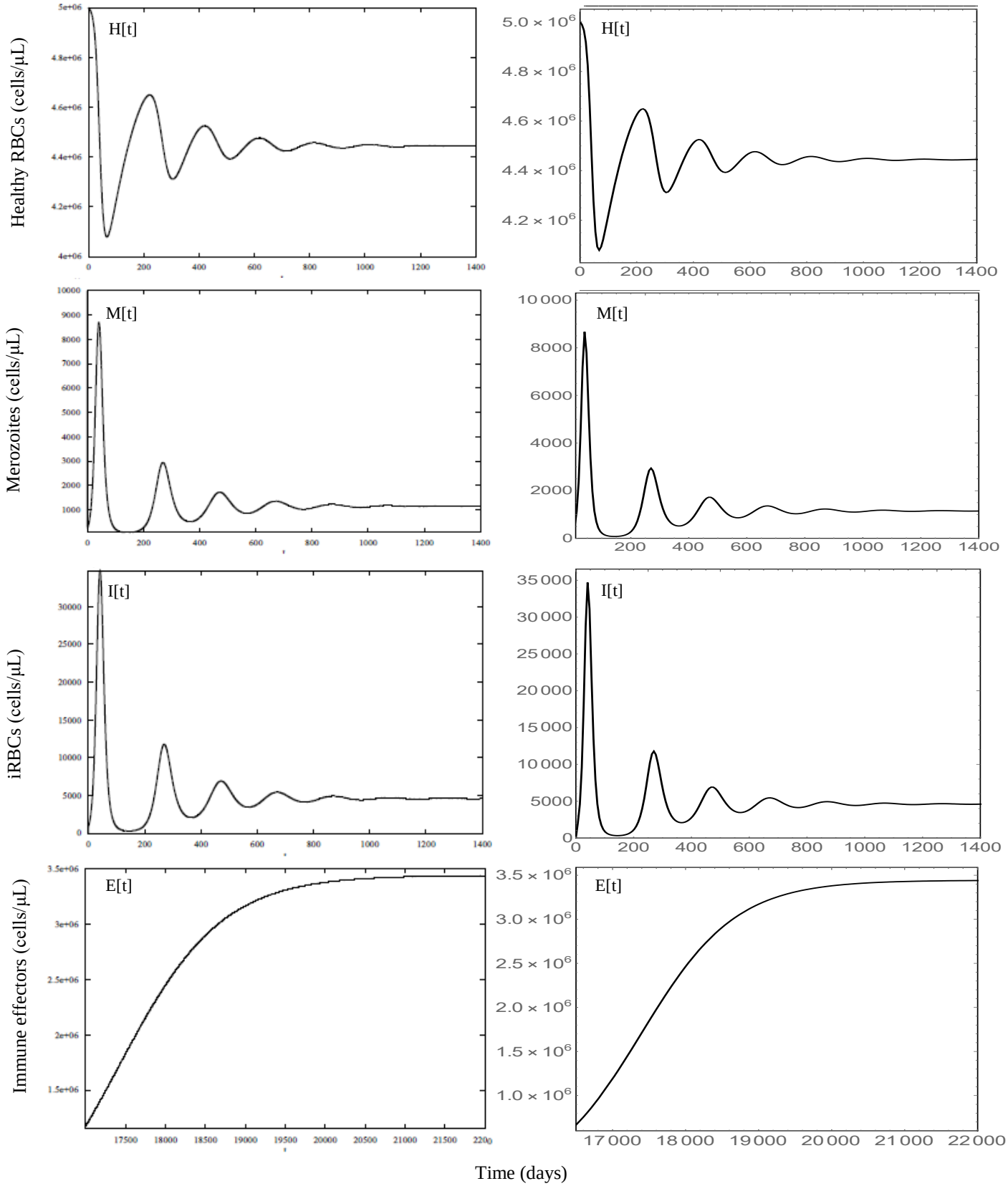

Figure A2.4: The results of the Li et al. [13] sub-model D showing an infection model at endemic equilibrium. Parameter values were used as in Table A2 except for $\alpha = 9 \times 10^{-7}$, $d_2 = 0.04$ *and* $k_1 = 1.03 \times 10^{-5}$. *On the left hand side are all the published graphs and on the right hand side the graphs that were reproduced.* $H[t]$ *represents the population of healthy RBCs;* $M[t]$ *merozoites;* $I[t]$ *iRBCs and* $E[t]$ *immune effectors.*

Stellenbosch University https://scholar.sun.ac.za

A.3. Niger *et al.* [15]

Table A3. Parameter and initial values of the Niger et al. [15] model, showing values for sub-model A and B, a disease free model and parasite present model, respectively.

Parameter	Description	SM-A	SM-B
$\boldsymbol{\lambda_X}$	Production rate of RBCs from the bone marrow	41664	41664
$\boldsymbol{\lambda_B}$	Production rate of immune cells	30	30
$\boldsymbol{\mu_X}$	Natural death rate of uninfected RBCs	0.8	0.8
$\boldsymbol{\mu_{Yi}}$ $\boldsymbol{(i = 1 - 4)}$	Natural death rate of infected RBCs	0.5	0.5
$\boldsymbol{\mu_{Y5}}$	Natural death rate of infected RBCs	1.0	1.0
$\boldsymbol{\mu_M}$	Natural death rate of merozoites	3.0	3.0
$\boldsymbol{\mu_B}$	Death rate of immune cells	1.53	1.53
$\boldsymbol{\mu_A}$	Deterioration rate of antibodies	0.4	0.4
$\boldsymbol{\mu}$	Loss of merozoites due to infection of RBCs	1	1
$\boldsymbol{\beta}$	Rate of infection	8×10^{-4}	8×10^{-4}
$\boldsymbol{\gamma_i}$ $\boldsymbol{(i = 1 - 5)}$	Progression rate of iRBCs from Stage (i) to Stage (i+1)	0.3	1.5
$\boldsymbol{k_i}$ $\boldsymbol{(i = 1 - 5)}$	Immunosensitivity of iRBCs	0	0.01
$\boldsymbol{k_M}$	Immunosensitivity of merozoites	0	0.3
$\boldsymbol{\rho_1}$	Immunogenecity of iRBCs and merozoites	0.001	0.001
$\boldsymbol{\rho_i}$	Immunogenecity of iRBCs and merozoites	10^{-5}	10^{-5}
$\boldsymbol{\eta}$	Maximum rate of increase of antibodies	0.6	0.6
$\boldsymbol{r}$	Number of merozoites	16	16
$\boldsymbol{X}$ $\boldsymbol{(0)}$	Initial concentration of healthy RBCs	500	500
$\boldsymbol{Y_1}$ $\boldsymbol{(0)}$	Initial concentration of iRBCs	–	–
$\boldsymbol{M}$ $\boldsymbol{(0)}$	Initial concentration of merozoites	1	1
$\boldsymbol{B}$ $\boldsymbol{(0)}$	Initial concentration of immune cells	–	–
$\boldsymbol{A}$ $\boldsymbol{(0)}$	Initial concentration of antibodies	–	–

Initial values are not given as the model shows that the initial values should not affect the steady states of the different variables that would be reached with the model. However, as stated previously, at least one merozoite is needed for the start of infection. Two different model outputs were achieved, with one

Stellenbosch University https://scholar.sun.ac.za

showing a parasite free steady state, where the $\gamma_i (i = 1 - 5)$ value denoting the progression rate of iRBCs from one stage to the next is lower, thus demonstrating a slower progression than that for the second model. The second model incorporates a stable parasite-present, or endemic, steady state. There is also no immunosensitivity of iRBC and merozoites in the parasite-free model. Model outputs are presented in Figures A3.1 and A3.2.

Stellenbosch University https://scholar.sun.ac.za

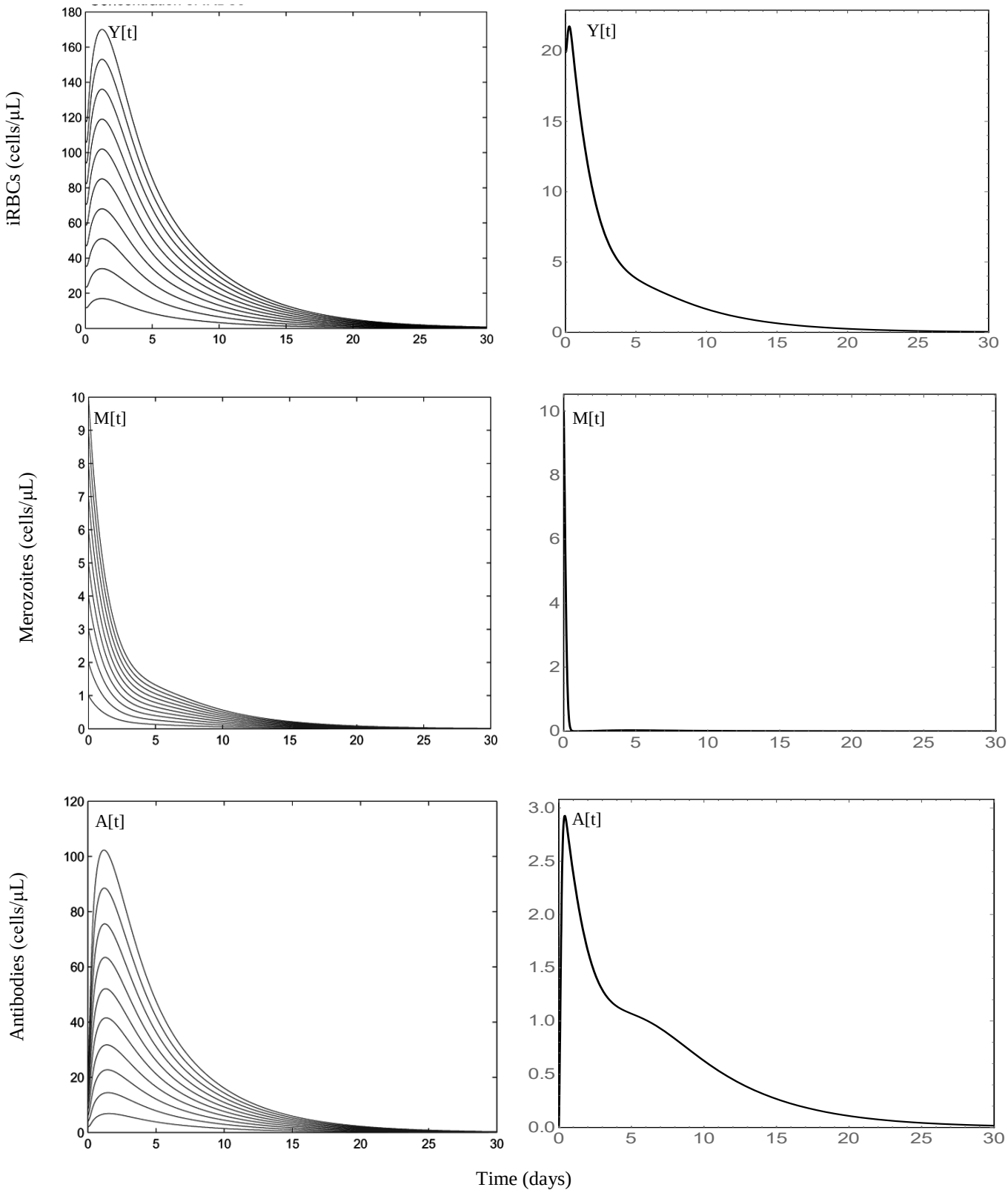

Figure A 3.1: The parasite-free equilibrium for the Niger et al. [15] model. Parameter values were used as in Table A3. On the left hand side are all the published graphs and on the right hand side the graphs that were reproduced. $Y[t]$ represents the combined population of iRBCs; $M[t]$ merozoites and $A[t]$ antibodies.

Stellenbosch University https://scholar.sun.ac.za

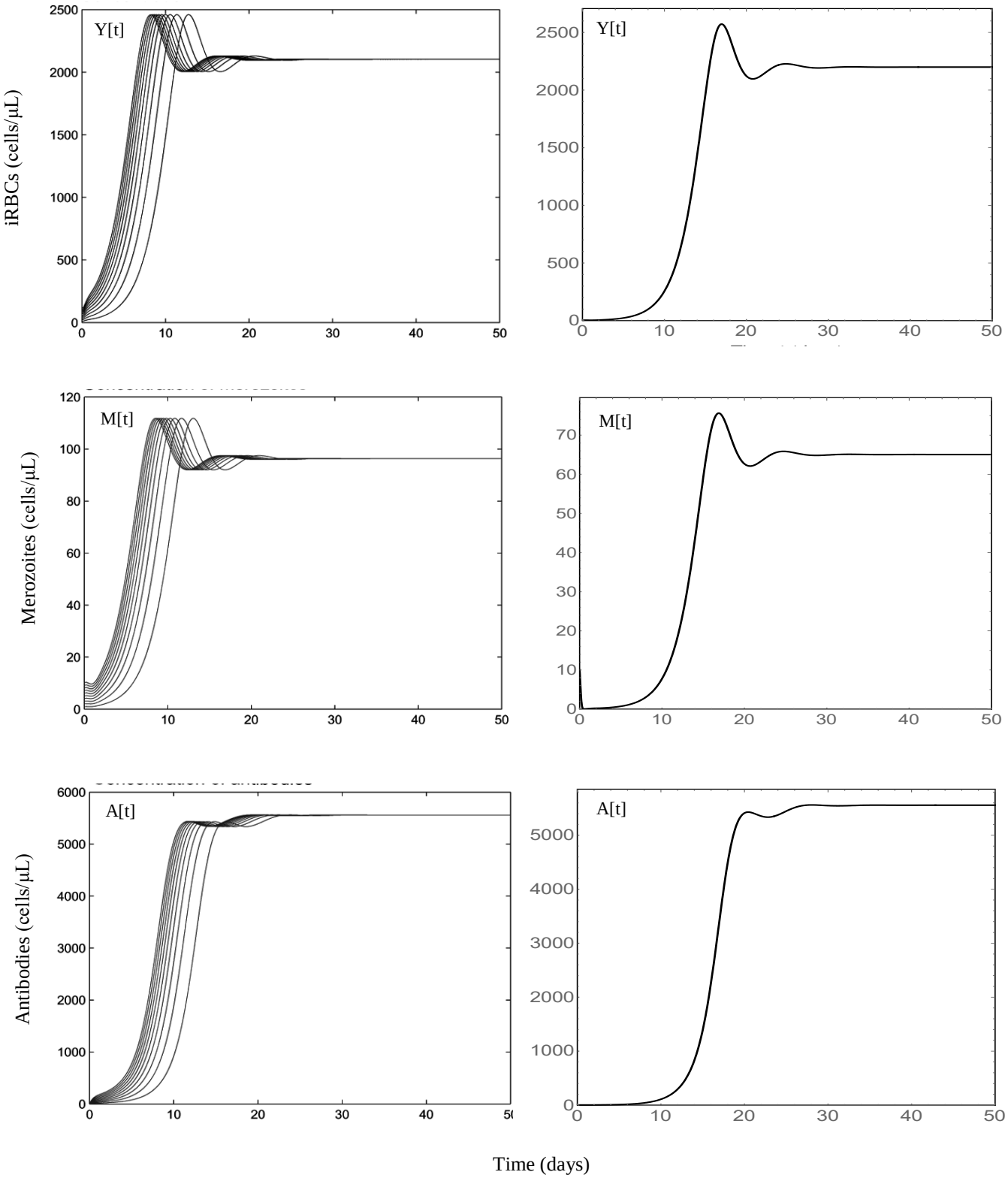

Figure A3.2: The parasite present equilibrium for the Niger et al. [15] model. Parameter values were used as in Table A3. On the left hand side are all the published graphs and on the right hand side the graphs that were reproduced. $Y[t]$ represents the combined population of iRBCs; $M[t]$ merozoites and $A[t]$ antibodies.

Stellenbosch University https://scholar.sun.ac.za

A.4. Okrinya [16]

Table A4. Parameter and initial values for Okrinya [16].

Parameter	Parameter Description	Value	Unit
λ_x	Rate at which RBCs are recruited	$4.15\ x\ 10^4$	$cells/\mu l/day$
β_x	Rate constant for infection rate of RBCs	$4.9\ x\ 10^{-6}$	$\mu l/cell/day$
μ_x	Natural per capita death rate of RBCs	0.0083	$/day$
μ_n	Natural death rate of iRBCs	0.055	$/day$
μ_y	Conversion rate of iRBCs to merozoites	0.5	$/day$
r	Number of merozoites released per bursting schizont	16	–
μ_m	Death rate of merozoites	48	$/day$
θ	Fraction of merozoites converting to gametocytes	$6.4\ x\ 10^{-3}$	–
μ_g	Natural per capita death rate of gametocytes	0.02	$/day$
c_0	Efficiency of antibodies in blocking merozoite invasion	0.6	$cell/mol$
c_1	Efficiency of antibodies in blocking merozoite release	1.12	$cell/mol$
k_a	Antibodies induced Fc-dependent killing rate of iRBCs	1.38	$cell/mol$
k_b	Antibody induced Fc-dependent killing rate of merozoites	12	$cell/mol$
k_c	Antibody induced Fc-dependent killing rate of gametocytes	1.26	$cell/mol$
k_y	Elimination rate of iRBCs by innate immune cells	0.9	$\mu l/cell/day$
k_m	Elimination rate of merozoites by innate immune cells	$1.18\ x\ 10^2$	$\mu l/cell/day$
k_g	Elimination rate of gametocytes by innate immune cells	1.4	$\mu l/cell/day$
b_m	Supply rate of immune cells from stem cells	0.038	$cell/\ \mu l/day$
η_1	Parasite induced innate immune cell production rate	$1.3\ x\ 10^{-7}$	$/day$
η_2	Parasite induced specific immune cell production rate	$3\ x\ 10^{-7}$	$mol\ \mu l/cell^2/day$
Φ	Phagocyte growth difference between merozoites and iRBCs	2	–
g_2	Antibody production difference between merozoites and iRBCs	0.85	–
k_d	Deterioration rate of innate immune cells due to iRBC killing	$2.8\ x\ 10^{-9}$	$\mu l/cell/day$
k_n	Deterioration rate of innate immune cells due to interaction with merozoites	$3.1\ x\ 10^{-9}$	$\mu l/cell/day$
η_3	Deterioration rate of antibodies due to interaction with iRBCs	$4.5\ x\ 10^{-8}$	$\mu l/cell/day$

Stellenbosch University https://scholar.sun.ac.za

$\boldsymbol{\eta_4}$	Deterioration rate of antibodies due to interaction with merozoites	$3.4\ x\ 10^{-8}$	$\mu l/cell/day$
$\boldsymbol{\mu_p}$	Death rate of innate immune cells	0.3	$/day$
$\boldsymbol{A_0}$	Starting density of antibodies	0	$mol/cell$
$\boldsymbol{\mu_a}$	Death rate of antibodies	0.3	$/day$
$\boldsymbol{X(0)}$	Initial concentration of RBCs	$5\ x\ 10^6$	$mol/cell$
$\boldsymbol{Y(0)}$	Initial concentration of iRBCs	0	$mol/cell$
$\boldsymbol{M(0)}$	Initial concentration of merozoites	0.105	$mol/cell$
$\boldsymbol{G(0)}$	Initial concentration of gametocytes	0	$mol/cell$
$\boldsymbol{P(0)}$	Initial concentration of innate immune cells	0.127	$mol/cell$
$\boldsymbol{A(0)}$	Initial concentration of antibodies	0	$mol/cell$

The Okrinya model was published in the non-dimensionalised form and reproduced graphs are presented in Figure A4.1. The graphs for the dimensionalised form are shown in Figure A4.

Stellenbosch University https://scholar.sun.ac.za

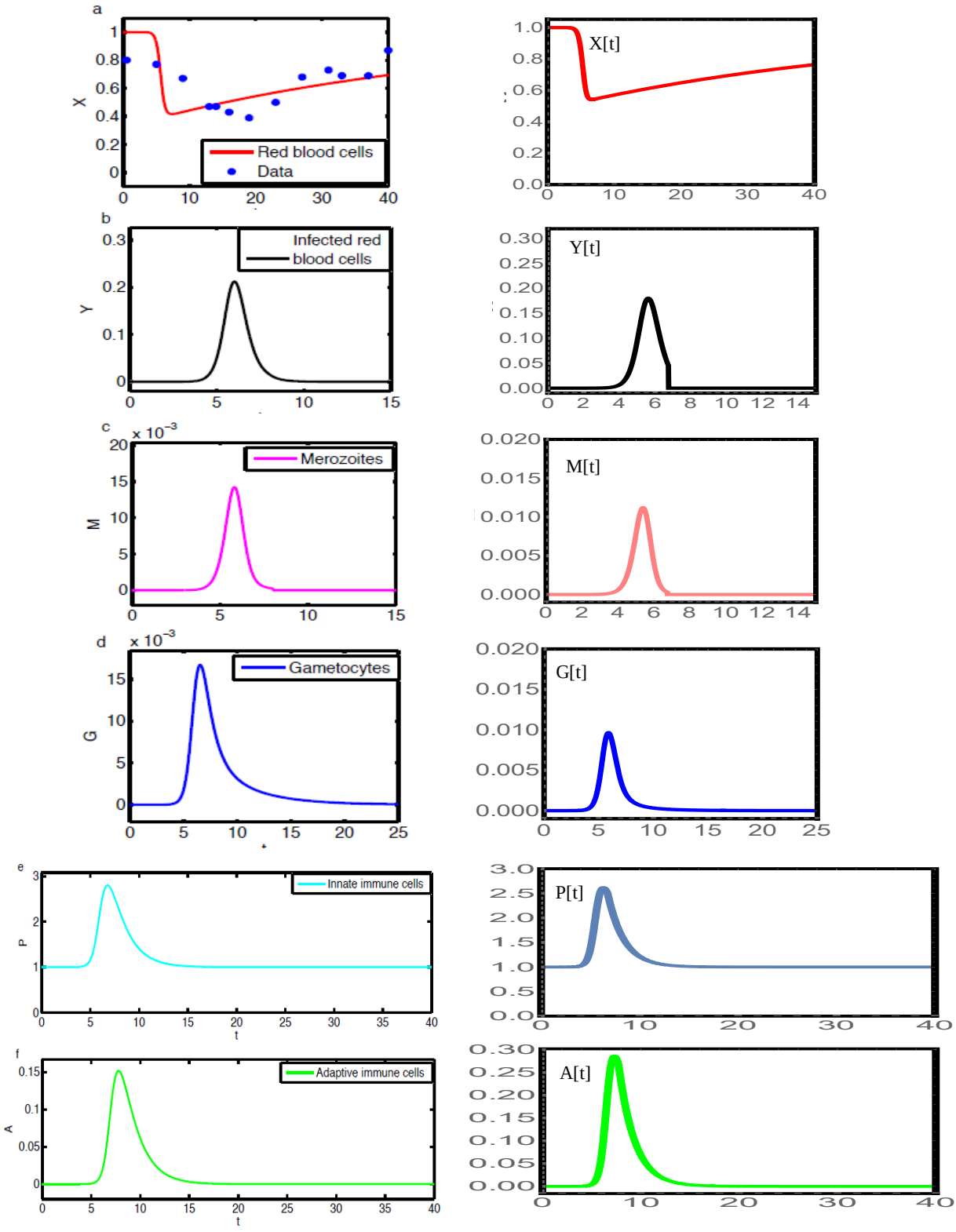

Figure A4.1: The parasite-present non-dimensionalised dynamics of malaria infection with immune response of the Okrinya [16] model. Graphs from the Okrinya [16] publication is shown on the left and reproduced graphs on the right. The red graphs show healthy RBCs; black shows iRBCs; pink/red- merozoites; dark blue- gametocytes, light blue- innate immune cells and green- adaptive immune cells.

Stellenbosch University https://scholar.sun.ac.za

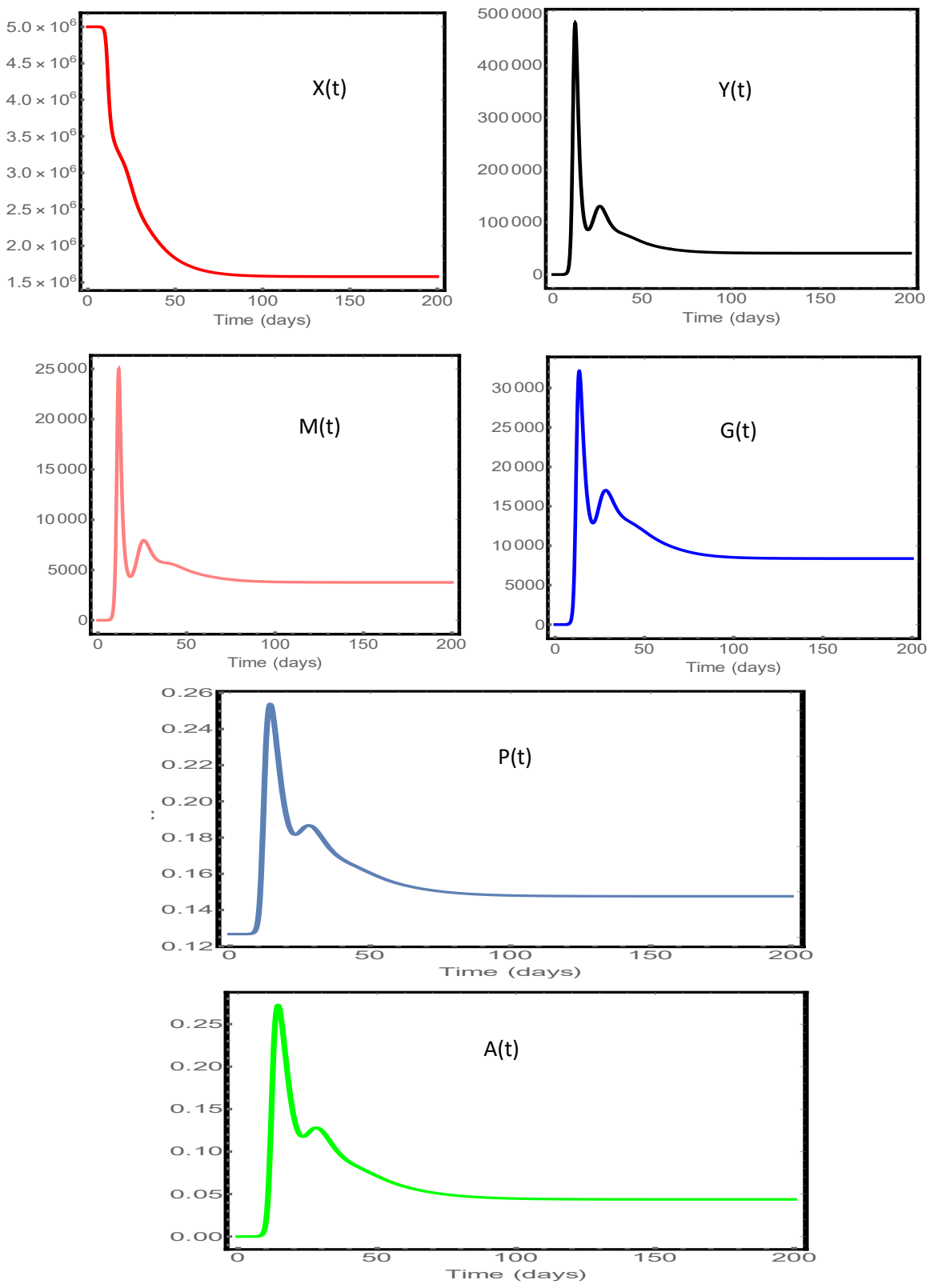

Figure A4.2: The parasite-present dimensionalised dynamics of malaria infection with immune response. Parameter values were used as in Table A4. The graphs show steady states are reached for the different variables when using the dimensionalised model form. The red graphs show healthy RBCs; black shows iRBCs; pink/red- merozoites; dark blue- gametocytes, light blue- innate immune cells and green- adaptive immune cells.